INVESTIGATING THE UNDERLYING IMMUNLOGICAL MECHANISMS OF PREVIOUSLY INFECTED SARS-CoV-2 INDIVIDUALS IN A UNIVERSITY SETTING: A CROSS-SECTIONAL, SEROPREVALENCE STUDY

by

Benjamin Hewins

Submitted in partial fulfillment of the requirements

for the degree of Master of Science

at

Dalhousie University

Halifax, Nova Scotia

December 2023

DEDICATION

I would like to formally dedicate this dissertation to my mother and father. Throughout my scholastic journey, my parents provided me unwavering support to help see me through each challenge. During times of uncertainty, I could always phone my parents or take a trip home to Kentville knowing that they would have my back. Not a day goes by that I do not remind myself how fortunate I am to be surrounded by such caring, loving, and supportive role models; I am eternally grateful.

TABLE OF CONTENTS

LIST OF TABLES

LIST OF FIGURES

ABSTRACT

Since December 2019, the COVID-19 pandemic has resulted in more than 770 million cases of the disease and over 6.9 million deaths worldwide. Although over 70% of the global population has been vaccinated against the coronavirus (over 13 billion doses administered), many individuals remain at risk of developing infection as novel sublineages of the Omicron variant continue to emerge. Gaps exist in our current understanding of COVID-19 disease pathogenesis in young individuals, particularly surrounding vaccine and infection-induced antibody durability and “long COVID-19". To address these gaps, we conducted a seroprevalence study at the Dalhousie University campus in Halifax, Nova Scotia, in the fall of 2022 and recruited N=77 students aged 18-35 years old. Rapid antigen testing and serum immunology were performed to measure the levels of previous infections on campus. I also assessed the serum concentration of twelve distinct blood biomarkers to characterize the long-COVID-19 immune response in this cohort. The sensitivity of rapid antigen testing was also compared to the gold standard RT-qPCR. My results suggest that young individuals mount a robust humoral immune response to COVID-19, and experience elevated levels of biomarkers associated with endothelial disruption during long-COVID-19 (i.e., ICAM-1 and VCAM-1). It is also evident that the COVID-19 nucleocapsid protein remains detectable up to 270 days post infection, indicative of mechanisms of viral persistence. Finally, I show that rapid antigen testing is comparable to RT-qPCR at detecting asymptomatic COVID-19 infections. This study provides a better understanding of the SARS-CoV-2 immune response in young individuals (18-35 years) and also a framework for the predisposing biomarkers associated with long-COVID-19 in this cohort.

LIST OF ABBREVIATIONS USED

aa	Amino acid
ACE2	Angiotensin converting enzyme 2
AM	Alveolar macrophage
ANG-2	Angiopoietin-2
ANOVA	Analysis of Variance
APCs	Antigen presenting cells
ARDS	Acute respiratory distress syndrome
BAL	Bronchoalveolar lavage
BSL2+	Biosafety level 2+
CCL2	CC motif ligand 2
CCL20	CC motif ligand 20
CD_4+ T-cell	Clusters of differentiation 4 T-cells, helper T-cells
CD_8+ T-cell	Clusters of differentiation 8 T-cells, cytotoxic T-cells
CDC	Centers for Disease Control and Prevention
CL2	Containment level 2
COPD	Chronic obstructive pulmonary disease
Cq	Quantitation cycle
CTD	C-terminal domain
CTL	Control
CXCL1	CXC motif ligand 1
CXCL2	CXC motif ligand 2
CXCL10	CXC motif ligand 10
DAMPs	Damage associated molecular patterns
DC	Dendritic cell
ddH_2O	Double distilled water
E-SEL	E-selectin
ELISA	Enzyme-linked immunosorbent assay
HCoV	Human coronavirus
HCoV-OC43	Human coronavirus OC43
HRP	Horseradish peroxidase
ICAM-1	Intercellular adhesion molecule 1
ICF	Informed consent form
IFN	Interferon
IFN-γ	Interferon gamma
IgA	Immunoglobulin A
IgG	Immunoglobulin G
IgM	Immunoglobulin M
IL-1	Interleukin 1
IL-2	Interleukin 2
IL-6	Interleukin 6
IL-8	Interleukin 8
IL-10	Interleukin 10
IL-17	Interleukin 17
IM	Intramuscular

IN	Intranasal
LC	Long COVID-19
MERS	Middle Eastern Respiratory Syndrome
MHC	Major histocompatibility complex
MPO	Myeloperoxidase
mRNA	Messenger ribonucleic acid
NAATs	Nucleic acid amplification tests
N protein	Nucleocapsid protein
NK cell	Natural killer cell
NLRs	Nod-like receptors
NSP	Non-structural protein
NTD	N-terminal domain
ORF	Open reading frame
P-SEL	P-selectin
PAMPs	Pathogen associated molecular patterns
PASC	Post-acute sequalae SARS-CoV-2
PRRs	Pattern recognition receptors
RBD	Receptor binding domain
RNase P	Ribonuclease P
ROS	Reactive oxygen species
RT-qPCR	Reverse transcriptase-quantitative polymerase chain reaction
S protein	Spike protein
S1	S1 subunit- spike protein
S2	S2 subunit- spike protein
SD	Standard deviation
ssRNA	Single stranded ribonucleic acid
TCR	T-cell receptor
Tfh cells	T-follicular helper cells
TLRs	Toll-like receptors
TMB	Tetramethylbenzidine
TMPRSS2	Transmembrane protease, serine 2
TNF-α	Tumor necrosis factor alpha
VCAM-1	Vascular cell adhesion molecule 1
VEGF	Vascular endothelial growth factor
VOC	Variant of concern
VOI	Variant of interest
VUM	Variant under monitoring
x G	Times gravity

ACKNOWLEDGEMENTS

First, I would like to thank each of my current and former lab members for their tutelage, support, and friendship both in and outside of the lab. This includes Dr. Nikki Kelvin, Dr. Anuj Kumar, Dr. Pacifique Ndishimye, Dr. Gustavo Sganzerla Martinez, Dr. Motiur Rahman, Ali Toloue Ostadgavahi, Mahya Kamrani, and formerly Abdullah Mahmud-Al-Rafat and Katie Lucki. I would like to make special mention of Ali; his calm demeanor and willingness to share his expertise in the lab were crucial to my development as a young scientist. I also acknowledge Gustavo, Motiur, Anuj, and Pacifique, who are some of the most hardworking, collaborative, and engaged scientists I've encountered. I am thankful for the integral roles each of you played in the completion of my thesis. I would also like to acknowledge my thesis supervisory committee, including Dr. Christopher Richardson, Dr. Jason Leblanc, and Dr. Todd Hatchette. Each committee meeting was mentally stimulating and provided many teachable moments regarding my approach(es) to scientific inquiry. I enjoyed getting to know each of you and thank you for taking time out of your schedules to assist with my research. I'd also like to thank the faculty, staff, and administrators in the Department of Microbiology and Immunology. The program was well orchestrated and inclusive.

Finally, I would like to thank my supervisor, Dr. David Kelvin. Dr. Kelvin is thoughtful in his approach to supervision, providing both the freedom and flexibility for students to carve a path of self-discovery. Dr. Kelvin's mentorship, knowledge, and selfless demeanor allowed me to refine my scientific potential and I will always be grateful for the role he played in shaping my future endeavors.

CHAPTER 1: INTRODUCTION

Viruses are globally ubiquitous, submicroscopic collections of genetic code (either DNA or RNA), which rely on host cell machinery for replication and survival. Viruses infect a diversity of living organisms, such as bacteria, plants, and animals and are the causal agents responsible for many of the pathogenic diseases observed in humans today(1). The persistence of a given virus within a population is largely influenced by viral evolution, where mutations to the genetic code of the virus allow immune evasion, also known as "viral escape". A virus's capacity to mutate is driven by factors such as the environment, where stressors to viral survival, such as recognition by neutralizing antibodies induced by infection or vaccine, cause rapid changes to the viral genome. Generally, RNA viruses mutate faster than DNA viruses and single-stranded viruses (such as severe acute respiratory syndrome coronavirus-2, SARS-CoV-2) mutate faster than double-stranded viruses(2).

Disease burden caused by the emergence and re-emergence of infectious diseases is increasing worldwide, as the global population continues to rise. Recent examples of emerging infectious diseases include (but are not limited to) Ebola, MPox, Zika Virus (ZIKV), Middle East Respiratory Syndrome (MERS), and recently SARS-CoV-2(3). The impact and disease burden of a particular virus is subject to many factors; I will discuss how the origin, distinct morphology, genetic factors, and mechanisms for immune evasion have contributed to the widespread burden of SARS-CoV-2 during the COVID-19 pandemic. To address gaps in our understanding of the immune response to COVID-19, we conducted a seroprevalence study at the Dalhousie University campus in Halifax, Nova Scotia, in the fall of 2022 and recruited N=77 students aged 18-35 years old

1.1 Introduction to coronaviruses

CoVs encompass a large family of enveloped, positive-sensed, spherical, single-stranded RNA (ssRNA) viruses. CoVs belong to the family *Coronaviridae* and contain genomes that range from 26 to 32 kilobases in length(4). There are currently four "common" human CoVs that are endemic in the global population; these include HCoV-229E (αCoV), HCoV-NL63 (αCoV), HCoV-OC43 (βCoV), and HCoV-HKU1 (βCoV)(5). Additional CoVs such as MERS-CoV (βCoV), SARS-CoV (βCoV responsible for severe acute respiratory syndrome, or SARS), and recently SARS-CoV-2 (responsible for coronavirus disease 2019, or COVID-19) have zoonotic origins. Infection caused by the four "common" CoVs is typically associated with mild symptoms while, in contrast, MERS-CoV, SARS-CoV, and SARS-CoV-2 are highly pathogenic, causing moderate to severe lower respiratory tract illnesses in humans.

1.1.1 Zoonotic origins of Coronaviruses pathogenic to humans

Collectively, the previously mentioned CoVs originated in animals and crossed the species barrier to infect humans, a concept otherwise known as zoonosis(6). Evolutionary trend analyses have been performed to reveal the specific origin of each CoV pathogenic to humans, which are summarized in Table 1.1.

Table 1.1 Comparison of the proposed zoonotic origin, typical clinical manifestation, classification, route of transmission, and case fatality rate in seven human Coronaviruses (HCoVs)(7,8).

	Species						
	HCoV-229E	**HCoV-NL63**	**HCoV-OC43**	**HCoV-HKU1**	**SARS-CoV**	**MERS-CoV**	**SARS-CoV-2**
Zoonotic origin (natural & intermediate host)	African hipposiderid Bats	Bats	Rodents Bovines	Rodents	Chinese horseshoe bats Masked palm civet (*Paguma larvata*)	Bats Dromedary camels	Bats (*Rhinolophus affinis*) Pangolins (*Manis javanica*)
Subgenus	*Duvinacovirus*	*Setracovirus*	*Embecovirus*	*Embecovirus*	*Sarbecovirus*	*Embecovirus*	*Sarbecovirus*
Classification	αCoV	αCoV	βCoV	βCoV	βCoV	βCoV	βCoV
Common clinical manifestation	Common cold symptoms in healthy adults	Mild fever, cough, sore throat, rhinitis	Mild upper-respiratory tract infections Sore throat	Cough, nasal congestion, fever, sore throat, chills	Fever, dry cough, shortness of breath	Fever, shortness of breath, cough, diarrhea, nausea	Fever, cough, lethargy, loss of smell/taste, headache
Route of transmission	Respiratory droplets Fomites	Respiratory droplets Fomites	Respiratory droplets Fomites	Respiratory droplets Fomites	Respiratory droplets Fomites Fecal-oral	Respiratory droplets Fomites	Respiratory droplets Fomites Fecal-oral
Peak case fatality rate	Unknown	Unknown	Unknown	Unknown	10%	34%	~6%

Noteworthy is the fact that all seven human coronaviruses (HCoVs) were evolutionarily confirmed to have originated from bats(4). For bats, CoVs are non-pathogenic and thus facilitate the acquisition of genetic diversity for CoVs without compromising the health of the host. This leads to more virulent forms of the virus with greater potential for spillover to other species, resulting in major global epidemics and pandemics. Importantly, the natural and intermediate

hosts for both SARS-CoV and SARS-CoV-2 are still under investigation. Phylogenetic analyses indicate that bats are likely the primary intermediate hosts responsible for animal-human zoonotic spillover, although other species such as pangolins and raccoon dogs were also species of interest(9,10). A source of debate regarding the origin of the SARS-CoV-2 pandemic was whether the virus was natural (i.e., spillover from animals to humans), or was a product of a laboratory leak from the Wuhan Institute of Virology. In any case, there remains no definitive consensus on the origin of SARS-CoV-2 and increased investigation into plausible methods is required. Understanding the origin of SARS-CoV-2 is fundamental to obviating future outbreaks by directing resources to increasing surveillance of host species and mitigating spillover events.

1.1.2 Distinct morphology

Perhaps one of the defining characteristics of CoVs is their distinct corona, or "crown-like" spike protein projections. Collectively, CoVs contain some of the largest viral RNA genomes described, averaging roughly 27 to 32 kilobases (kb)(7). CoV virions are spherical and measure 100-120 nm in diameter. Much of the CoV genome is used to code for two large, open reading frames (ORFs). ORFs 1a and 1b encode for several non-structural proteins (NSPs) (11). The remaining viral genome codes for the structural proteins, which include spike (S), envelope (E), nucleocapsid (N), and membrane (M), proteins, respectively (Figure 1.1).

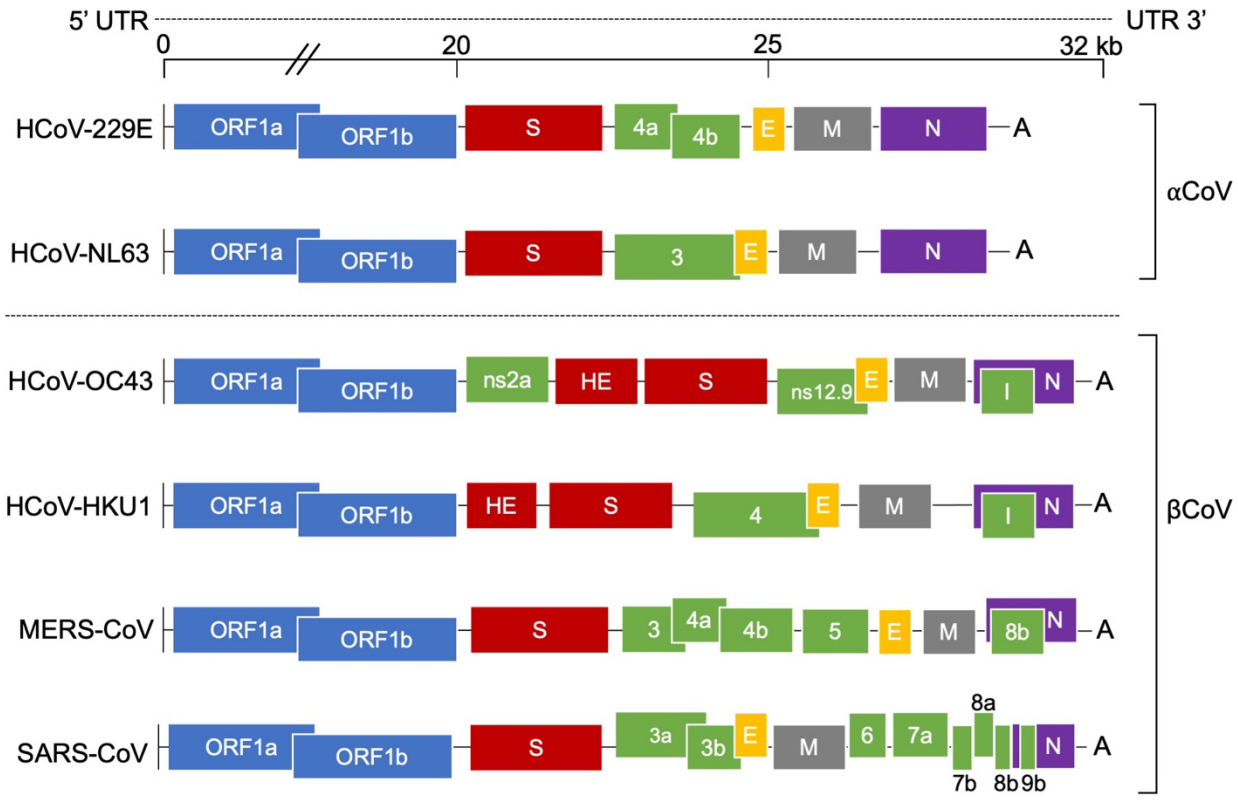

Figure 1.1 Genome structure of human coronaviruses.

The genome structures of six of the seven human coronaviruses (HCoVs) are shown above, demonstrating genome homology and preservation between the viruses. Each of the human coronaviruses are roughly 30-32kb in length and contain large open reading frames (ORFs 1a and 1b), which are both translated into large polyproteins at the 5' end. Much of the remaining genome contains ORFs for structural proteins (HE-S-E-M-N) as well as a number of accessory proteins, which are involved in mechanisms relating to viral pathogenesis(7). The genome structures are separated as alpha and beta coronaviruses, respectively. Abbreviations: HCoV: human coronavirus; MERS-CoV: Middle East respiratory syndrome coronavirus; SARS-CoV-severe acute respiratory syndrome coronavirus; HE: hemagglutinin-esterase; S: spike; E-envelope; M: membrane; and N: nucleocapsid.

Importantly, the structure of SARS-CoV-2 largely overlaps with the structure of the previously mentioned HCoVs, which I'll discuss in the next section.

1.2 SARS-CoV-2

In December 2019, a pneumonia-like disease of unknown cause was discovered in Wuhan, Hubei Province, China. The virus responsible for the outbreak was identified as a novel coronavirus, which was later named severe acute respiratory syndrome coronavirus 2 (SARS-CoV-2). The novel coronavirus 2019 (COVID-19) is structurally similar to other HCoVs, including severe acute respiratory syndrome (SARS-CoV) and the Middle East Respiratory Syndrome (MERS-CoV). In March 2020, the World Health Organization (WHO) declared the COVID-19 outbreak a global pandemic(12). Since then, the COVID-19 pandemic has rapidly swept the globe and is responsible for over 770 million cases and greater than 6.9 million deaths worldwide. The virus has placed marked stress on healthcare systems around the world, causing saturated emergency rooms, inpatient wards, and ICUs, while also drastically increasing wait times for other healthcare services(13). Many hospitals are having to channel valuable resources and space to create (at times makeshift) COVID-19 dedicated floors and wards. Furthermore, elective treatments in other disciplines have been reduced or canceled altogether to accommodate surges in cases and increased COVID-19 related hospitalizations, further exacerbating conditions and reducing quality of life for those on waiting lists. To add additional context to the disease burden caused by the global COVID-19 pandemic, it is estimated that the pandemic has cost the global economy roughly $114 trillion USD (low-end estimate) since 2020(14). Experts predict that this evaluation will continue to increase due to the continued emergence of virulent SARS-CoV-2 variants, supply chain disruptions, and restoration of previous healthcare systems. To understand how and why the COVID-19 pandemic has caused such global devastation, it is important to understand the unique biology and clinical characteristics of SARS-CoV-2.

1.2.1 SARS-CoV-2 structure

The SARS-CoV-2 virus belongs to the B lineage of the β-CoVs, which is a family comprised of an enveloped, non-segmented, positive-sense, single-stranded RNA virus genome(15). Like other HCoVs, the SARS-CoV-2 virion is characterized by a unique, corona "crown-like" shape with "club-like" spike glycoproteins projecting from the surface (Figure 1.2).

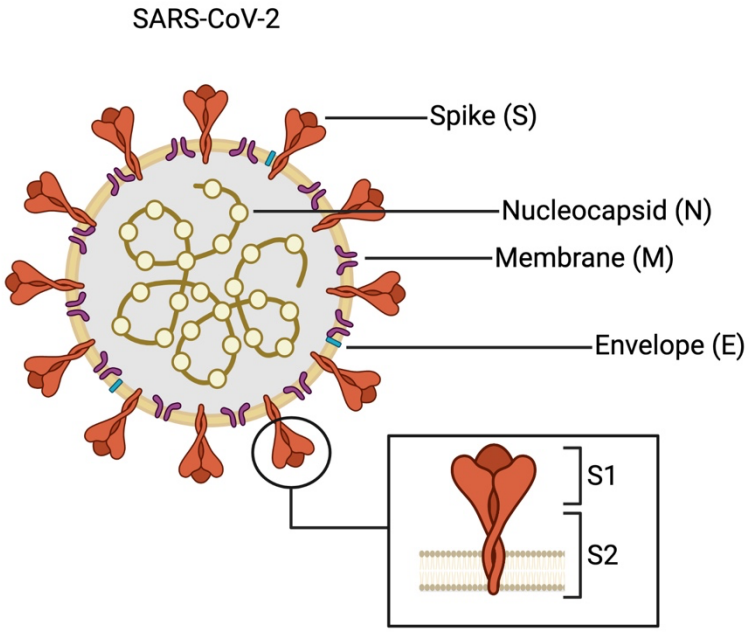

Figure 1.2 Virion structure of SARS-CoV-2.

Severe acute respiratory syndrome coronavirus 2 (SARS-CoV-2) is an enveloped, positive-sense, single-stranded RNA virus. The virion of SARS-CoV-2 consists of structural proteins, such as spike (S), envelope (E), membrane (M), and nucleocapsid (N). The S protein facilitates viral interaction with receptors on the host cell, where its S trimers (S1) protrude from the viral envelope, providing specificity for cellular entry receptors. The two non-covalently, functionally distinct subunits of S are called S1 and S2. S1 contains the receptor binding domain (RBD) while S2 anchors the S protein to the virion membrane, mediating membrane fusion (8,16). Image created using BioRender.

1.2.2 Viral entry & infection

SARS-CoV-2 viral entry is mediated by the binding of the S protein to its corresponding receptor, angiotensin-converting enzyme 2 (ACE2). A similar modality is observed for other HCoVs, such as SARS-CoV and HCoV-NL63, where these coronaviruses rely on ACE2 as their obligate receptor(16). Viral entry begins with S protein attachment and fusion to the host cell membrane. Multiple copies of the S protein trimeric structure are inserted into the SARS-CoV-2 virion membrane (resulting in the "crown-like" surface), which ensures a multitude of readily available attachment points for the virus(16,17). Additionally, human ACE2 is expressed on epithelial cells of multiple tissue types, such as lung, intestine, kidney, heart, adipose, and reproductive tissues.

For viral entry to occur, SARS-CoV-2 uses human ACE2 as an entry receptor and human proteases as entry activators. The S protein is trimeric and divided into two primary subunits, subunit 1 (S1), which contains three receptor binding domain (RBD) S1 heads and binds ACE2, and subunit 2 (S2), responsible for anchoring the S protein to the membrane. Coronavirus entry is mediated by two S protein cleavage events. First, proteolytic cleavage occurs during virus maturation in an infected host cell at the S1/S2 boundary via the host cellular protease furin at a multibasic site (Arg-Arg-Ala-Arg) (Figure 1.4). Following furin cleavage, the S protein is comprised of two non-covalently associated S1/S2 subunits(16). This furin-like cleavage is necessary for fusion and viral infection(18).

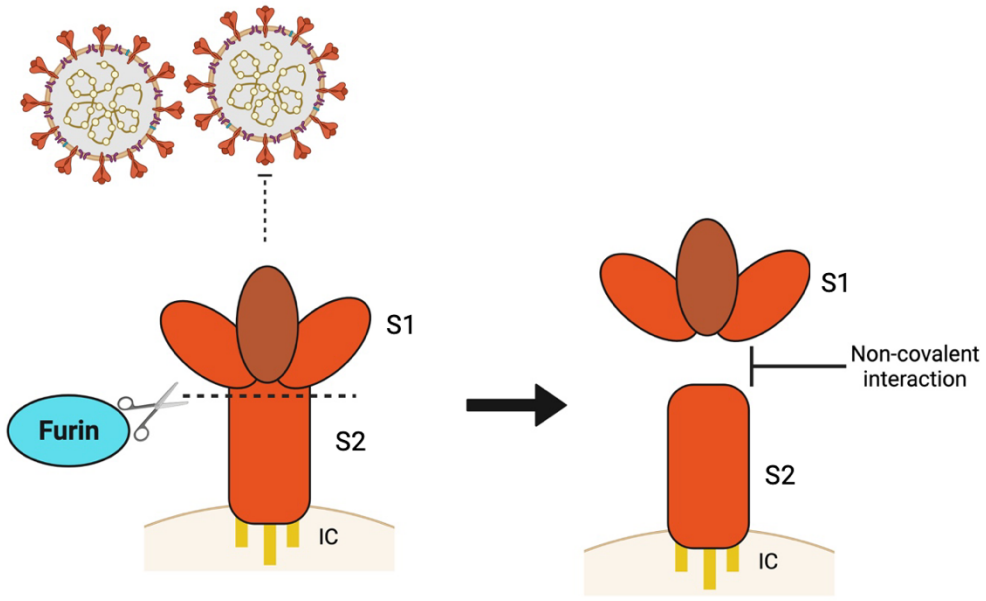

Figure 1.3 SARS-CoV-2 spike (S) protein schematic.

Schematic of the three-dimensional (*3D*) structure of the SARS-CoV-2 spike (S) protein. The junction between the S1 and S2 subunits represents a cleavage site for the protease furin. The cleavage activates the fusion machinery of SARS-CoV-2 viral glycoproteins and is generally referred to as the 'polybasic site'(19). Once furin cleaves S1 and S2, the protein is divided into two subunits held together by noncovalent interactions, while S2 remains anchored via the intracellular tail. Following this S priming, S1 undergoes a conformational change that exposes the receptor-binding domain (RBD) capable of recognizing the ACE2 entry receptor (20). Abbreviations: S1: subunit 1, S2: subunit 2, IC: intracellular tail. Image created using BioRender.

After the S protein is cleaved by furin in the host cell's Golgi apparatus, binding between SARS-CoV-2 and human ACE2 initially occurs through the S1 RBD, causing conformational changes in both subunits. The S1 domain is then shed from the viral surface to allow the S2 domain to fuse to the host cell membrane. S protein activation is further mediated by additional cleavage at the S2' site by a protease called transmembrane protease, serine 2 (TMPRSS2) at the cell surface(16,17,21). S2' TMPRSS2 cleavage exposes the S2' subunit, enabling fusion and pore formation between the viral capsid and the host cell membrane, allowing viral RNA to access the cytoplasm and viral replication to commence (Figure 1.5).

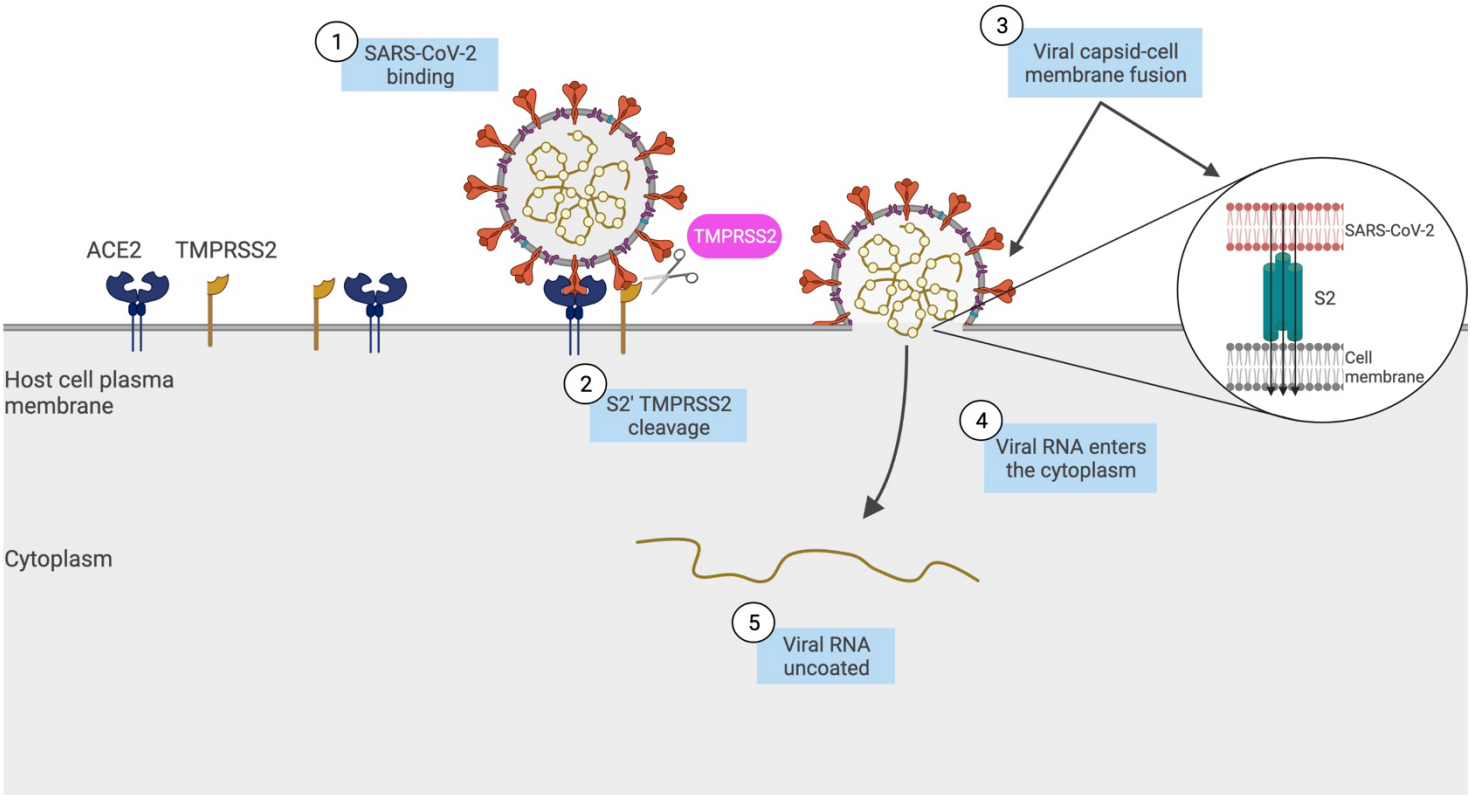

Figure 1.4 SARS-CoV-2 viral entry mechanisms into the host cell.

SARS-CoV-2 uses two distinct entry pathways into the host cell during infection, endosomal entry, and cell surface entry. Pictured above is the cell surface entry route, where the virus binds to transmembrane protease, serine 2 (TMPRSS2) and ACE2 receptors on the host cell surface (step 1). Binding to TMPRSS2 facilitates cleavage at the S2' subunit of the spike protein (step 2), exposing the fusion peptide. This cleavage event causes conformational changes in S2', forcing the fusion peptide into the cell membrane thereby forming a fusion pore (step 3) and allowing viral RNA to enter the host cell cytoplasm where viral uncoating and replication can proceed (steps 4 and 5). Alternatively, viral entry can proceed via the endosomal entry method. Endosomal entry proceeds when TMPRSS2 expression is low. Here S2' cleavage is facilitated by cathepsins following the internalization of the virus-ACE2 complex by clathrin-mediated endocytosis into endolysosomes(16). Abbreviations: TMPRSS2: transmembrane protease, serine 2, ACE2-angiotensin converting enzyme 2; S2': spike protein subunit 2. This image was adapted from Jackson et al. (2021). Image created using BioRender.

1.3.2 Viral replication within the host cell

SARS-CoV-2 tends to target tissues in the upper respiratory epithelia, where ACE2 is abundantly expressed(8). Once viral uptake and fusion has occurred and the SARS-CoV-2 endosome is formed, the viral RNA is subjected to uncoating, where viral genomic RNA enters the host cell cytoplasm. The SARS-CoV-2 genome varies from 29.8 kb to 29.9 kb in length; however, due to divergence and genome evolution from the ancestral strain, many COVID-19 lineages contain differing genome sizes(22). Additionally, the genome contains a 5' cap and 3' poly-A tail, which serves an important role in allowing SARS-CoV-2 to function as an mRNA for translation of the replicase polyproteins(15,23). After viral RNA uncoating, the genomic material immediately undergoes translation by host cell ribosomes to produce viral replicate enzymes, which function to generate new RNA genomes and synthesize viral particle assembly(24). Viral RNA translation begins with the two large, open reading frames ORF1a/b. The SARS-CoV-2 genome contains 14 ORFs in total; however, translation begins at the first ORF, which is comprised of ORF1a/b and constitutes roughly 67% of the viral genome (6). ORF 1a/b encodes a large replicase polyprotein (polyprotein 1ab) that is further cleaved into 16 non-structural proteins (Nsp), numbered nsp1 through nsp16 (Figure 1.3)(15,24). These Nsp form the replicase machinery.

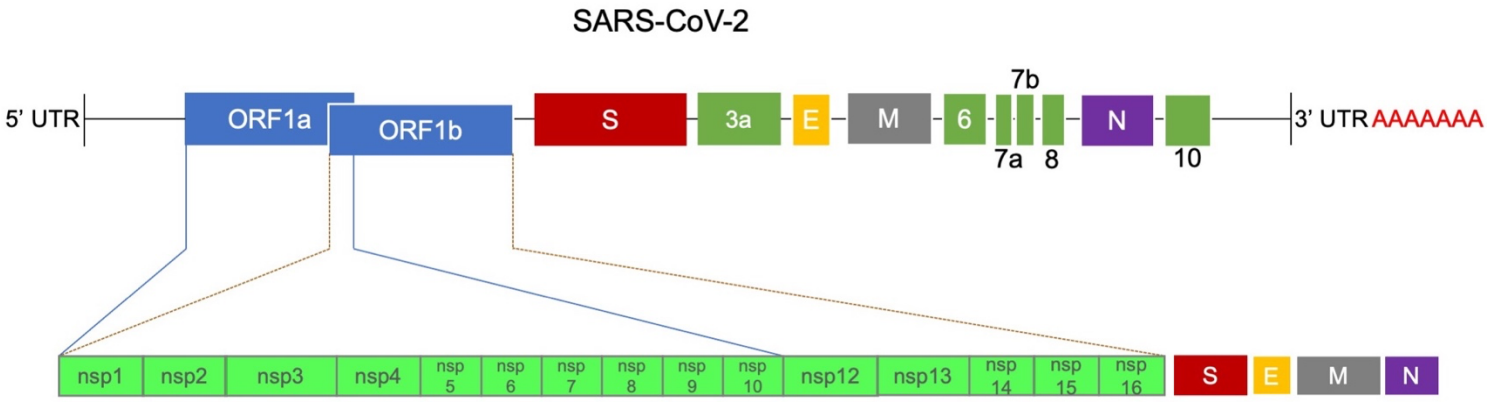

Figure 1.5 Genome structure of SARS-CoV-2.

From the 5' to 3' direction, a replicase complex (ORF1a and ORF1b) encodes a large polyprotein (polyprotein 1ab), which is further cleaved into 16 non-structural proteins (nsp1-16) that are responsible for maintaining key aspects of viral replication and transcription. The spike (S) structural protein is involved in host-receptor binding and membrane fusion, the membrane (M) structural protein facilitates viral assembly, the nucleocapsid (N) structural protein is involved in viral genome packaging and virion assembly, while the envelope (E) structural protein forms an ion channel, promoting virion assembly. Three of the four structural proteins (S, E, and M) are located within the viral membrane. Additionally, of the nine accessory proteins, ORF3a, ORF7a, and ORF7b are transmembrane proteins, which are predominantly involved in modulating the inflammatory response, pathogenesis, and host cell apoptosis(25). The 3' untranslated region also contains a large poly (A) tail. Figure adapted from: Rastogi et al. (2020)(26).

In addition to Nsps, the SARS-CoV-2 genome encodes the remaining ORFs and the four major structural proteins at the 3' end, including the spike surface glycoprotein (S), envelope (E), membrane (M), and nucleocapsid (N). The translated structural proteins are translocated into endoplasmic reticulum (ER) membranes and move through the ER-golgi intermediate compartment (ERGIC), where interaction with new genomic RNA results in budding into the lumen(8). Each of the four structural proteins play an important role in pathogenesis and release of viral particles and are each advantageous for SARS-CoV-2 establishment in a distinct way. Table 1.2 summarizes the location and unique function of each structural protein.

Table 1.2 The four major SARS-CoV-2 structural proteins, their location within the virus, and their distinct function during viral infection.

Structural Protein	Location on SARS-CoV-2 Virion	Function
Spike (S) glycoprotein 	A trimeric glycol-protein protruding from the viral membrane surface as a "club-like" projection.	The spike glycoprotein is a type I membrane protein that interacts with the human angiotensin-converting enzyme 2 (ACE2) receptor to enter the host cell. The spike protein represents the first step of infection, inducing a host antibody response. It is therefore an important target for therapeutics, modelling, diagnostics, and vaccines(27).
Envelope (E) 	The envelope protein is located on the virion surface. Forms an ion-channel.	The envelope protein plays an important role in assembly, release, and virulence phases of the viral life cycle. It is composed of 75 amino acid residues and is said to be multifunctional, as it is also involved in mediating the host immune response via a pore-forming transmembrane domain(28).
Membrane (M) 	The most abundant structural protein, it spans the virion membrane bilayer.	The membrane glycoprotein plays a key role in viral particle assembly by stabilizing the N protein-RNA complex inside the virion. M protein also closely interacts with and can bind to the other structural proteins(29).
Nucleocapsid (N) protein enclosing viral RNA 	N protein bound to viral RNA is in the cytoplasm of the virion and possesses a modular structure.	The nucleocapsid (N) protein is an RNA-binding protein involved in viral genome assembly and packaging. Structural studies have revealed that N protein interacts with RNA and other structural proteins, and undergoes self-association, meaning that it binds to a domain within the same polypeptide(30,31).

*Note: Protein diagrams created using BioRender.

1.3 The SARS-CoV-2 immune response

In response to viral pathogens, such as SARS-CoV-2, the host immune system is activated. This activation occurs in a two-prong process, where non-specific antiviral mechanisms act as a 'first line of defense' (innate immunity), followed by the priming and development of an antigen-specific immune response (acquired immunity). The pathogenesis of a given virus is largely dictated by the extent and duration in which the host immune system is activated. Certain clinical factors, including being immunocompromised, having a pre-existing or underlying health condition, or being elderly, are also predictors for disease risk, severity, and outcome. As viruses are transmitted throughout the population, they encounter antibodies and other immune mediators produced by natural infection and vaccination. With increasing specificity, these immune mediators cause increased selective pressure that can lead to both protein level and genetic mutations that force viral evolution. Understanding the interplay between the host immune system and the intricacies involved in viral evolution and antigen escape is of great importance to mitigate the emergence of novel SARS-CoV-2 variants.

1.3.2 Innate immunological mechanisms

The innate immune system represents the first of two fundamental defense systems that respond to foreign antigens, such as microbes, viruses, and toxins(32). Innate immunity refers to a collection of broad, non-specific defense mechanisms that respond to conserved molecular motifs within microbes, otherwise known as pathogen-associated molecular patterns, or PAMPS(32,33). A class of germline encoded receptor proteins found within the subcellular compartments (membrane-bound and cytosolic) of host immune cells called Pattern Recognition Receptors (PRRs) recognize PAMPS and initiate signal cascading events. This recognition by

PRRs is highly specific and typically serves as the first step in promoting pro-inflammatory or antiviral events with rapid onset (minutes to hours following challenge). PRRs are commonly grouped into sub-families, including the Toll-like receptors (TLRs), the nucleotide-binding oligomerization-like receptors (NLRs), and the retinoic acid-inducible gene-1-like receptors (RLRs)(33,34).

As viral nucleic acids are sensed by PRRs, type I and type III interferons (IFNs) are produced to activate inflammation(35). IFN production further stimulates the expression of interferon stimulated genes (ISGs), that play a role in establishing a broad, antiviral base state in neighboring cells(35,36). Some well-known classical ISGs include PKR, MX1, and OAS1, which are central to antiviral defense(37). Collectively, ISGs exert their antiviral function by impeding viral entry, replication, and budding. In addition to the rapid onset of the IFN response, PRRs stimulate the production and release of chemokines and cytokines, which promote cell migration and inflammation at the site of infection. Cytokines are small, secreted proteins, which serve as intercellular messengers for initiating or constraining an inflammatory response(38). The chemokines (or chemotactic cytokines) stimulate the migration and localization of innate immune cells (namely leukocytes) to the site of infection using cell surface G protein-coupled heptahelical chemokine receptors(39). The predominant innate immune cells include the granulocytes (basophils, neutrophils, eosinophils) and the mononuclear cells, such as mast cells and macrophages. Neutrophils are the most abundant and transient cells in circulation and typically increase in number during an immune response. During a viral infection, neutrophils are recruited to inflamed tissues (commonly lung tissues) by chemokines such as CXCL1, CXCL2, and IL-17(38,40). Once activated, neutrophils serve multiple effector functions in response to viral infection. Neutrophil activation can trigger degranulation, where neutrophils

secrete proteolytic enzymes; activation also mediates pathogen clearance by promoting reactive oxygen species (ROS) production and release(40). Mast cells also play important mediating roles in response to viral infection, such as degranulation events, effector cell/dendritic cell mobilization, and cytokine/chemokine expression for NK cell recruitment(41). Macrophages and monocytes also play key roles during viral infection. For example, during a SARS-CoV-2 infection, activated alveolar macrophages exhibit both phagocytic activity (engulf dead or virus infected cells in the lungs) and cytokine production following recognition of damage-associated molecular patterns (DAMPs) via PRRs(42). Following recruitment and activation, monocytes also display marked phagocytic activity during viral infection, where they acquire inflammatory macrophage and dendritic cell (DC)-like phenotypes for antigen presentation and tissue remodeling(42,43).

1.3.3 Adaptive immunological mechanisms

As previously discussed, the innate immune system functions non-specifically as the first line of defense in response to a foreign pathogen. While the innate system mounts a broad scale response, the adaptive immune system is being primed for specific, subsequent encounters to the original pathogen. The function of the adaptive immune system is complex, but may be broken into three primary foundational pillars, including: i) the recognition of "non-self", foreign antigens; ii) the development of immunological memory that can eliminate pathogens efficiently, should subsequent infections occur; and, iii) the generation and activation of pathogen-specific effector pathways that function to eliminate foreign pathogens or pathogen infected host cells(32,44). The structural feature of a foreign pathogen that allows an adaptive immune response to be mounted is called an antigen. Recognition of antigens by host cells is further dependent on small, distinct regions of the antigen called epitopes, or antigenic determinants(45).

There are two predominating cell types that constitute adaptive immunity, which include T- and B-lymphocytes and antigen presenting cells (APCs). T-lymphocytes, or T-cells, express unique antigen-binding receptors in their membranes called T-cell receptors (TCRs). The repertoire of TCRs is diverse and each can bind to a specific foreign peptide following antigen presentation by an APC(32). The most common APCs are dendritic cells, macrophages, B-cells, and epithelial cells. These cells express proteins referred to as the major histocompatibility complex (MHC), which are divided into class I MHC molecules, found on all nucleated cells, or class II MHC molecules, which are found on specific immune cell subsets. Importantly, MHC class I molecules present endogenous peptides, while MHC class II present exogenous (extracellular) antigen (peptides) to T-cells(32). An MHC-antigen complex is formed and functions to activate TCRs, allowing the T-cell to further mediate the immune response by releasing cytokines and eventually differentiating into either a cytotoxic (CD_8+ T-cell) or helper (Th) T-cell (CD_4+ T-cell). These mechanisms will now be discussed in the context of SARS-CoV-2.

1.3.4 SARS-CoV-2 immunopathogenesis

SARS-CoV-2 initially establishes infection in the upper respiratory tract via interaction with the human ACE2 receptor, which is expressed on the apical surface of epithelial cells. If disease is severe, the infection may progress to the lungs, where additional ACE2 receptor binding takes place. In the lungs, SARS-CoV-2 increases proinflammatory cytokine secretion, alters vascular leakage/tone, and disrupts mechanisms and cell types that govern lung homeostasis, such as alveolar macrophages and surfactant producing epithelial cells. Epithelial cells that first sense SARS-CoV-2 in the lungs mount a strong immune cascade, characterized by increased production/secretion of cytokines, chemokines, and growth factors to stave off the acute infection(46). Various immune cells (neutrophils, lymphocytes, macrophages) are then

recruited to begin mounting the innate immune response. Increased neutrophil levels drive polarization to an inflamed state by releasing numerous chemokines, thereby attracting additional APCs. Alveolar macrophages (AMs) can also be shifted to an M1 pro-inflammatory phenotype in the presence of interferon gamma (IFN-γ), which leads to further secretion of proinflammatory cytokines TNF-α, IL-1β, and IL-6(46,47). Furthermore, PAMPs initiate TLR signal transduction, where ssRNA fragments from the SARS-CoV-2 genome interact with TLR7/8 and NFκB, resulting in the transcriptional activation of proinflammatory cytokines (such as TNF-α, IL-6, and Type 1IFNs)(48). This increased inflammatory state leads to pryoptosis, which is inflammation-induced cell death. Pyroptosis of the alveolar epithelial cells releases DAMPs that interact with TLRs expressed on endothelial cells, causing further production of proinflammatory cytokines and chemokines. Prolonged, elevated levels of circulating cytokines can lead to a syndrome termed “cytokine storm” or “cytokine release syndrome”, which causes immune cell hyperactivation and systemic inflammation.

Studies investigating the immune profiles of bronchoalveolar lavage (BAL) samples in individuals with COVID-19 demonstrate elevated levels of neutrophils as well as dysregulated levels of biomarkers, including the chemokines CC motif ligand 20 (CCL20), CXC motif ligand 1 (CXCL1), CXC motif ligand 10 (CXCL10), proinflammatory cytokines TNF, IL-6, IL-8, IL-10, and IFN-γ, and markers of endothelial damage/transformation such as intercellular adhesion molecule 1 (ICAM-1), vascular cell adhesion protein 1 (VCAM-1), vascular endothelial growth factor (VEGF), D-dimer, Angiopoietin 1-7, and E-selectin(49–51).

It has been shown that the SARS-CoV-2 S protein triggers disruption of the endothelial and epithelial glycocalyx layer, which provides critical barrier function by protecting cells from shear stress(52). Additionally, SARS-CoV-2 contributes to thromboinflammation and endothelial

cell activation, both of which are shown predictors of disease outcome. The endothelial adhesion biomarkers ICAM-1 and VCAM-1 increase in circulation during COVID-19 infection, suggesting possible shedding of adhesion molecules and a highly inflamed endothelium during disease(53,54). Delineating the extent to which the vascular tone (vascular permeability and homeostasis) is affected in the pulmonary endothelium is critical for uncovering the immunopathological mechanisms that govern disease outcome. Understanding the interplay between inflammatory and endothelial biomarkers during various COVID-19 disease states may allow the development of rapid assessment devices to expedite triaging of sick patients.

Many of the current SARS-CoV-2 vaccine platforms were designed to stimulate the humoral immune response, characterized by the secretion of circulating IgA, IgG, and IgM neutralizing antibodies. Recent studies also suggest that messenger RNA (mRNA) vaccines induce higher anti-RBD antibody levels than natural immunity against SARS-CoV-2(55). Although circulating neutralizing antibody levels are effective at staving off severe disease caused by the virus, it is important to understand the role of adaptive immunity in controlling SARS-CoV-2 infection. The adaptive immune response to COVID-19 begins with a marked increase in cytotoxic CD_8+ T-cells, which remain elevated from one week following infection and peak at roughly the 14 day mark(56). These cytotoxic T-cells are responsible for controlling viral infection by killing virus-infected cells and also produce a suite of effector molecules, such as the antiviral cytokine IFN-γ(56,57). In contrast, patients with acute COVID-19 infection may display decreased levels of CD_8+ T-cells, a phenomenon known as lymphocytopenia, which is often associated with increased inflammation, severe disease, and death(58).

Effective, long-term viral control following COVID-19 infection also depends on the activation of CD_4+ T-cells. These cells have been found in greater numbers than CD_8+ T-cells

during COVID-19 infection, have been shown to increase over time, and are also linked to milder diseases in acute and convalescent cases(56,59). The polyfunctionality of CD_4+ T-cells is also advantageous during viral disease. For example, SARS-CoV-2 specific CD_4+ Th1 cells produce IFN-γ, TNF-α, and IL-2, which all play important antiviral roles during early infection(59). The CD_4+ Th1 cells also differentiate into T follicular helper (Tfh) cells, which assist in providing instruction to B-cells to maintain long-term humoral immunity.

Understanding the interplay between the subsets (CD4+ and CD_8+ T-cells) of the adaptive immune system and innate immunity is critical to obtain a broader picture of the various SARS-CoV-2 disease states. Research efforts are needed to explore novel methods of stimulating both humoral and adaptive immunity with vaccination and therapeutics, especially as the virus continues to mutate into increasingly transmissible forms in the population. This topic will be covered in the next two sections.

1.3.5 Variants of concern (VoCs)

Central to the COVID-19 pandemic has been the dynamic and rapidly evolving viral variant landscape. Since the onset of the COVID-19 pandemic in December 2019, there have been several mutations to the SARS-CoV-2 genome. The emergence (and re-emergence) of these viral variants has led to multiple pandemic waves, each distinct from the previous. The ancestral variant of SARS-CoV-2, which was first discovered in the Chinese city of Wuhan (Hubei province) was aptly named Wuhan-Hu-1 (referred to in this thesis as 'Wuhan virus'), and demonstrated 80% sequence homology with severe acute respiratory syndrome (SARS), the coronavirus responsible for the 2002-2004 outbreak in China(60). As novel variants of SARS-CoV-2 emerged, they were categorized by public health authorities as being a variant under monitoring (VUM), a variant of interest (VOI), or a variant of concern (VOC). A VUM is a

variant being monitored to assess its mutations and characteristics; a VOI has mutations and/or characteristics that are being monitored to assess their potential risk to public health; and a VOC has mutations and characteristics that pose a significant threat to public health(61).

In November 2020, the Alpha variant (B.1.1.7) of SARS-CoV-2 was the first to be identified as a VOC and was ~29% more transmissible than the original Wuhan virus. Shortly after the Alpha variant began driving global case numbers, the Delta variant (B.1.617.2) arose as the second VOC in late 2020. Delta was a highly mutated variant compared to the Wuhan virus, and was estimated to be 97% more transmissible(62). The Delta variant profoundly shifted the COVID-19 pandemic towards increased case numbers and severe cases, hospitalizations, and deaths. As Delta replaced Alpha as the dominating global variant, hospital intensive care units (ICUs) and emergency rooms were flooded with critically ill COVID-19 patients, severely restricting resources, and hospital beds for preexisting patients. By late 2021, a new VOC emerged in South Africa, which was termed the Omicron variant (B.1.1.529). The Omicron variant was flanked with a multitude of genetic and protein-level mutations compared to previous VOCs, leading to rapid global dissemination of the virus. Although Omicron was generally regarded as being a less severe variant of the virus, the sheer number of infections and high transmissibility (reproduction number for Omicron=3.4) led to unprecedented spikes in cases and deaths, especially in unvaccinated and medically vulnerable populations(63). The rapid evolution of the SARS-CoV-2 virus necessitated multiple rounds of vaccination due to immune evasion and instances of antibody waning, which will be discussed in the next section(s).

1.4 Immune evasion and vaccination

1.4.1 Mutations and selective pressure

Mutations in SARS-CoV-2 occur during viral replication where thousands of protein-level and genetic mutations have occurred since the beginning of the pandemic. Thankfully, many of these mutations are innocuous in nature; however, some mutations have equipped the virus with the ability to evade host immunity conferred by vaccination and previous infection as well as increasing transmissibility. The majority of COVID-19 mutations that have led to a more virulent virus, both in infectivity and severity, are located within the spike protein(64). Mutations in this region are more likely to shift the antigenic profile of the virus away from immunity previously acquired by vaccination or previous infection, a phenomenon known as “immune escape”. Immune escape coupled with waning protection from circulating neutralizing antibodies can lead to breakthrough infections, where fully vaccinated individuals become reinfected. As SARS-CoV-2 continues to mutate, increased instances of booster doses have also been required to maintain protection from the virus, especially for older individuals and those with underlying health conditions.

When the Omicron (B.1.1.529) variant began to spread around the globe, healthcare systems saw a massive influx in cases, hospitalizations, and deaths. This was partially explained by the highly mutated nature of the virus, which contained roughly 30 amino acid (aa) substitutions, 6 aa deletions, and 3 aa insertions in the spike protein, compared to ancestral strains(65). This caused rapid spread of the virus and drove rates of vaccine-variant mismatch, where earlier iterations of the SARS-CoV-2 vaccine did not offer robust protection from infection with novel strains. The extensively transformed Omicron spike contributed to increased binding interaction with ACE2 and the NTD, while also causing active interference in

recognizing vaccine and infection-induced antibodies, the surrogate marker of protection to COVID-19(66).

The spike protein facilitates viral binding and host cell entry and has been the main target for neutralizing antibodies, and thus vaccine development. Spike is also the component of SARS-CoV-2 that is incorporated into both mRNA and adenovirus-based vaccines(64,67), which will be discussed in the next section. Most mutations in spike occur in the S1' region where the N-terminal domain (NTD) and C-terminal domain (CTD) comprise the receptor binding domain (RBD), which interacts with human ACE2 receptors(68). Below is a table (Table 1.3) summarizing the main spike mutations observed in VoCs in relation to the Wuhan strain since the beginning of the COVID-19 pandemic.

Table 1.3 Outlining the primary SARS-CoV-2 variants and their respective genetic mutations in the Spike protein region compared to the Wuhan strain. This table was adapted from the European Centre for Disease Prevention and Control(69).

SARS-CoV-2 Variant	Genetic Mutation	Region on Spike Protein	Date of Emergence
Alpha (B.1.1.7)	E484K, N501Y, D614G	RBD	Sep 2020
Beta (B.1.351)	E484K, N501Y, D614G, K417N	RBD	May 2020
Gamma (P.1)	E484K, N501Y, D614G, K417T, H655Y	RBD	Feb 2021
Delta (B.1617.2)	D614G, L452R, T478K, P681R, N501Y, G339D, S371L, S373P, S75F, N440K	RBD, NTD, and furin-cleavage site on the S2' region of spike	June 2021
Omicron (B.1.1.529)	A67V, Δ69-70, T95I, G142D, G339D, G496S, Δ143-145, Δ211, L212I, ins214EPE, N440K, G446S, G496S, S477N, T478K, T547K, Q498R, Q493K, Q439R, Q954H, E484A, Y505H, D796Y, N769K, P681H, N764K, N856K, N969K, L981F	NTD and RBD	Dec 2021
Omicron BA.2 (B.1.1.529.2)	T191, A27S, V213G, S371F, T376A, D405N, R408S	NTD and RBD	Jan 2022
†Omicron BA.4/BA.5 (B.1.1.529.4/.5)	L452R, F486V, R493Q	NTD and RBD	Jan-Feb 2022
Omicron BQ.1	K444T, N460K	NTD and RBD	Oct 2022
Omicron XBB.1.5	N460K, F490S	NTD and RBD	Jan 2023
Omicron BA.2.86 "Pirola"	*Unknown	*Unknown	Aug 2023

†: grouped together as spike mutations were identical for BA.4 and BA.5.
*: given the recency of this variant, the mutational profile and specific regions of spike are still unknown
Abbreviations: ins: insertion, Δ: mutation

Omicron quickly replaced Delta as the dominating global variant in late 2021 and was said to infect 3-6 times as many people as Delta(70). Scientists believe that the Omicron variant may have evolved mutations in one person, as part of a long-term prolonged infection(71). Interestingly, Omicron has persisted in the population and all novel variants appear to be sublineages of the ancestral Omicron (B.1.1.529) variant. Just as Omicron abruptly replaced Delta in December 2021, a novel Omicron sublineage called Pirola (BA.2.86) emerged in August 2023, which contains greater than 35 amino acid changes compared to the recently circulating XBB.1.5 Omicron sublineage. As with previous VoCs, the question remains as to whether current vaccine models will be protective against emerging sublineages. In the next section, mRNA vaccines will be discussed as well as proposed alternative vaccination methods aimed at improving long-term, robust protection from SARS-CoV-2.

1.4.2 Messenger RNA (mRNA) vaccines

Pivotal to the COVID-19 pandemic was the rapid development and global administration of SARS-CoV-2 vaccines. Since the beginning of the pandemic in December 2019, more than 5.55 billion people worldwide (~72.3% of the global population) have received a COVID-19 vaccine, which is equal to greater than 13 billion doses administered. The rapid mobilization of government leaders, academia, and the pharmaceutical industry working towards a vaccine resulted in an unprecedentedly expedited timeline for vaccine rollout and global distribution. Historically, vaccine development could take 10-15 years before entering the public, but thanks to accelerated emergency approval and review timelines, the first COVID-19 vaccines began rolling out in December 2020(72,73). Prior to this, the fastest that a vaccine has been developed was for mumps in the 1960s; this process took four years(72). This scientific achievement

redefined the timeline for vaccine rollout, while also demonstrating that vaccines could be developed rapidly without compromising safety and efficacy. The first vaccine developed and approved for emergency use was from Pfizer, in partnership with the German biotech company BioNTech, and was soon followed by a similar platform vaccine from Moderna. Both companies used a novel mRNA platform for delivering the vaccine. The primary COVID-19 vaccine platforms that were granted emergency use approval included: i) protein subunit vaccines: Covovax (Serum Institute of India) and Nuvaxoid (Novavax); ii) non-replicating viral vector vaccines: Convidecia™ (CanSino), Jcovden (Janssen), Vaxzevria (Oxford/AstraZeneca), Covishield (Serum Institute of India), and Sputnik V (Gamaleya Research Institute of Epidemiology and Microbiology); iii) inactivated vaccines: Covaxin (Bharat Biotech), Covilo (Sinopharm), and CoronaVac (Sinovac); and iv) RNA vaccines: SpikeVax® (mRNA-1273-Moderna) and Comirnaty® (BNT162b2- Pfizer-BioNTech)(74,75). Although each of these vaccines played an integral role in reducing the global burden caused by the COVID-19 pandemic, the focus for the remainder of this section will be on the mRNA vaccines, which were heavily administered and redeveloped to accommodate the mutating virus. Importantly, additional vaccines not listed here were approved or are in a clinical trial stage of development.

mRNA vaccines rely on synthetic messenger ribonucleic acid (mRNA) encoding the spike protein of SARS-CoV-2, which upon receipt, causes the natural production of spike protein to be displayed on host cells. This leads to the broad production of circulating neutralizing antibodies, which confers protection against COVID-19 similar to the protection acquired following natural infection. These vaccines replace the uridine (U) nucleotide with a pseudouridine (ψ), which is thought to reduce the immune response to the mRNA. The mRNA is

delivered using a fatty lipid nanoparticle system, composed of a phospholipid, cholesterol, ionizable lipid, and polyethylene glycol (PEG) lipid(76,77).

The durability of mRNA vaccines has been their largest limitation thus far. mRNA vaccines are administered intramuscularly (IM) in a two dose prime-boost format. Following the first dose series, the Comirnaty® vaccine was 91.3% effective through six months of follow-up and up to 96.7% effective against severe disease(78). Despite this, beyond six months of follow-up, neutralizing antibody titers and IgG levels begin to decrease, especially in individuals who are immunocompromised, older than 65, or are male(79,80). Similar statistics were observed for the Spikevax® mRNA vaccine from Moderna. Decreasing antibody titers, coupled with a rapidly mutating virus, necessitated multiple rounds of booster doses and vaccine re-development to maintain protection against novel COVID-19 variants, where some individuals received up to five doses of an mRNA vaccine. As novel variants such as Omicron emerged, cases climbed as the heavily mutated virus was able to evade immunity. For example, neutralizing activity against Omicron following full vaccination (2+ doses) with Comirnaty® dropped 33-fold compared to the B.1 (D614G spike mutation) variant, and 74-fold for Spikevax®(81).

To obviate the need for continually receiving booster doses following COVID-19 vaccination, it is thought that moving towards alternate platforms may be beneficial. Currently being investigated are intranasal (IN) vaccines, which are more likely to provide sterilizing immunity at the site point of infection (the upper respiratory tract). Sterilizing immunity stimulates the secretion of neutralizing antibodies (largely IgA) at the mucosal site of infection, including the nose and throat, rather than solely relying on the systemic response induced by IM vaccines(82). This approach may be more effective at blocking infection and potentially reducing transmission. Currently, IN vaccine candidates include virus-vectored vaccines,

recombinant subunit vaccines, and live attenuated vaccines which are in varying stages of clinical trial development(83,84).

1.5 Clinical Presentation of COVID-19

1.5.1 Risk factors that govern disease severity

The clinical spectrum of COVID-19 is variable in the general population. A portion of infected individuals (17.9-33.3%) remain asymptomatic and most asymptomatic cases occur in children and young adults(85,86). Typical clinical presentation for symptomatic COVID-19 is characterized by fever, cough, shortness of breath, nausea, fatigue, sore throat, and anosmia, with symptoms generally subsiding within a few days to a few weeks. Some infected individuals may experience persistent symptoms that can last greater than four weeks following infection, a condition termed “long COVID-19”, which will be discussed in depth in the next section(87). Although vaccines are effective at preventing severe disease, groups such as the elderly, those with underlying health conditions, or immunocompromised individuals may be at risk of developing clinical illness.

A proportion of patients infected with SARS-CoV-2 will develop severe disease, where approximately 15-20% of cases require hospitalization and 3-5% require critical care(88). For those who develop critical COVID-19, progression to acute respiratory distress syndrome (ARDS) or ventilation occurs roughly 10 days post symptom onset(89). Age is perhaps the greatest risk factor for developing a severe COVID-19 infection, where those aged 85 years and older are at the highest risk. Comorbidities such as diabetes, obesity, hypertension, and COPD also predispose individuals to developing a severe infection. Severe COVID-19 manifests as a pneumonia-like infection characterized by respiratory failure, septic shock, and multi-organ failure, as well as a pronounced level of viremia, which occurs when SARS-CoV-2 virus enters

the bloodstream. The immunological phenotypes observed during a severe COVID-19 infection include an overreactive adaptive immune response, characterized by reduced T follicular helper (Tfh) cells in circulation and hyperreactive CD_4+ and CD_8+ T-cells(90). Hallmark biomarker profiles have also been identified in critically ill patients. During the state of dysregulated immune function observed during severe infection, biomarkers associated with vascular damage (such as D-dimer, GDF-15, and sICAM-1) as well as proinflammatory cytokines (IL-1, IL-2, IL-6, and IL-8 TNF-α) are elevated in critically ill patients(91). Interestingly, some individuals recovering from COVID-19 may encounter symptoms that do not resolve after the initial infection, a difficult to diagnose complication referred to "long COVID-19".

1.5.2 Post-Acute Sequelae of SARS-CoV-2 (PASC), or "long COVID-19"

Individuals with a SARS-CoV-2 infection may develop symptoms that persist beyond the phase of acute infection. COVID-19 symptoms that linger for greater than four weeks following the initial infection is termed long COVID-19 (referred to as "LC" for the remainder of this dissertation) and occurs in roughly 10-30% of infected individuals, although this number varies in the literature(92). LC occurs in patients of all ages; however, those aged 36 to 50 years are the most afflicted, while a female gender also predisposes infected patients to developing prolonged symptoms. Acute COVID-19 tends to involve the upper respiratory tract and lungs and follows a similar disease course in mild cases. In contrast, LC has been described with greater than 200 symptoms and impacts multiple organ systems, including the heart, lungs, immune system, pancreas, gastrointestinal tract, neurological system, kidney, spleen, blood vessels, and reproductive system. Multiple causes for LC have been proposed, such as persisting reservoirs of SARS-CoV-2 in tissues, autoimmunity, immune dysregulation (potential reactivation of dormant

viruses), microvascular disruption, and endothelial impairment, among others(93–95). Given the myriad of symptoms and probable causes, LC is difficult to clinically diagnose and treat.

A growing body of literature has now linked LC to endothelial dysfunction. The endothelium is a single cell layer that lines every blood vessel, and when the system is disrupted, can affect organ/tissue homeostasis, inflammation, vascular tone, and oxidative stress. Angiogenesis may therefore represent a key pathophysiological mechanism for targeting the diagnosis of LC. A blood biomarker study revealed that the biomarkers angiopoietin 1 (ANG-1) and p-selectin (P-SEL) were highly correlated to LC and that these markers provided LC classification accuracy at 96%(96). A separate paper found that at three months after discharge, cytokines related to vascular injury/repair, such as ICAM-1 and VCAM-1, had not returned from an elevated state in patients with LC compared to those in healthy controls at the same timepoint(97). In addition to increased vascular/endothelial activity, persistent SARS-CoV-2 viral antigen in different tissues may also play a key role in diagnosing LC.

The idea of viral persistence in "sanctuary tissues" has been previously demonstrated in Ebola virus, where viral proteins can remain, and become reactivated, despite being cleared from the blood. One plausible explanation for LC is that a similar phenomenon is occurring following a COVID-19 infection. Persistent SARS-COV-2 and latent pathogen reactivation may contribute to experiencing prolonged symptoms(98). One study detected viral antigen (spike, nucleocapsid, or the S1 subunit) in > 70% of patients experiencing persistent COVID-19 symptoms and spike protein was the most abundantly detected(95). Interestingly, the same study found that patients who reported gastrointestinal or neuropsychiatric symptoms were more likely to exhibit measurable, persistent viral proteins. To fully delineate, and consequently diagnose/treat LC, continued investment in LC research and staged clinical trials is necessary. The United States

National Institutes of Health (NIH) *ClinicalTrials.gov* currently lists 386 trials pertaining to Long COVID-19 and among those, 94 are interventional studies and 12 are testing pharmacological interventions(99). To augment our understanding of LC in younger individuals, one of the secondary objectives of this study was to compare the biomarker levels in students experiencing LC symptoms with students whose symptoms were relieved following acute infection.

1.6 Seroprevalence studies

The objective of a seroprevalence study is to estimate the fraction of individuals within a population infected with a particular infectious agent by drawing blood and using the serum to measure antibody levels, hence the name, sero- (relating to serum) and prevalence- (commonness). The results of epidemiological seroprevalence studies are generally stratified based on age, sex, and particular risk factors for a given disease, such as obesity, asthma, COPD, or diabetes. The scientific community, policy makers, and public health leaders may use these results to evaluate the magnitude of an outbreak and establish public health measures and control strategies accordingly. In the context of SARS-CoV-2, a common enzyme-linked immunosorbent assay (ELISA) method was used to discern antibodies induced by previous infection from vaccine induced antibodies by measuring the levels of anti-nucleocapsid (anti-N) antibodies(100). Measuring antibodies produced by the spike protein of the virus, versus the spike-like particles incorporated in many of the mRNA vaccine platforms, would not allow the estimation of previous infection. Instead, by measuring antibodies against N (a structural protein in SARS-CoV-2), it is possible to differentiate between infection and vaccine-induced antibodies.

A common theme among COVID-19 seroprevalence studies is the age ranges most likely to have been previously infected. Prior to the arrival of the infectious Omicron variant, seropositivity ranged from 10-30% in the general population, with younger individuals (17-26 years old) most likely to exhibit SARS-CoV-2 seropositivity(101,102). In a seroprevalence study conducted in Canada, 9% of individuals had antibodies against SARS-CoV-2 in 2021 and by March of 2023, 76% of individuals were seropositive(103). The spike in infection-induced antibodies was most pronounced in younger individuals aged 18-29. This young demographic represents a unique cohort for understanding infectious disease dynamics. Most campuses contain a diverse student body, where students travel from different areas of the world. This poses a threat of introducing novel variants of SARS-CoV-2 to the campus, as well as to any cities or communities in proximity. In settings such as high schools, colleges, or universities, the average age is significantly younger than that of the general population and the frequency of social interactions are also increased. During the lockdown phases of the COVID-19 pandemic, many campuses enforced vaccination mandates, curfews, social distancing, and masking policies; limited social gathering sizes/interactions; and transitioned to remote lectures in an attempt to curb the spread of the virus(104). Additionally, campus housing such as dorms, residences, and student houses are characteristically crowded, with housemates living near one another and at times in shared rooms.

The student age range (18-35) was therefore a suitable target for this project and provided valuable information regarding the broader immune response to COVID-19 in young persons as well as whether this group is afflicted by long COVID-19 similarly to older groups. This cohort also adds to our understanding of how to manage pathogenic threats on campus and provides a

seropositivity baseline for the province, as Dalhousie University contains the largest student body in Nova Scotia and is centered in the province's most populated metropolitan area.

1.7 Rationale and Objectives

As of 2021, there were 210,863 COVID-19 papers published, which covered a range of disciplines from biology and immunology to social factors, behaviour, economics, and global trade(105). An extensive literature review revealed that many COVID-19 studies neglect to fully interpret the immunological underpinnings and consequences for young individuals following SARS-CoV-2 infection, as this cohort represents a low-risk, generally healthy population. Even less reported is the isolated incidence of COVID-19 infections in a university setting. With that, I investigated various aspects of the immune response to COVID-19 in N=77 university aged students (18-35 years) by conducting a seroprevalence study on the Dalhousie University Halifax campus. This included the levels of antibody waning following infection, the presence or absence of viral antigen in the bloodstream, and social/demographic trends followed by university students prior to study enrollment. Additionally, I measured a variety of immune biomarkers in serum and sub-stratified students based on their long COVID-19 status to explore relationships between the two. To determine whether students were positive for COVID-19 during enrolment, rapid antigen testing was performed. All nasal/throat samples were also banked, and reverse transcriptase-quantitative PCR (RT-qPCR) was performed to determine whether rapid tests were comparable to the gold standard PCR, and whether any asymptomatic cases were missed during enrolment. Thus, this project will test the following hypothesis: 1) a varied SARS-CoV-2 immunological history elicits a broad systemic immune response and heightened endothelial biomarker signatures in long COVID-19 subjects in a young population.

CHAPTER 2: MATERIALS AND METHODS

2.1 Ethical clearance

To obtain biological samples for this study (blood, serum, plasma, and throat swabs), non-interventional research ethics approval was required before subject recruitment could commence. The Nova Scotia Health Research Ethics Board (NSH-REB) approved the study entitled "Investigating Previously Infected SARS-CoV-2 Individuals in a University Setting for Antibody Waning and Variant Incidence: *A Cross-Sectional, Seroprevalence Study*" (ROMEO file #: 1028052) in May 2022. Subject recruitment and enrolment began on 2022-09-05 and closed on 2022-10-25. Students were recruited using a flyer recruitment poster distributed by email and on posterboards around the Dalhousie campus. Inclusion criteria for the study included any Dalhousie University registered students (undergraduate, graduate, professional studies, post-doctorate, or resident) between the ages of 18-35. Participants who did not satisfy the age requirements were not enrolled in this study. Participants who met inclusion (N=77) were scheduled for a one-time study appointment at the Tupper Medical Building, where informed consent was obtained by the sub-investigator. The study overview is displayed below (Figure 1.7).

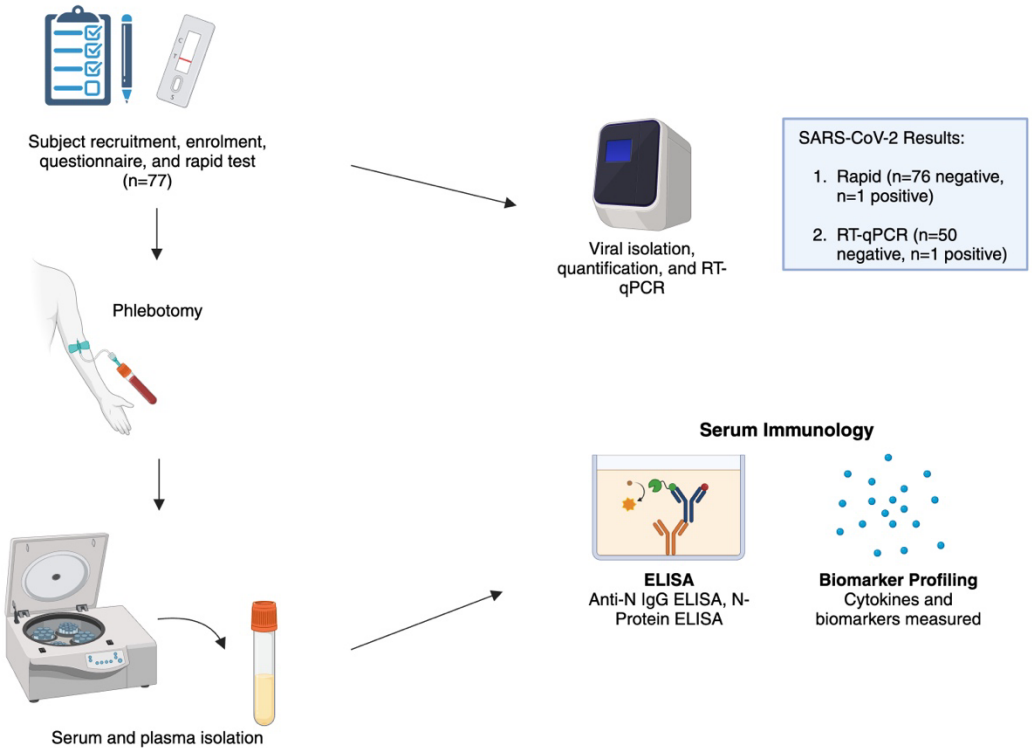

Figure 2.1 Graphical overview of the study procedure and primary methods used.

Students were informed of the study via email and campus-wide poster canvasing. Interested students were directed to book a one-time study visit at the Tupper Medical Building where a member of the research team met with the prospective participant. Enrolment then proceeded with consenting, a questionnaire (demographic, social, COVID-19 related), rapid testing, and a venous blood draw. Serum was isolated from the blood and subjected to various immunological assays such as biomarker profiling and ELISAs. Additionally, the rapid test samples were banked, and viral RNA was isolated. Real-time quantitative PCR (RT-qPCR) was then performed on these samples. Image created with BioRender.

2.2 Rapid Antigen Testing and Questionnaire

To protect the researchers, students, and phlebotomists who were assisting with enrolment, each prospective participant was required to complete a rapid antigen SARS-CoV-2 test (Abbott Panbio™ Ag Rapid Test Device) prior to enrollment. At the time of enrollment, the most accurate method of rapid testing was determined to be swabbing the back of the throat, tonsils, and tongue. Students were therefore directed to perform a 10-15 second throat swab

before placing five drops of buffer in the lateral flow cartridge. Importantly, those who were uncomfortable or unable to swab the throat proceeded with nasal swabbing for 5-10 seconds per nostril. The rapid test result was recorded, and the remaining buffer (250µl) was placed in a 1.5 mL Eppendorf tube (Eppendorf Tubes®, DNA LoBind Tube 1.5 mL), labeled with the corresponding study code, and banked at -80°C.

Following the rapid testing procedure, participants were asked a series of social, behavioral, and COVID-19-related questions before proceeding to phlebotomy. To be eligible for study compensation, participants were required to satisfy the following requirements: signing the informed consent form (ICF), completing a rapid antigen test, completing the questionnaire, and providing an 8CC sample of venous blood. Demographic information for the study cohort can be found in Appendix I.

2.3 Phlebotomy

Phlebotomy services were performed by trained phlebotomists from Nova Scotia Health (NSH) at a small, temporary clinic in laboratory 10A in the Tupper Medical Building. Blood was obtained using 20-, 21-, or 25-gauge butterfly assembly needles (BD Vacutainer® Safety-Lok™ Blood Collection Set) with separate, attachable holders (BD Vacutainer® One-Use Holder). Four milliliters of blood were apportioned into both EDTA tubes (BD Vacutainer® Blood Collection Tubes with K2 EDTA; lavender cap) and serum tubes (BD Vacutainer® Blood Collection Tubes with silica-coated activator; red cap). Collected blood was labelled with a unique study code and left undisturbed in an upright configuration for one hour before being transferred to a refrigerator (4°C) prior to centrifugation. At the end of each study day, the blood tubes were transferred to a biosafety-level 2+ (BSL2+) laboratory (10A, Tupper Medical Building) where they were placed

in a benchtop centrifuge (Thermo Scientific™ Sorvall ST4 Plus) and spun for 15 minutes at 1500 x G at 4°C with the brake set to two. The samples were transferred to a Class IIA biosafety cabinet (BSC) and 500µl of serum and plasma were apportioned into pre-labelled 2mL cryogenic vials (Corning Brand) at -80°C. The 8CC venous blood sample from each patient yielded approximately three serum-containing vials (500µl each) and three plasma-containing vials (500µl each).

2.4 Viral RNA Isolation

The nasal/throat swab samples were further used for viral RNA isolation (Life Technologies™ MagMax™ Viral RNA Isolation Kit). First, samples were pulled from the -80°C freezer and thawed on ice. Carrier RNA (22µl) was added to 4.4mL of lysis/binding solution concentrate and 4.4mL of isopropanol to create the lysis/binding solution. The bead mix was then prepared by adding 110µl RNA binding beads to 110µl of lysis/binding enhancer; this mixture was vortexed and placed on ice. Two wash buffers were also prepared by adding absolute ethanol and isopropanol, respectively.

Samples were then prepared by combining 200µl of throat/nasal isolate to 200µl of nuclease free water (Invitrogen™ Ambion Nuclease-Free Water) and 802µl of prepared lysis/binding solution in a 1.5mL Eppendorf tube. To this mixture, 20µl of the previously prepared bead mix was added before being briefly vortexed and placed on a shaker (Fisherbrand™ Microplate Shaker) for four minutes at a speed of 60. The samples were then briefly centrifuged (~2 sec) and placed in a magnetic rack for three minutes to capture the beads. The supernatant was discarded and two washes with each wash buffer (wash buffer 1 and 2) was performed, with vortex and pull-down steps between each. Following the final wash, the beads

were left to dry for two minutes before 50µl elution buffer was added to each. The samples were then vortexed for four minutes before being placed in the magnetic rack. It was at this stage the eluted RNA was retained and placed in separate, labeled 1.5mL Eppendorf DNA LoBind tubes and stored at -20°C.

2.5 Viral RNA Quantification

Following viral RNA extraction, levels of viral RNA were quantified for each sample using the Qubit™ 4 benchtop fluorometer (ThermoFisher Scientific, Qubit™ 4 Fluorometer). Each sample was prepared using a broad range RNA detection kit (Qubit™ RNA BR Assay Kit, lot #: 2181628). A working solution was first prepared by adding 14µl dye to 2786µl buffer. The two standards were then prepared by adding 10µl of each standard to the appropriate tube with 190µl of the previously prepared working solution, for a total volume of 200µl. To prepare each sample, 2µl of isolated RNA was added to 198µl of working solution in a 1.5mL Qubit™ specific assay tube. Once standards and samples were prepared, they were briefly vortexed (~2-3 sec) and incubated at room temperature for two minutes before being read on the fluorometer.

2.6 RT-qPCR of isolated RNA

Isolated viral RNA samples were prepared for reverse transcriptase-quantitative polymerase chain reaction (RT-qPCR) processing using the Luna® SARS-CoV-2 RT-qPCR multiplex assay kit (New England BioLabs, Ipswich, MA). First, the assay mix was prepared for n=96 samples (including a positive and negative control; samples were run as duplicates) by combining 517µl of master mix containing UDG (uracil-DNA glycosylase) with 206.8µl SARS-

CoV-2 primer-probe mix (primer/probe sequence included in Appendix II), and 310.2µl of nuclease-free water on ice.

Next, 10µl of prepared assay mix was aliquoted into 96 qPCR wells in a 96-well qPCR plate. Each test sample well then received 10µl of test sample while the positive control well received 2µl of SARS-CoV-2 positive control (SARS-CoV-2 nucleocapsid gene cloned into a plasmid) with 8µl of nuclease free water. Finally, the negative control was prepared by adding 10µl nuclease free water to the assay mix in the negative control well. Each reaction contained a total reaction volume of 20µl. The contents of each well were then pipetted to ensure components were mixed.

The plate was then sealed with optically transparent film and centrifuged for 1 minute at 3,000 rpm. The RT-qPCR machine (Applied Biosystems 7500 fast real-time qPCR machine, Waltham, MA) was programmed (7500 software version 2.3) with the following thermocycling protocol (Table 2.1):

Table 2.1 RT-qPCR thermocycling protocol for quantifying isolated SARS-CoV-2 viral RNA.

Cycle Step	Temperature (°C)	Time	Number of Cycles
Carryover prevention	25	30 seconds	1
Reverse transcription	55	10 minutes	
Initial denaturation	95	1 minute	
Denaturation	95	10 seconds	45
Extension	60	30 seconds	

Table adapted from New England Biolabs® Luna® SARS-CoV-2 RT-qPCR Multiplex Assay Kit (NEB #E3019S/L)

During the reaction set-up, the following three fluorophores were assigned: VIC (for the N1 target), FAM (for the N2 target), and Cy5 (for the internal control, RNase P target). The primers for this reaction were obtained from two specific regions of the SARS-CoV-2 nucleocapsid gene, which were modified to contain different fluorophores for simultaneous observation on two different channels of a real-time instrument. The RNase P target is included to amplify the human RNase P gene to ensure input material integrity and absence of inhibition, thus serving as an internal control. Primer sequences for the N1, N2, and internal control may be found in Appendix I.

2.7 Nucleocapsid (N-protein) ELISA

Human SARS-CoV-2 N ELISA kits (ThermoFisher Scientific, Waltham, MA) were obtained and stored at -80°C. The ELISA protocol was performed in a Class IIA BSC inside a BSL2+ laboratory at Dalhousie University. Frist, a 1X wash buffer was prepared following a 20-fold dilution of the 20X wash buffer concentrate with ddH_2O. The assay diluent was diluted 5-fold. 100µl of biotin conjugate concentrate was prepared and diluted 80-fold with the previously prepared assay diluent. A standard curve was then prepared by diluting the reconstituted standard provided in the kit in a descending series using the prepared 1X assay diluent. The sample and standards were then added to the 96-well pre-coated microplate (100µl to each well) and duplicates were run for all samples. The plate was then covered and incubated at room temperature with gentle shaking for 2.5 hours on a shaker (Fisherbrand™ Microplate Shaker). The plate was then placed in an automated plate washer (BioTek™ 50 TS Washer) where four washes were completed with 1X wash buffer. Next, 100µl of biotin conjugate was added to each well and incubated for one hour and washed as in the previous step. The Streptavidin-HRP was

diluted 100-fold using 1X assay diluent and 100µl was added to each well before another 45-minute incubation with gentle shaking. The wash was repeated and 100µl of TMB substrate was added to each well with a multichannel micropipette (Eppendorf Research® Plus 12-Channel). The plate was incubated in the dark, at room temperature, with gentle shaking. Finally, 50µl of Stop Solution was added with a multichannel pipette to each well before gentle tapping on the side of the plate to mix. The absorbance was read at 450 nm using a plate reader (BioTek™ Synergy LX), where plate layout and absorbance were selected using Gen5 software (version 3.04).

2.8 Anti-Nucleocapsid IgG ELISA

Human SARS-CoV-2 Anti-N IgG ELISA kits (Abcam, Cambridge, UK) were obtained from a -80°C freezer and transferred to a class IIA BSC. The sample diluent and assay diluent B were diluted 5-fold with ddH_2O. Next, 20 mL of wash buffer concentrate was diluted in 380 mL of ddH_2O, yielding 1X wash buffer solution. The Streptavidin-HRP concentrate was diluted 800-fold with assay diluent. The biotinylated antibody was prepared by mixing 200µl of assay diluent with the antibody concentrate. The provided standard control was serially diluted to create a standard curve (see ab274339 protocol). Once the reagents were prepared, the samples were diluted 1500X with sample diluent; 1µl of serum was added to 1499µl of 1X sample diluent. Next, 100µl of each standard and sample were added to a precoated microplate, with samples being run as duplicates. The plate was covered and incubated with gentle shaking on a plate shaker for one hour at room temperature and the plate was washed four times with 1X wash buffer in a plate washer. 100µl of prepared biotinylated antibody was added to each well with a multichannel pipette before a 30-minute incubation and subsequent washing step. 100µl of

streptavidin-HRP was added to each well with a multichannel pipette and incubated for 30 minutes, followed by a washing step. 100µl of TMB substrate was then added to each well and the plate was incubated in the dark, at room temperature, with gentle shaking for 15 minutes. 50µl of stop solution was added to each well with a multichannel pipette and plates were gently tapped to mix before being read at 450 nm with Gen5 software (version 3.04).

2.9 Biomarker Analysis

A total of 24 distinct biomarkers were grouped and analyzed based on their immunological function. The tailored biomarker panels were measured using the Ella-SimplePlex™ Immunoassay (Bio-Techne, Minneapolis, Minnesota) and selected according to their broad biological role in viral disease and SARS-CoV-2 pathogenesis(51,96). The biomarkers in this study were subdivided based on their specific immunological function during disease and a subset of biomarkers (Table 2.2) were selected for analysis based on their previously documented involvement during long COVID-19. Comparison group serum collected from LC subjects in Saskatchewan [(Age (SD)=45.8 (13.3); N (male)=71 (36%), N (female)=124 (64%)] was also subjected to biomarker analysis and used for intergroup comparisons in the results section. The entire list of measured biomarkers can be found in Appendix 2 (Table A.2.3).

Table 2.2 The biomarker type and relative function during SARS-CoV-2 infection(51).

Biomarker	Type	Role in Infection
Inflammatory:		
CXCL10	Chemokine	Attracts macrophages/monocytes during infection (involved in cytokine storm). CXCL10 is released by monocytes, endothelial cells, and fibroblasts.
IL-15	Cytokine	Progresses septic shock by maintaining natural killer cell populations
TNF-α	Cytokine	Inflammatory– contributes to the progression of acute respiratory distress syndrome
IFN-γ	Cytokine	Provides early defence against viral challenge
IL-6	Cytokine	Contributes to pulmonary inflammation
CCL2	Cytokine	Recruits immune cells and increases inflammation
Endothelial/vascular Repair and/or Transformation:		
ANG-2	Cytokine (proangiogenic factor)	Induces vascular sprouting, upregulated in inflammatory diseases
D-dimer	Fibrin degradation product	Elevated during COVID-19 in the lungs due to increased rate of thromboembolic complications
E-selectin	Adhesion molecule	Marker of endothelial activation
ICAM-1	Adhesion molecule	Regulates endothelial barrier function
VCAM-1	Adhesion molecule	Regulates inflammation associated with vascular adhesion
Neutrophil Degranulation:		
MPO	Peroxidase enzyme	Released by stimulated neutrophils and can increase reactive oxygen species production during infection leading to oxidative stress

Student serum samples were diluted according to their pre-defined panels to the following concentrations: CXCL10, ANG-2, and IL-6 (2:1); CCL-2, IL-15, IFN-γ, and TNF-α (2:1); D-dimer and E-SEL (50:1 dilution); ICAM-1, VCAM-1, and MPO (1:100). All samples were run in triplicate using the Ella SimplePlex™ Immunoassay Runner (V.3.9.0.28) and processed according to the manufacturer's protocol.

3.0 Statistics

All Master data was stored in a password-encrypted Microsoft Excel spreadsheet and statistical analyses were performed using GraphPad Prism 9.3.1 (350) for macOS. Additionally, the ELISA standard curves were interpolated using GraphPad Prism 9. Results with a p-value ≤ 0.05 were considered statistically significant. For the comparison of two groups, a normality test (Shapiro-Wilk test) was first performed to assess the distribution of the data. Based on the result of this test, non-normally distributed data were subjected to a Mann Whitney U test while data following a Gaussian distribution were subjected to an unpaired T-test. Furthermore, for data comparing three or more groups, the one-way analysis of variance (ANOVA) and Kruskal-Wallis tests were used with Tukey's multiple comparisons post-hoc test. For the biomarker analysis, either a Bonferroni correction test or Dunn's multiple comparisons test was used for post-hoc comparison of each group(96). To determine whether there was a relationship between the time since infection and levels of both nucleocapsid protein and anti-N IgG levels, simple linear regression and correlation analyses were used. Simple linear regressions were also performed on the biomarker levels as a comparison between long-COVID-19 symptomatic students and healthy student controls.

CHAPTER 3: RESULTS

Prior to the arrival of the Omicron variant in Canada, the seroprevalence of COVID-19 remained relatively low (0.05% - 9%) as measured using anti-S or anti-N antibody ELISAS(103). However, these percentages increased as the virus continued to mutate and spread throughout the population. By March 2023, seroprevalence reached 76% in Canada, a statistic similar to those found in our study cohort, which included N=77 students aged 18-35 years old. On enrolment, N=50 (65%) of subjects reported previously being infected with COVID-19, as confirmed with either rapid antigen or PCR testing. Following anti-N IgG ELISA testing of serum samples, we found that N=71 (92%) had detectable antibody titers in their serum ($\bar{x}$=34ng/mL, IQR=27.5ng/mL). The level of viral nucleocapsid protein in serum was also measured, and N=27 (35%) of the study population tested positive. These discrepancies will be explored in the discussion of this dissertation.

3.1 Nucleocapsid (N-protein) ELISA and Anti-N IgG ELISA are effective methods for detecting previous COVID-19 infection and levels of antibody waning.

To determine the number of previous infections and levels of antibody waning in our study population, serum-based enzyme-linked immunosorbent assays (ELISAs) were used. First, the SARS-CoV-2 Nucleocapsid protein (N) ELISA was used to elucidate whether lingering viral proteins were present in subject serum. The aim of targeting the N protein was to determine whether diagnosis of previous SARS-CoV-2 infection could be achieved by directly measuring specific antigens of the virus in serum. The N protein is an important RNA-binding structural protein involved in viral genome packaging. The N protein is also highly conserved between other coronaviruses and among COVID-19 variants, thus potentially representing a reproducible detection method in the face of rapidly evolving viral variants(30).

The results indicated that 35% (N=27) of the study population contained measurable levels of N protein in serum ranging from 0.3-9.0 ng/mL (Figure 3.1). Following the first attempt using this assay, it was determined that a standard ELISA serum dilution of 1:4 was too dilute to detect N protein in serum. Following this, subsequent trials revealed that running the samples neat (i.e., no serum dilution) yielded measurable levels of N protein. To validate our findings and to ensure that cross-reactivity and non-specific binding were not occurring with the increased serum concentration, both positive and negative controls were also tested. Three positive controls, which were collected from severely ill COVID-19 patients in a continuing care home and 43 negative controls (collected prior to the COVID-19 pandemic) were used. All positive controls returned measurable N protein levels ranging from 0.9-3.1 ng/mL, while negative controls were measured in a non-detectable range (a concentration < 0.07 ng/mL).

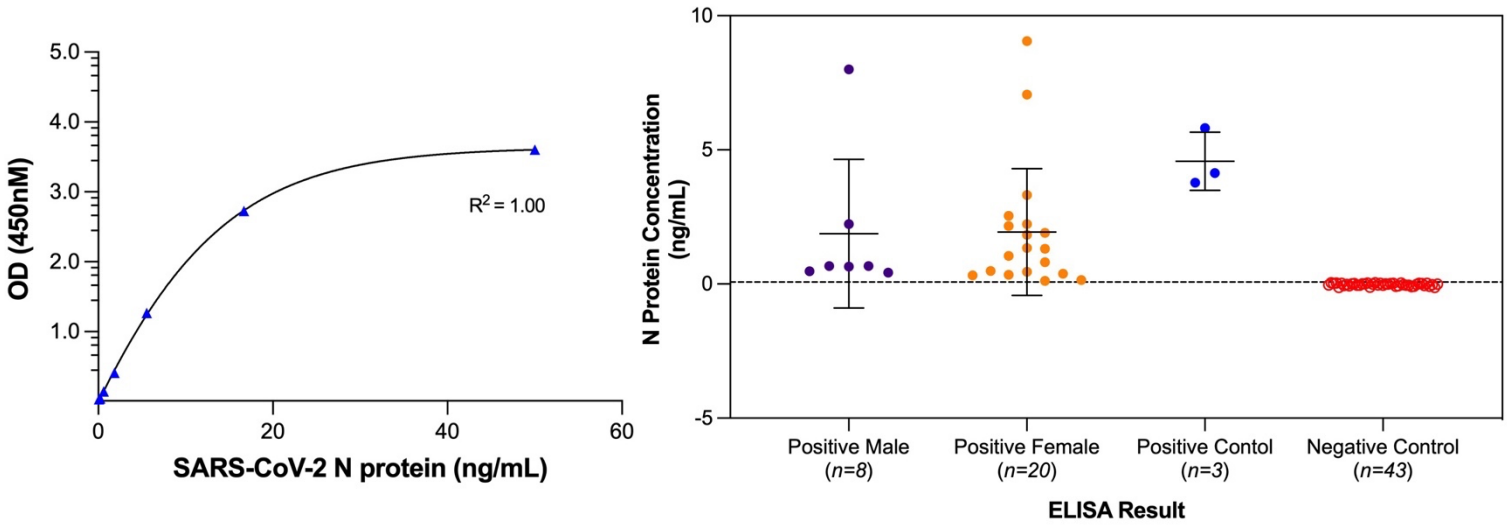

Figure 3.1 ELISA standard curve and serum nucleocapsid protein levels, stratified by sex and control group.

Serum samples reveal measurable N levels for males, females, and positive controls, while the negative control samples did not return measurable levels of N. The seropositivity for male subjects was [(N=7/22 (32%)] and [(N=20/55 (36%)] for females. The dotted line represents the 0.07 ng/mL minimum detection baseline, and the error bars represent the mean ± SD. The figure was generated using GraphPad Prism 9.3.1 (350) for MacOS.

Factors that commonly influence disease outcome such as sex, body mass index (BMI), long COVID-19 (LC) status, and vaccine combination on N levels were also explored (Figure 3.2, A-D). The role of sex did not significantly influence N levels (P=0.1827), nor did BMI (P=0.7481) or the presence of LC symptoms (P=0.2454). Interestingly, the specific combination of COVID-19 vaccines that subjects were exposed to seemed to impact the level of N, where those who received three doses of Pfizer-BioNTech's Comirnaty® mRNA vaccine (BNT162b2) had significantly lower (P=0.0368) N levels ($\bar{x}$=1.04) compared to those with two doses of Comirnaty® and one dose of Moderna's Spikevax® mRNA vaccine (mRNA-1273) ($\bar{x}$=3.52) (Figure 3.2 D).

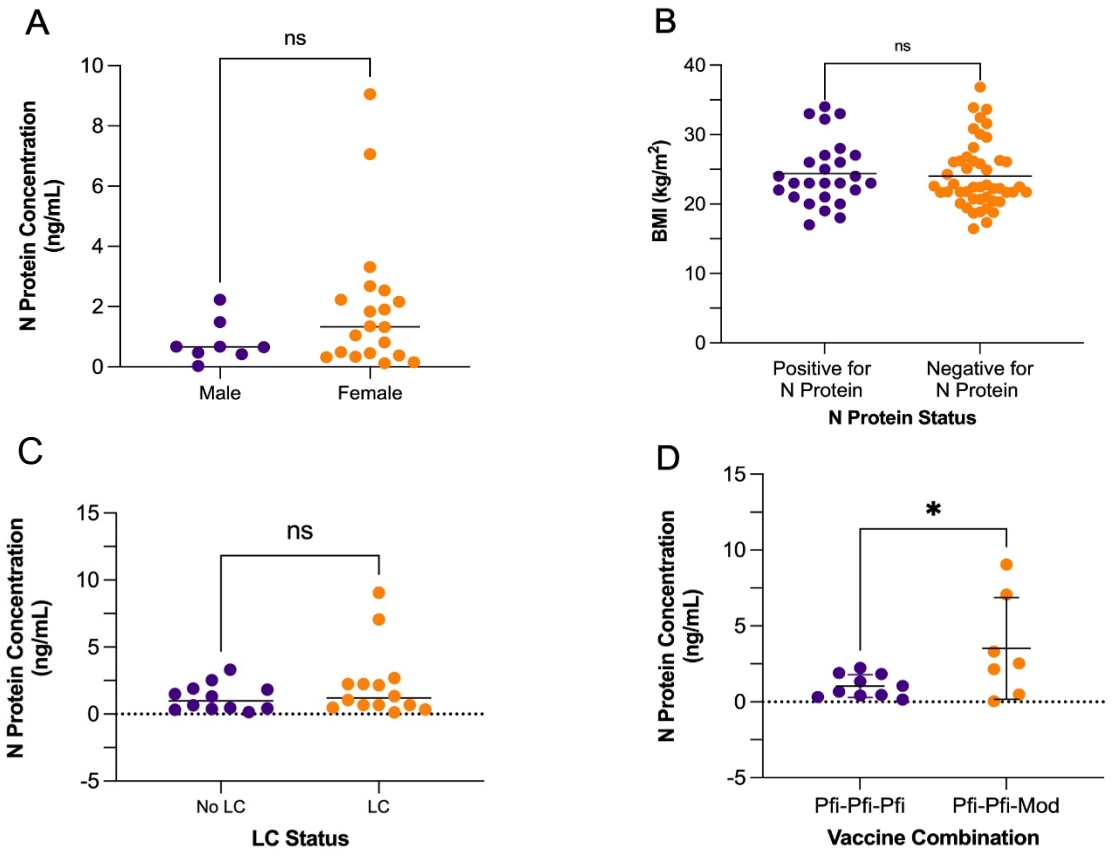

Figure 3.2 (A-D) N protein levels were influenced by the combination of vaccine received; however, BMI, sex, and LC status did not alter N protein levels.

Comparison of N levels based on sex, BMI (kg/m^2), LC status, and vaccine combination at sampling following serum ELISA. The dotted line (- - -) represents the lowest detection limit (0 ng/mL) for N. Statistical significance is denoted as follows: (ns: non-significant, where $P > 0.05$; *, $P \leq 0.05$; **, $P \leq 0.01$; ***, $P \leq 0.001$; ****, $P \leq 0.0001$). A Mann Whitney U test was used for comparing two groups with non-normally distributed data, as in A-D. Straight line bars represent mean, while error bars represent the mean ± SD.

(A) Comparison of N levels based on reported sex. **(B)** BMI comparison between negative and positive N protein status. **(C)** Comparing N levels between those with LC symptoms and those without LC symptoms. **(D)** Comparing N concentration based on the vaccine prime, and boost received by subjects with detectable N (P=0.0368). Abbreviations: LC: Long COVID-19; Pfi: Pfizer; Mod: Moderna. The results and figures were generated using GraphPad Prism 9.3.1 (350) for MacOS.

Finally, the correlation between time since infection and levels of N was explored to determine whether N levels wane with time similar to vaccine- and infection-induced antibodies. The correlation analysis revealed a weakly positive (r=0.4936; P=0.0441) correlation between

time since infection and N concentration (Figure 3.3, A, B), suggesting that the number of days since infection did not significantly affect the level of N in circulation. This phenomenon has also been observed for the spike protein (S), where latent viral persistence of S can last up to 15 months following infection(106)

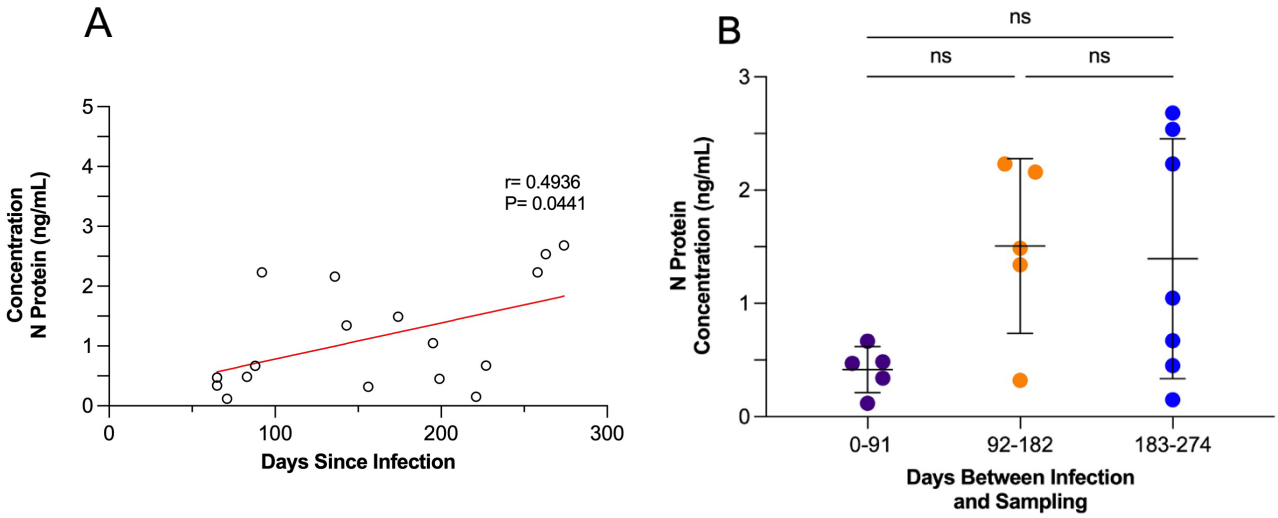

Figure 3.3 (A, B) A weakly positive correlation between time since infection (days) and the concentration of N in circulation was observed.

(A) Correlation between the time since infection in days and the level of N in circulation. Results demonstrated a weakly positive correlation (r=0.4936; P=0.0441). **(B)** Stratified time periods since infection and the level of N. Results do not suggest statistical intergroup difference between the time since infection and the level of N in circulation ((0-91 vs. 92-182) P=0.1218; (0-91 vs. 183-274) P=0.1362; (92-182 vs 183-274) P=0.9699). Statistical test used for (A) was a simple linear regression with correlation analysis and a one-way ANOVA with a post-hoc Tukey test (B). The error bars represent the mean ± SD. The results and figures were generated using GraphPad Prism 9.3.1 (350) for MacOS.

The magnitude of the humoral immune response was then assessed by measuring the levels of Anti-N IgG antibodies. Anti-N IgG antibodies were selected to differentiate between infection-induced and vaccine-induced antibody levels and these antibodies have been reported as indicators of natural infection in the literature(107). In our cohort of 77 subjects, the total number of participants positive for anti-N IgG antibodies (n=71, 92%) outnumbered the

percentage of participants who previously reported testing positive for SARS-CoV-2 (n= 50, 65%). Predictors of disease outcome were assessed (age, sex, vaccine, and diet) for their effect on anti-N IgG levels (Figure 3.4, A-D). Students on a plant-based diet (vegetarian/vegan) had significantly (N=15, x~=10.72, P=0.0093) lower anti-N IgG antibody concentrations compared to those with no dietary restrictions (N=54, x~=27.35), and younger students aged 18-26 had significantly (P=0.0132) higher antibody levels (N=37, x~=29 ng/mL), than those aged 27-36 (N=34, x~=13.1 ng/mL). Subject sex and vaccine makeup did not significantly affect antibody titers. These results should be interpreted with caution, however, given the likely presence of cofounders and the low sample size.

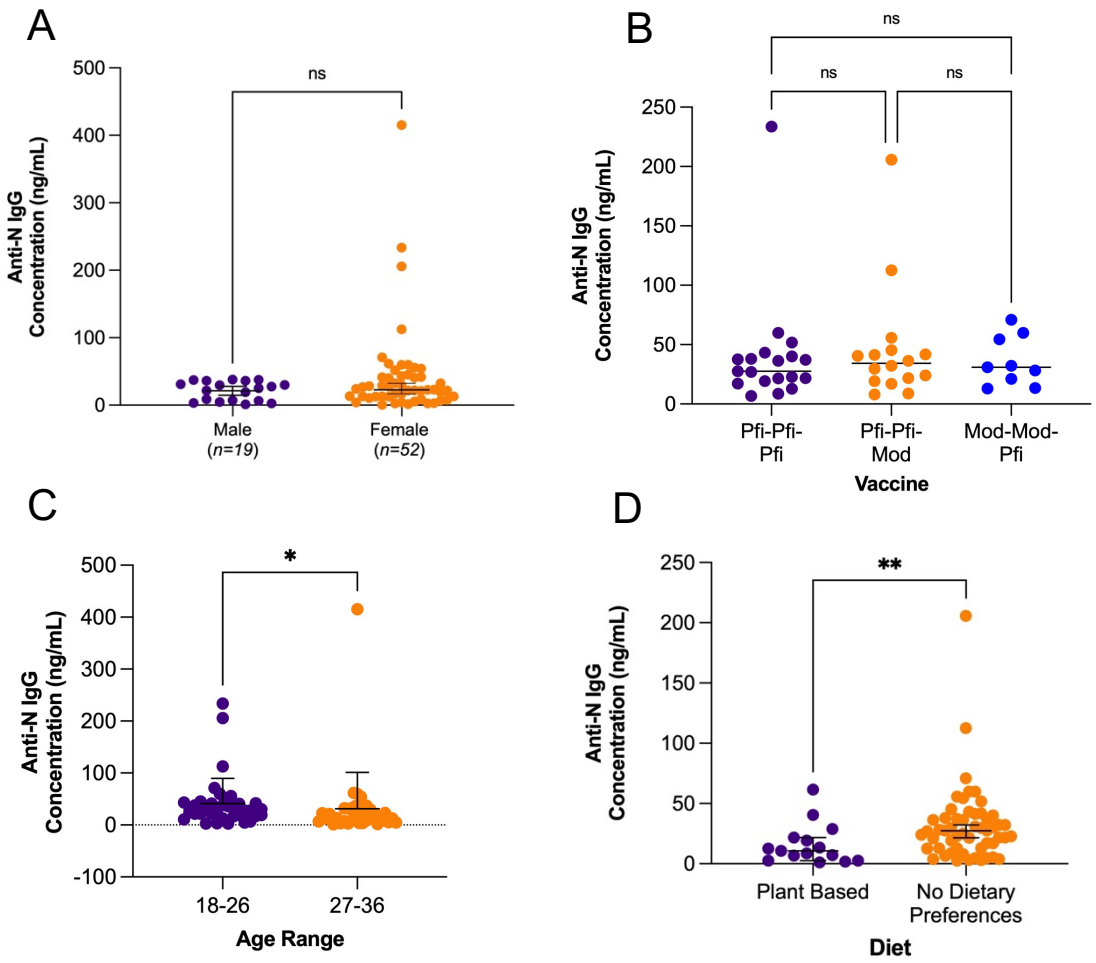

Figure 3.4 (A-D) Anti-N IgG levels are minimally influenced by factors associated with COVID-19 disease outcome.

(A) Comparison of anti-N IgG concentration based on sex (P=0.1947). **(B)** Anti-N IgG levels based on the combination of mRNA vaccines received, no intergroup statistical differences were observed ((Pfi-Pfi-Pfi vs. Pfi-Pfi-Mod, P=0.1962; Pfi-Pfi-Pfi vs. Mod-Mod-Pfi, P=0.9716; Pfi-Pfi-Mod vs. Mod-Mod-Pfi, P=0.8485). **(C)** Comparison of anti-N IgG levels based on an age sub-stratification of the student cohort (P=0.0132). **(D)** Anti-N IgG levels based on dietary preference (P=0.0093). Statistical test used for (A) was an unpaired t-test, a one-way ANOVA with a post-hoc Tukey test (B), and a Mann-Whitney U test (C, D). Straight line bars represent mean, while error bars represent the mean ± SD. Abbreviations: Pfi: Pfizer; Mod: Moderna. The results and figures were generated using GraphPad Prism 9.3.1 (350) for MacOS.

The relationship between time since infection and anti-N IgG levels was then explored to determine if antibody levels in younger individuals wane similarly to those in older individuals.

Anti-N COVID-19 antibodies have been shown to peak at 6-7 weeks following infection and positivity rates in previously infected individuals can reach 98.8%(108,109). A correlation analysis revealed a weakly negative correlation of anti-N IgG antibody titers ($r=-0.3393$, $P=0.0159$) with increasing time; however, it was not possible to determine whether the antibody levels peaked at 6-7 weeks following infection as most subjects were recruited after this timepoint. By stratifying time since infection, it was apparent that antibody titers were highest ($\bar{x}=93.32$ ng/mL) for individuals 0-91 days between infection and sampling while those at 91-182 days ($\bar{x}=31.90$ ng/mL) and 183-295 days ($\bar{x}=34.44$ ng/mL) were both lower (Figure 3.5, A, B).

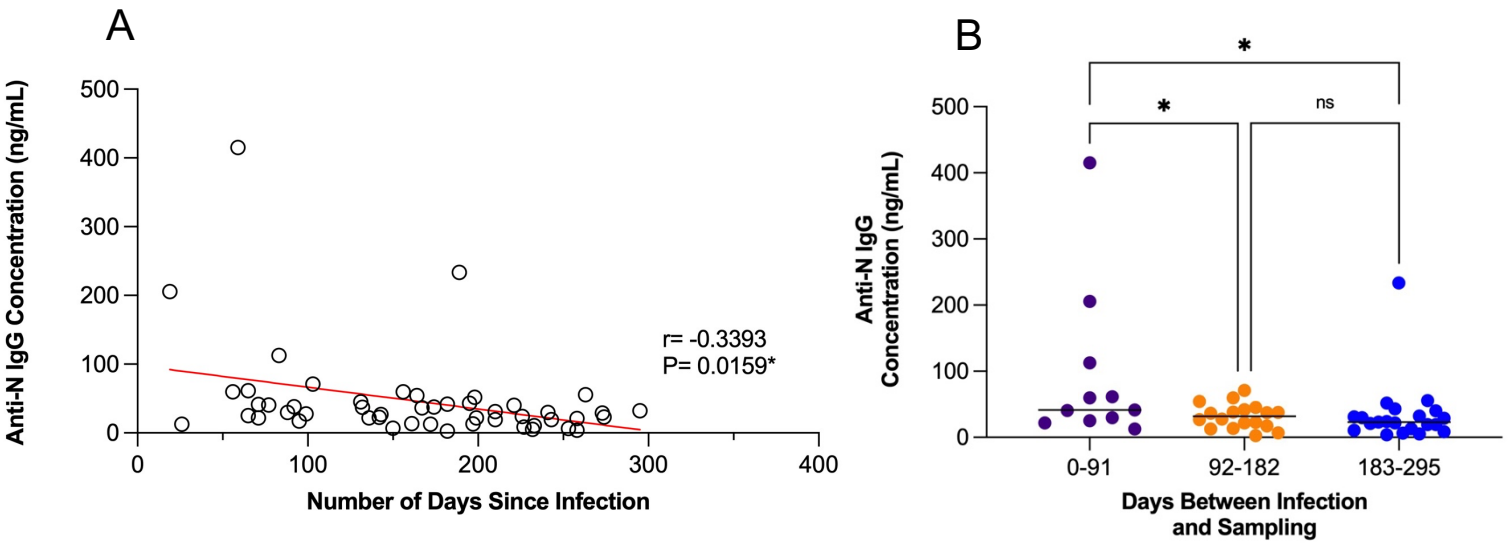

Figure 3.5 (A, B) A weakly negative correlation between time since infection and anti-N IgG titers in circulation was observed.

(A) A weakly negative correlation (r=-0.3393, P=0.0159) between the time (days) since infection and sampling. **(B)** Time stratification between the time since infection and circulating anti-N IgG titers (0-91 vs. 91-182, P=0.0429; 0-91 vs. 183-295, P=0.0468; 92-182 vs. 183-295, P=0.9915). Statistical test for (A) was a simple linear regression and correlation analysis and (B) was a one-way ANOVA with a post-hoc Tukey test; the straight-line bars indicate the mean. The results and figures were generated using GraphPad Prism 9.3.1 (350) for MacOS.

3.2 Comparing various aspects of the LC immune response in symptomatic students compared to those with no LC symptoms. A significantly increased level of endothelial damage/transformation biomarkers was observed in LC symptomatic students.

To better understand the underlying immune response for students with LC symptoms, both humoral and cellular immune mediators were investigated. The main symptoms associated with LC in our cohort were respiratory issues; loss of smell (anosmia) and taste (ageusia); lethargy/malaise; cough; headache; difficulty thinking or concentrating (brain fog); and congestion (Figure 3.6 C). These symptoms are similar to those generally reported in the literature for LC and closely match symptoms reported by the Centers for Disease Control and Prevention (CDC)(87). Additionally, the number of subjects in our group (N=30, 39%) with LC

symptoms appears higher than ranges reported in the literature (10-25%) for the general population. There was no significant difference (P=0.1875) in the levels of anti-N IgG antibodies based on the frequency of symptoms reported (Figure 2.4 C), although antibody titers did appear higher for those with anosmia, ageusia, and respiratory issues (despite no significant difference). Furthermore, we determined that anti-N IgG concentrations between those with LC symptoms and healthy students were not significantly different (P=0.2966), nor were levels of N in circulation (P=0.2454) (Figure 3.6, A, B).

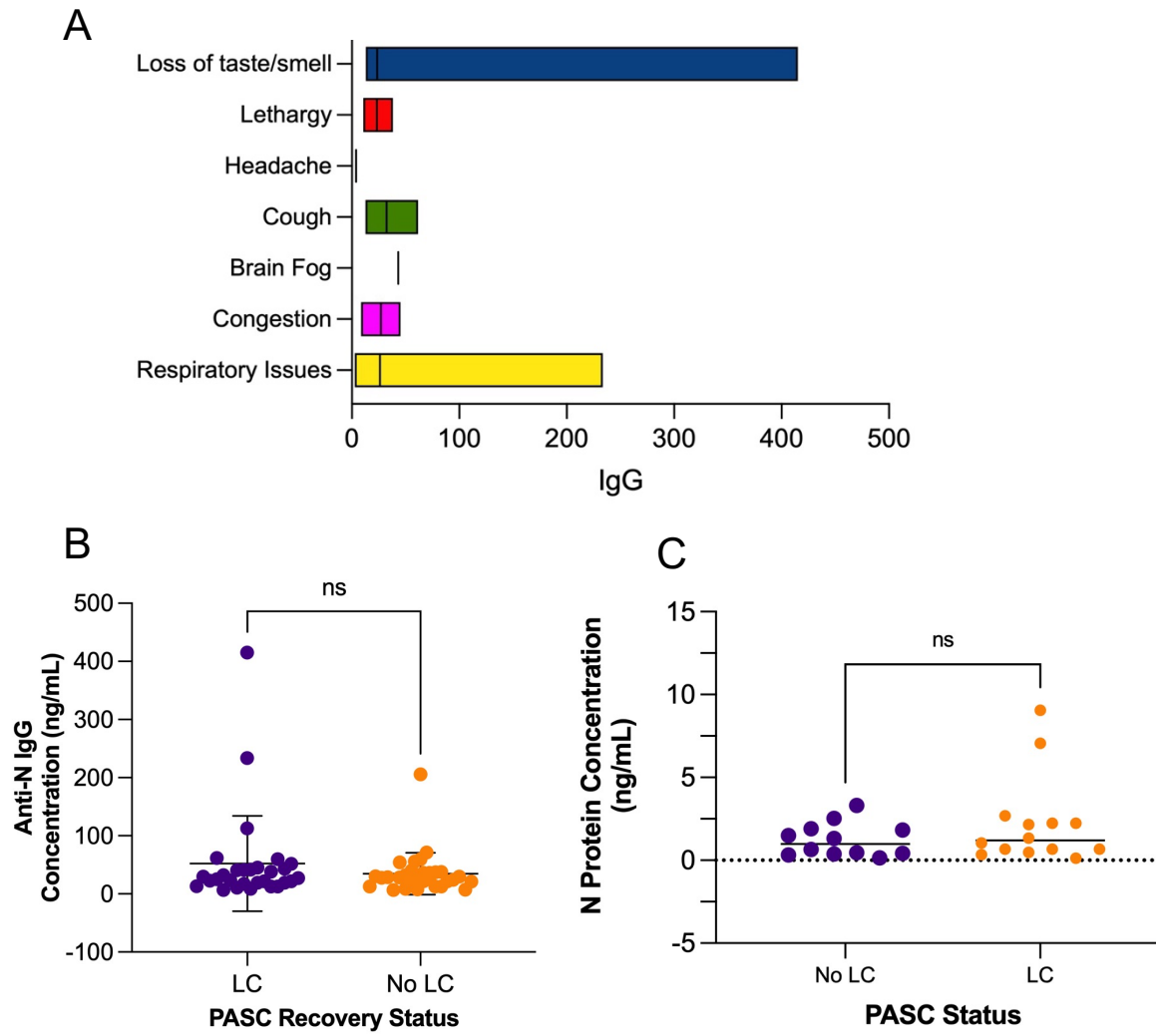

Figure 3.6 (A-C) LC status does not affect the circulating levels of anti-N IgG or N.

(A) Anti-N IgG antibody levels based on LC symptoms experienced in our cohort (P=0.1875). **(B)** Comparison of anti-N IgG antibody levels in students with LC symptoms and healthy student controls (P=0.2966). **(C)** Comparison of N levels in students with LC symptoms and healthy student controls (P=0.2454). Statistical test for (A) was a one-way ANOVA with a post-hoc Tukey test and an unpaired t-test was applied for (B, C); straight line-bars represent the mean and error bars represent the mean ± SD. The results and figures were generated using GraphPad Prism 9.3.1 (350) for MacOS.

To further evaluate the host immune response to COVID-19 in the context of LC, I examined the levels of 13 immune biomarkers. Biomarker levels were compared in students with LC symptoms, students with no LC symptoms (healthy student controls), and in a comparison

group of older individuals with LC symptoms [(Age (SD)=45.8 (13.3); N (male)=71 (36%), N (female)=124 (64%)]. The specific biomarker panels were custom tailored to cover the immunological spectrum of LC, based on previous work in our laboratory as well as available literature. The LC immune response is multifaceted, and is thought to be caused by a combination of factors, including prolonged tissue-specific inflammation, viral antigen persistence, and microvascular dysfunction (among others)(110). To elucidate LC in younger individuals, biomarkers such as IL-6, IL-15, TNF-α, IFN-γ, CCL2, and the proinflammatory chemokine CXCL10 (recruiter of macrophages, monocytes, neutrophils, etc.) were chosen to understand the inflammatory cascade. Biomarkers such as ICAM-1, VCAM-1, E-selectin, Ang-2, and D-dimer were chosen to study the level of vascular transformation/damage associated with LC. Finally, myeloperoxidase (MPO) was selected based on its involvement in the stress response and neutrophil recruitment during acute COVID-19 infection.

Proinflammatory cytokines such as TNF-α and IL-6 are commonly upregulated during infection and have been shown to contribute to the cytokine storm phenomenon observed in acute cases of COVID-19, where a state of hyperinflammation can cause organ failure and acute respiratory distress syndrome (ARDS)(111). Similarly, LC studies have shown persistent upregulation of inflammatory cytokines TNF-α and IL-6; however, age may play a role in which cytokines are elevated (e.g., patients 21-40 years had higher TNF-α, while those over 60 had higher IL-6)(112,113). Our results show that TNF-α (R^2=0.01484, P=0.5139) is weakly correlated with increased time post infection, while IL-6, CCL2, IL-15, and CXCL10 showed no clear correlation with time (Figure 3.7). Given the low number of samples collected beyond 10 months post infection, these results need to be validated with a follow-up study and remeasuring.

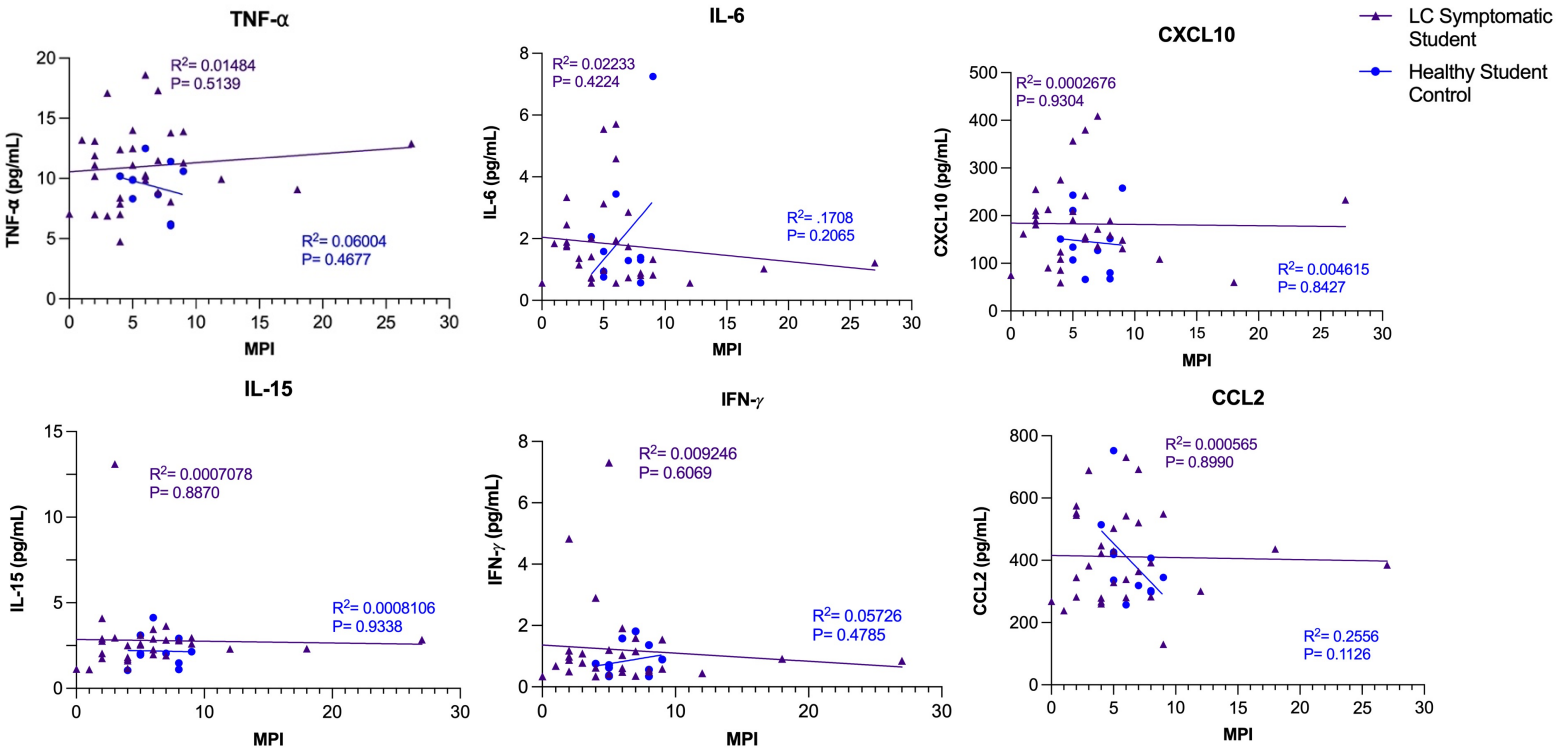

Figure 3.7 Cardinal proinflammatory cytokine levels begin to gradually decrease over time.

Linear regression analysis of serum proinflammatory cytokine levels and months post infection (MPI). Both LC symptomatic (N=30) and healthy student controls (N=11) were compared by linear regression analysis over time. The results and figures were generated using GraphPad Prism 9.3.1 (350) for MacOS.

The levels of each proinflammatory marker were also compared among the LC symptomatic participants, healthy student controls, and comparison groups to determine the role of age on LC progression and outcome. Interestingly, TNF-α appeared to have significantly higher cytokine concentrations (LC student vs. Comparison, P=0.0389; LC student vs. Healthy Student Control, P > 0.9999; Comparison vs. Healthy Student Control, P=0.0055) in the comparison group, compared to the LC symptomatic and healthy student control groups. This effect was not observed for the other proinflammatory cytokines IL-6, IL-15, IFN-γ, CCL2, and

CXCL10 (Figure 3.8), although IL-6 levels do appear slightly elevated in the older comparison group compared to both student groups.

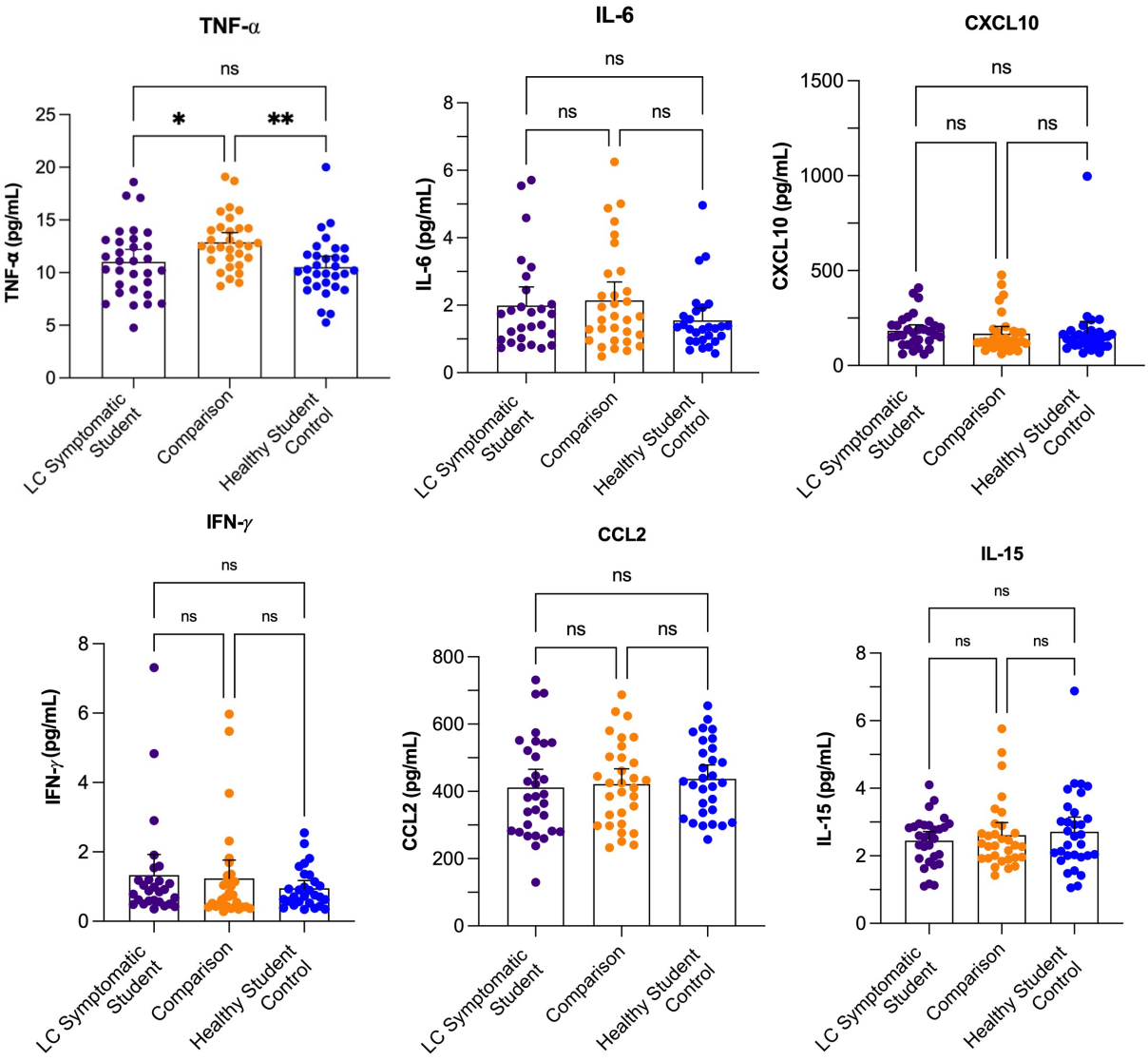

Figure 3.8 Proinflammatory cytokine concentrations remain consistent across the three groups; however, concentrations of TNF-α are upregulated in the older comparison group.

Comparing proinflammatory biomarker concentrations between the LC symptomatic student group (N=31), the comparison group ((N=31, Age (SD)=45.8 years (13.3)), and the healthy student control (N=31). Statistical differences were observed for TNF-α where (LC student vs. Comparison, P=0.0389; LC student vs. Healthy Student Control, P > 0.9999; Comparison vs. Healthy Student Control, P=0.0055). Non-normally distributed data (CXCL10, IFN-γ, IL-15, and CCL2) were subject to a Kruskal-Wallis test with a Dunn's post-hoc test, while normal data (TNF-α and IL-6) underwent a one-way ANOVA with a post-hoc Bonferroni correction. The results and figures were generated using GraphPad Prism 9.3.1 (350) for MacOS.

Next we investigated endothelial biomarkers to determine whether vascular damage and/or transformation biomarker levels are also altered in younger individuals with LC. One recent study determined that a serum biomarker profile consisting of ANG-1 and P-SEL was highly predictive (96%) of LC using a machine learning approach(96). Although there were no significant group differences for ANG-2, E-selectin, or D-dimer in our study, our results did indicate that ANG-2 (R^2=0.01830, P=0.4681), E-selectin (R^2=0.01396, P=0.5267), and D-dimer (R^2=0.06438, P=0.1684) are weakly positively correlated with increased time post infection (Figure 3.9). Interestingly, D-dimer levels have been correlated to LC and were found to be elevated at the six months post infection timepoint(114). Similar results were demonstrated in the LC symptomatic group compared to results in healthy student controls. Again, these results would benefit from a re-enrolment and follow-up sampling to examine whether these trends are observed at longer time points post infection.

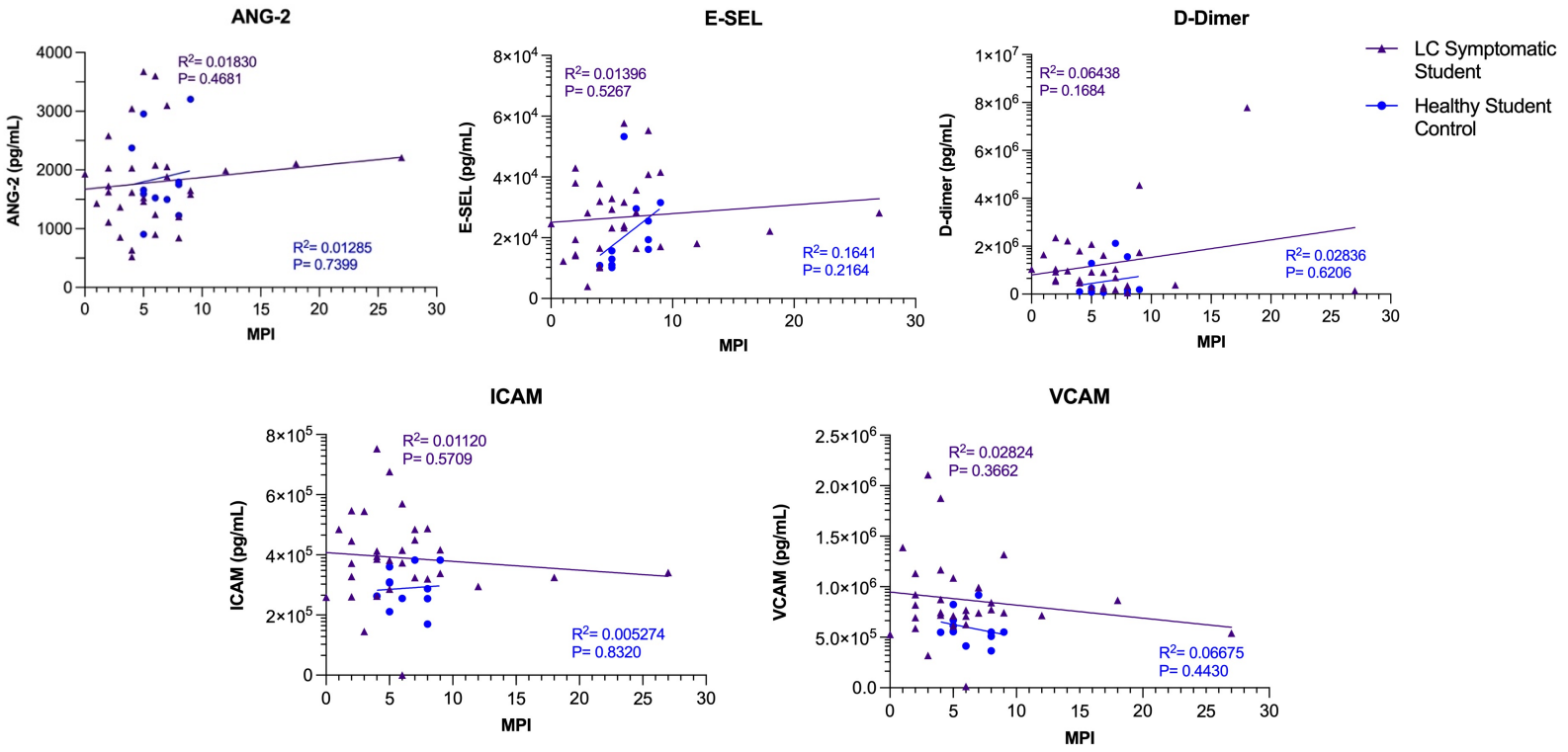

Figure 3.9 ANG-2, E-selectin, and D-dimer levels are correlated with time and remain elevated while other endothelial biomarkers grade off with time post infection.

Linear regression analysis of endothelial transformation/damage biomarkers commonly associated with SARS-CoV-2 infection. Both LC symptomatic (N=30) and healthy student controls (N=11) were compared by linear regression analysis over time. The results and figures were generated using GraphPad Prism 9.3.1 (350) for MacOS.

The remaining biomarkers associated with endothelial transformation were not correlated with increased time (i.e., ICAM-1 and VCAM-1); however, these two biomarkers displayed significant group differences among the three groups. The LC symptomatic group displayed elevated ICAM-1 levels (Symptomatic Student vs Comparison, P=0.0022; Symptomatic Student vs. Healthy Student Control, P=0.0009; Comparison vs. Healthy Student Control, P > 0.9999) compared to those of the comparison and healthy student control groups as did VCAM-1 (Symptomatic Student vs Comparison, P=0.0073; Symptomatic Student vs. Healthy Student Control, P=0.0003; Comparison vs. Healthy Student Control, P > 0.9999) (Figure 3.10, A, B),

while the other endothelial biomarkers (i.e., ANG-2, E-selectin, D-dimer) did not display significant group differences.

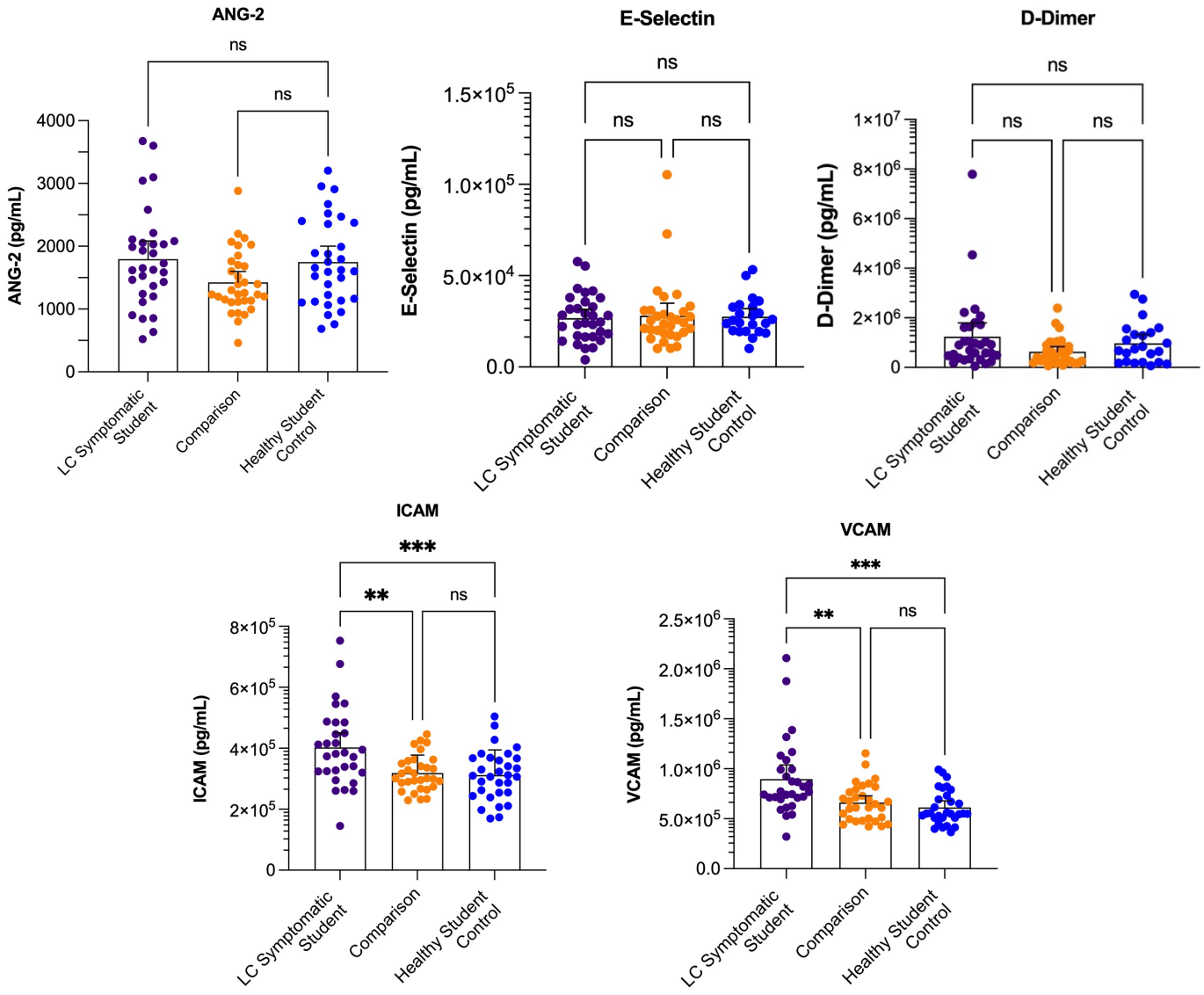

Figure 3.10 Endothelial biomarker levels are similar among the three comparison groups, while ICAM-1 and VCAM-1 levels are increased in the LC symptomatic student group.

Comparing proinflammatory biomarker concentrations among the LC symptomatic student group (N=31), the comparison group (N=31), and the healthy student control group (N=31). Statistical differences were observed for ICAM-1 (LC student vs. Comparison, P=0.0022; LC student vs. Healthy Student Control, P=0.0009; Comparison vs. Healthy Student Control, P > 0.9999). Non-normally distributed data (ICAM-1 and VCAM-1) were subject to a Kruskal-Wallis test with a Dunn's post-hoc test, while normal data (ANG-2, E-selectin, and D-dimer) underwent a one-way ANOVA with a post-hoc Bonferroni correction. The results and figures were generated using GraphPad Prism 9.3.1 (350) for MacOS.

The final biomarker explored in this work was myeloperoxidase, or MPO. SARS-CoV-2 infection can trigger neutrophils to release MPO. MPO is a pro-oxidative leukocyte heme-enzyme that serves a variety of functions during viral infection. For example, MPO increases the production of reactive oxygen species (ROS) and promotes neutrophil recruitment and cytokine production. MPO also catalyzes H_2O_2 and superoxide, which generates hypochlorous acid that is capable of microbial killing and host tissue damage(115). Previous research in our laboratory used an artificial neural network to demonstrate that the upregulation of MPO increases the disease severity level in COVID-19 sepsis and septic shock patients, suggesting the role of this biomarker during severe infection(116). In our cohort, MPO levels were weakly negatively correlated with time post infection (R^2=0.03853, P=0.2899); however, MPO levels were significantly elevated in the LC symptomatic group (Symptomatic Student vs Comparison, P=0.0016; Symptomatic Student vs. Healthy Student Control, P > 0.9999; Comparison vs. Healthy Student Control, P=0.0100) and the healthy student control group, compared to the older comparison group (Figure 3.11).

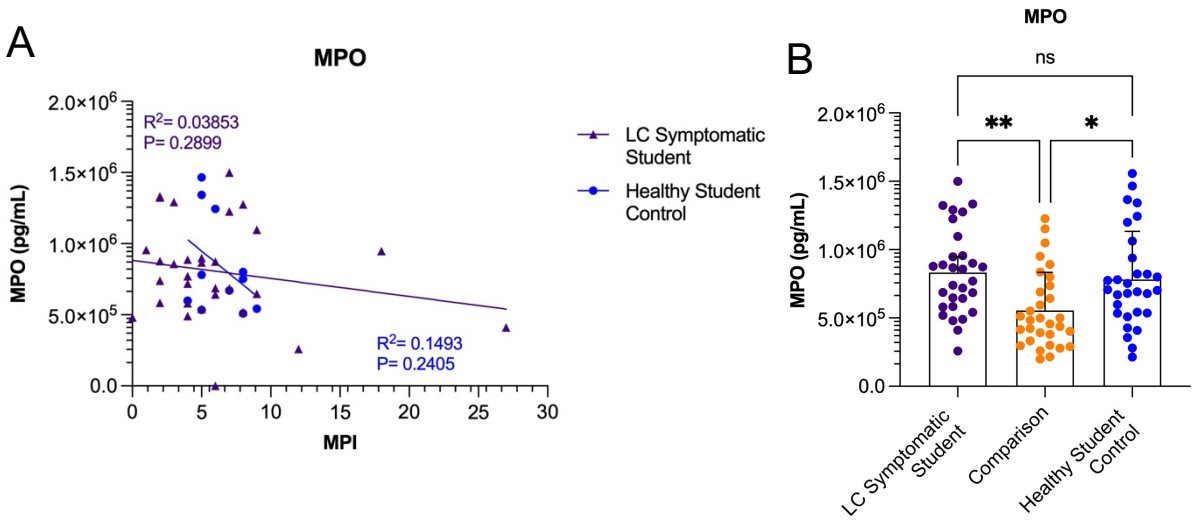

Figure 3.11 MPO levels are not sustained with time post infection and are elevated in younger cohorts.

(A) Linear regression analysis of MPO (R^2=0.03853, P=0.2899) comparing LC symptomatic students (N=30) and healthy student controls (N=11) over time. **(B)** Comparing MPO concentrations between the LC symptomatic student group (N=31), the comparison group (N=31), and the healthy student control group (N=31). Statistical differences were observed for MPO (LC student vs. Comparison, P=0.0016; LC student vs. Healthy Student Control, P > 0.9999; Comparison vs. Healthy Student Control, P=0.0100) following a Kruskal-Wallis test with a Dunn's post-hoc test. The results and figures were generated using GraphPad Prism 9.3.1 (350) for MacOS.

3.3 SARS-CoV-2 rapid antigen testing yields the same results as RT-qPCR and can accurately detect the highly mutated Omicron variant.

Central to the COVID-19 pandemic was heavy public health investment in the ongoing testing and reporting of new cases. As case numbers increased during periods of more transmissible variants (such as Delta, Omicron, and Omicron's sublineages), it became more difficult and costly to subject all positive cases to RT-qPCR testing and sample sequencing. With that, many individuals began resorting to home testing with rapid antigen COVID-19 tests. During enrolment in our study, all students were required to perform a rapid antigen test upon arrival via a five second throat swab or nasal swab depending on the comfort level of the

individual. Of the N=77 students in the study, only one student tested positive on enrolment; the test was administered a second time to rule out a false positive.

We then compared the accuracy of rapid antigen testing with PCR testing by subjecting N=50 (65%) banked throat/nasal buffer samples to RT-qPCR processing and analysis. We also included N=10 known positive sample controls, which were collected and banked during the Halifax Omicron wave of January 2022. Interestingly, all samples except the positive rapid test on enrolment provided negative results (meaning Cq > 40), and N=8/10 known positive controls returned a positive result (Table 3.1). These results are in direct agreement with those collected following the rapid testing. The reaction was set up using the three specific fluorophores of highly conserved regions of the SARS-CoV-2 genome: VIC (for the N1 target), FAM (for the N2 target), and Cy5 ((for the internal control, ribonuclease P (RNase P) target)). The pre-defined primers for this reaction were obtained from two specific regions of the SARS-CoV-2 N gene, which were modified to contain different fluorophores for simultaneous observation on two different channels of a real-time instrument. The RNase P target was included to amplify the human RNase P gene to validate the input material integrity and absence of inhibition, thus serving as an internal control. The amplification plot for this reaction can be found in Appendix II.

Table 3.1 RT-qPCR analysis of student samples and known positive COVID-19 samples (controls) collected in 2022.

Sample Number	Rapid Test Result	RT-qPCR Result	Cq Value
S1-S35	−	−	Cq > 40
S36	+	+	23.12
S37-S50	−	−	Cq > 40
CTL1	+	+	26.22
CTL2	+	+	27.64
CTL3	+	+	31.80
CTL4	+	+	24.76
CTL5	+	+	32.50
CTL6	+	+	34.54
CTL7	+	+	22.76
CTL8	+	+	24.30
CTL9	−	−	Cq > 40
CTL10	−	−	Cq > 40
PC	+	+	23.50

† S1-S50 are student samples
† † CTL1-CTL10 are samples collected during the January 2022 Omicron wave in Halifax
† † † PC is positive control

CHAPTER 4: DISCUSSION

The COVID-19 pandemic caused by the Severe Acute Respiratory Syndrome Coronavirus 2 (SARS-CoV-2) has resulted in significant global burden across a variety of sectors. As the virus continues to mutate and spread, many vulnerable populations remain at risk of developing an infection. The evolutionary interactions between the virus and the host means that as COVID-19 gains mutations (predominantly in the RBD region of spike), previously acquired immunity from vaccination and infection may not provide adequate protection. In this cross-sectional study, I aimed to explore various concepts relating to the immune response to COVID-19 in an underrepresented cohort, such as the level and durability of infection-induced antibodies; the presence of persistent viral antigen in the bloodstream; the incidence of LC and the immune biomarkers associated with LC in young individuals; and the sensitivity of rapid antigen testing compared to PCR.

4.1 Anti-N IgG antibody titers and nucleocapsid protein levels represent methods of characterizing seropositivity and immune status

Throughout the COVID-19 pandemic, many techniques were optimized and developed for the rapid, reproducible, and cost-effective diagnosis of SARS-CoV-2. To quantify levels of previous infection in our study cohort, two specific ELISA assays were used. We chose to directly measure SARS-CoV-2 viral proteins in blood (nucleocapsid protein) as a benchmark for previous exposure and infection. Additionally, we decided to target N as opposed to Spike (S) to ensure we were detecting previous infection, rather than vaccine-induced proteins. For example, one recent study linked post-mRNA vaccine myocarditis to elevated levels of free circulating,

full-length spike antigen in young individuals(117). Interestingly, the spike protein was unbound by circulating antibodies.

Although pre-existing literature regarding the measurement of N is sparse, studies have demonstrated the diagnostic value of measuring this protein. One study measured this protein in early course COVID-19 infection and compared the sensitivity to viral RNA testing. Their results found that measuring N was most sensitive (diagnostic sensitivity of 90.9%; 95% CI: 85.1%-94.6%) between 2 and 7 days post symptom onset and quickly declined after antibody levels increased(118). The study also acknowledged that this assay does not possess the diagnostic sensitivity to detect N in asymptomatic cases. In our study, only 35% of our cohort had detectable levels of N. This level is low, but unsurprising, given that all enrolled subjects except one tested negative for active infection. Interestingly, this subject had no detectable N in serum and a low anti-N IgG titer (2.68 ng/mL), while the Cq value was 23.12. This result suggests that for early disease course or for asymptomatic infection, serum N detection likely lacks the necessary sensitivity to diagnose infection. For these cases, the gold standard of viral RNA isolation and PCR should be considered, rather than serology. Importantly, repeating this experiment with a larger sample size of individuals who had confirmed symptomatic and mild/asymptomatic COVID-19 would allow this trend to be statistically validated.

As anti-N antibody levels increase in response to infection, the level of N antignemia is reduced. In our study, N=71 (92%) of participants had detectable levels of anti-N IgG antibodies; however, only a fraction (35%) had detectable N in circulation. In students with detectable N, mean anti-N IgG antibody titers were 31 ng/mL (95% CI: 20.7%-41.2%), while those with no detectable N had a mean antibody titer of 44 ng/mL (95% CI: 20.6%-66.7%). Although no significant difference was detected between the means of each group, it is worth noting that those

with no detectable N had higher anti-N IgG levels, suggesting that viral clearance had occurred for these individuals.

Interestingly, the number of individuals who identified as having previously been infected with SARS-CoV-2 (via rapid testing or PCR) on enrollment was 65%. This discrepancy likely stems from the increase in mild and undiagnosed asymptomatic COVID-19 cases, which increased during the highly transmissible Omicron wave(85). Using the anti-N IgG antibody titers as a surrogate for previous infection, 27% of individuals in the study had seroconverted with no prior knowledge of infection. Studies have estimated that 44.1% of people remain asymptomatic following SARS-CoV-2 infection, and that these rates are highest in children and young individuals and lowest in older individuals (lowest at 90.5 years of age, 8.1%)(85). Enrollment for our study commenced in September 2022 and closed in early October of the same year, suggesting that individuals may have been exposed to the Omicron sublineage variants BA.4 and BA.5. Given the short incubation period of this variant, the fast speed of viral transmission, and reduced stringency during this outbreak period in Nova Scotia, it is not unreasonable to assume that a portion of exposed individuals remained asymptomatic in our study(119,120). This is compounded by the young age ($\bar{x}$=26.7 years, ± SD: 4.4) of our cohort (and thus less likelihood of exhibiting symptoms) and the social nature of a university campus, where students are more likely to engage in social functions regardless of restriction measures. A similar study conducted in a university setting in Cameroon in February 2022 found that 92% of students enrolled (N=90, mean age=24 years) had detectable Anti-N antibodies(121).

In the context of LC, one of the contributing mechanisms proposed to explain persistent infection is the lingering of viral proteins, and/or continued viral shedding in reservoir tissue sites throughout the body. In our study, viral N protein was detected in serum up to 274 days post

infection and, following a linear regression analysis, it appeared that levels of this protein followed a weakly positive association (r=0.4936). This result suggests that there are possibly mechanisms at play allowing viral components to persist following acute infection. Viral proteins and/or viral RNA have been found in the reproductive system, cardiovascular system, brain, appendix, eyes, and lung tissues following acute COVID-19 infection(94). Studies have also documented the recovery of replication competent SARS-CoV-2 virus at 78 days after symptom onset in immunosuppressed individuals(122). Although we were unable to detect persistent positive RT-qPCR testing in our study, it is possible that repeating this experiment with samples from the lower airway or lungs may have returned PCR positive results in individuals with LC symptoms. A separate study found circulating spike antigen in 60% of a cohort of individuals suffering from LC 12 months post infection(95). These results indicate that there are possibly reservoir tissues hosting replicating virus, or viral components, which promote continued immune system activation/exhaustion, a syndrome commonly associated with long COVID-19. Again, the results from our study should be interpreted with caution given the low sample size; however, a future aim would be to re-sample serum from our cohort to determine whether those with detectable N maintained measurable levels of this protein.

4.2 The influence of factors such as sex, diet, vaccine, and BMI on N and anti-N IgG antibodies

The levels of both N protein and anti-N IgG antibodies were also evaluated based on factors such as subject sex, BMI, dietary preferences, and particular vaccine combination. First, the sex of the individual did not appear to have any significant effect on the levels of these proteins. In the literature, studies have demonstrated that individual sex does not significantly impact antibody concentrations following a mild disease course(123). For severe cases of

COVID-19, females generally mount a more robust immune response, characterized by higher antibody titers and a more pronounced antiviral response. Females also seroconvert more quickly compared to males, where protective RBD-specific IgG antibody levels against COVID-19 peak in the fourth week post symptom onset for women, and the seventh week for males(124). In our young cohort, there were no reported instances of severe disease in previously infected participants, and this possibly explains why there were no significant differences in N and IgG between the two sexes. Other factors commonly associated with disease severity, such as smoking status, BMI, and alcohol consumption also had no significant impact on N and IgG levels in our study cohort. This may be attributed to disease severity, where those who smoke or have higher body mass indexes are more likely to progress to ARDS and death during severe infection(125). In our group, reported infections were mild and smoking rates were low (less than 5% of the cohort); BMI was also low ($\bar{x}$=25.03 kg/m^2) compared to that of the general population, which likely mitigated the impact of these factors on serum markers such as N and IgG.

The results did suggest that antibody levels were significantly impacted by both diet and age. Subjects on a plant-based diet (vegetarian or vegan) appeared to have lower antibody titers ($\bar{x}$=16.0 ng/mL) than individuals with no dietary restrictions ($\bar{x}$=32ng/mL). This finding indicates that individuals on a plant-based diet may be mounting a suppressed humoral immune response during pathogenic challenge, although there is little evidence in the literature to support this claim. One study compared the immune responses between participants following plant-based diets and participants following nonvegetarian diets, and found those on a plant-based diet had significantly reduced white blood cell counts, phagocytic activity, and suppressed T-cell proliferation(126). More thorough investigation into the role of diet on the SARS-CoV-2

humoral response is necessary to support our findings, where our results were possibly impacted by confounding factors, such as BMI, immune system status, or blood type of participants, which have all been shown to impact SARS-CoV-2-specific antibody kinetics(127).

The vaccine combinations of enrolled participants were then compared to determine their effect on N and anti-N IgG levels. Our results suggested that those with a mixed vaccine combination consisting of two doses of the Pfizer-BioNTech Comirnaty® (BNT162b2) and one dose of the Moderna SpikeVax® (mRNA-1273) vaccine had higher levels of N protein in serum than those who received three doses of Comirnaty®. The vaccine combination had no significant effect on anti-N IgG antibody levels, which was to be expected, given the mRNA vaccines were designed to elicit a broad, anti-spike antibody response rather than anti-N IgG antibodies. Given the small sample size for those who tested positive for N, the level of significance should be interpreted with caution. As the mRNA vaccines were not designed either with N viral components or to target N, the impact of time since infection should not be overlooked as a potential confounding variable for this result.

Finally, following age stratification of enrolled participants, those aged 18-26 had higher median antibody titers (x~=29 ng/mL), than those aged 27-36 (x~=13.1 ng/mL). Given the closeness in age range, similar levels of trained immunity, and low levels of comorbidities, this result would benefit from further analysis by comparing IgG levels in an older group. Interestingly, children and young adults appear to have a narrower antibody profile and lower antibody titers following COVID-19 exposure than older adults (aged 50 and above), where those aged 19-30 years had significantly lower IgG levels compared to children (mean age 11 years) and adults (mean age 49 years)(128,129).

4.3 Endothelial biomarkers are elevated in younger individuals and associated with increased time post infection in LC subjects

In the literature, the number of previously infected individuals who will progress to develop LC symptoms ranges from 7.5%-41%(130). In our study, (N=30/77) 39% of participants reported experiencing prolonged symptoms following primary COVID-19 infection. The most common LC symptoms experienced by students in our group were loss of taste and smell, respiratory issues, congestion, cough, and lethargy, and no significant differences were observed in IgG concentrations based on symptoms. Furthermore, no significant differences in N concentrations were observed for LC and non-LC subjects.

Biomarker profiling revealed that that there were no significant intergroup differences between LC symptomatic students, healthy student controls (no LC symptoms), and a comparison group with LC symptoms (age [SD]: 45.8 [13.3]) for inflammatory cytokines IL-6, IFN-γ, IL-15, and the chemokines CXCL10 and CCL2. However, the older comparison group had significantly elevated TNF-α levels compared to the two student groups. Similarly, linear regression analysis revealed that these inflammatory biomarkers (aside from TNF-α) do not appear to be associated with time, post infection (weakly negative associations). Inflammatory markers commonly associated with acute infection (IL-6 and TNF-α) have been found to remain elevated in LC subjects(112,131). These biomarkers were not elevated in our student groups; however, the older comparison group had elevated TNF-α compared to the student groups and TNF-α also displayed a weak positive association with time post infection, suggesting levels of this biomarker remain elevated following acute infection. This finding indicates that older subjects may be experiencing a more pronounced persistent state of inflammation during LC, contributing to the hallmark immune exhaustion/dysregulation associated with LC(132).

Importantly, this trend should be explored further by extending sampling timepoints to determine whether TNF-α levels are maintained beyond 10 months post infection.

Levels of CXCL10, CCL2, and IFN-γ were not elevated in LC subjects and their levels do not appear to be sustained with time post infection. IFN-γ is an important antiviral cytokine that helps drive the differentiation of Th1 cells. Reduced expression of this cytokine during LC has been documented in other studies and indicates a state of immune dysfunction or exhaustion (133). CCL2 and CXCL10 are chemokines that are heavily involved in the recruitment and infiltration of immune cells in the lungs during acute infection in COVID-19(134). Decreased expression of these cytokines is also a common feature of LC and supports a dysregulated cellular immune response and skewed immune cell trafficking during prolonged infection.

A series of endothelial biomarkers (ICAM-1, VCAM-1, D-dimer, E-selectin, and ANG-2) were investigated to determine whether vascular injury/involvement was associated with LC in our cohort. No intergroup differences were observed between the student groups and comparison group for ANG-2, E-selectin, and D-Dimer; however, ICAM-1 and VCAM-1 were significantly elevated in LC symptomatic students. Interestingly, ICAM-1 and VCAM-1 were not associated with time post infection, while ANG-2, E-selectin, and D-dimer all showed weakly positive associations with time post infection. ICAM-1 and VCAM-1 are cell adhesion molecules expressed on the surface of endothelial cells that mediate leukocyte adherence and recruitment to the endothelium during inflammation. These cytokines have been correlated with symptoms during acute COVID-19 infection and contribute to vascular leakage and pulmonary oedema(135). Our results suggest that ICAM-1 and VCAM-1 levels are significantly increased in younger individuals with LC, although levels of these markers appear to grade off with time (a common feature of LC). One explanation is that younger individuals experience increased

vascular transformation during acute infection, and these biomarkers remain elevated (compared to other endothelial markers) for an extended period. A separate study classified vascular transformation biomarkers associated with LC and found that ANG-1 and P-SEL were highly predictive of LC (96%) following the application of a machine learning algorithm(96). The authors also measured ICAM-1 and VCAM-1 and found no clear association between these biomarkers and LC. In our study, there were no group differences in the levels of ANG-2 or E-selectin; however, these biomarkers do show a weakly positive association with time. Taken together, our results suggest that age plays a role in ICAM-1 and VCAM-1 levels and that other biomarkers associated with vascular repair (D-dimer, ANG-2, and E-selectin) may remain elevated with time during LC.

Finally, MPO was measured to determine whether oxidative stress was associated with LC. Previous research in our laboratory using an artificial neural network and machine learning model found that MPO levels were upregulated during severe COVID-19 disease and septic shock (116). MPO is a pro-oxidative enzyme released by neutrophils during acute COVID-19 infection, which can increase the production of reactive oxygen species(136). Our results demonstrated increased MPO levels in both LC symptomatic and healthy student controls compared to the comparison group, and a weak negative association between MPO and time post infection. Recent studies suggest that the impact of acute COVID-19 on the symptoms of LC are partially mediated by oxidative damage and antioxidant defences, where increased MPO production contributes to post-viral somatic and mental symptoms(137). MPO has also been linked to endothelial glycocalyx shedding in COVID-19, exacerbating the degradation of an already compromised endothelial barrier(115). Importantly, our findings indicate increased

neutrophil and MPO activity in young subjects during acute disease, which may carry over and contribute to the pathogenesis of post-acute infection.

Despite the low sample size and minimal sampling beyond 10 months post infection, these results contribute to our understanding of the role of age on biomarkers associated with LC and provide additional framework towards the development of a rapid screening device for LC diagnosis. Currently, LC diagnosis is challenging due to the breadth of clinical manifestations and lack of consensus in the literature regarding risk groups, consistent biomarker profiles, the role of cellular immunity, and long-term consequences of LC. Increasing our cohort sample size and adding an additional elderly age group (70+ years of age) would provide a comprehensive framework for delineating the role of age (young, middle aged, older) and its contribution to the LC immune response at substantial post-infection timepoints.

4.4 Rapid antigen and RT-qPCR testing are both effective at detecting Omicron and asymptomatic infection

Rapid antigen testing was performed during enrollment to determine the level of active infection among the student cohort. Of the N=77 students enrolled, only N=1 subject tested positive for COVID-19. This subject displayed no symptoms associated with infection and a second rapid antigen test was performed to rule out a false positive result. Rapid testing buffer was also banked for subsequent RT-qPCR testing to determine whether additional asymptomatic infections were missed by rapid antigen screening.

Rapid lateral flow tests are regarded as being less sensitive at diagnosing early and asymptomatic COVID-19 infection compared to PCR(138). In comparison to the gold standard nucleic acid amplification tests (NAATs) such as RT-qPCR, which detect and amplify the presence of viral nucleic acids, rapid antigen tests rely on the presence of viral antigens, which

are measured by bindings interactions between the antigen and antigen-specific capture antibodies. Rapid antigen test sensitivity has been found to peak four days after illness onset with a sensitivity of 68.7% compared to RT-qPCR testing; rapid test sensitivity increased to 81% for symptomatic patient testing(139,140). Students in our cohort were enrolled in September-October 2022, a period that was dominated by the highly infectious Omicron sublineages BA.4 and BA.5. Recent studies have validated rapid antigen testing for measuring Omicron, where they were shown to detect the Omicron variant with similar sensitivity (78%) to the Delta variant (81.5%) within a 48-hour window of RT-qPCR positivity(138). Our results suggest that rapid antigen testing accurately detected asymptomatic infection during the Omicron wave with similar sensitivity to RT-qPCR processing of nasal samples. One limitation of this finding was the likelihood of non-specific isolation of host RNA in addition to viral RNA. Viral RNA input levels would have been very low and fragmented, given that no students reported active, symptomatic infection on enrolment; therefore, we cannot discount the possibility that asymptomatic infections were not detected due to low/degraded viral RNA input material. Despite this limitation, these findings suggests that rapid antigen testing can detect early, asymptomatic infection with similar sensitivity to RT-qPCR.

Importantly, rapid antigen testing remains a reliable method of detecting COVID-19 and controlling infection, especially as new sublineages of Omicron emerge. The cost of rapid antigen testing is roughly one tenth the cost of NAATs and should remain the first option for diagnosing individuals who are less likely to develop severe disease(141). This approach would reserve costly RT-qPCR diagnostic processing for at-risk populations who require early, accurate detection of the virus, such as the elderly, immunocompromised, or those with underlying health conditions.

4.5 Limitations of the study

This study has potential limitations that should not be overlooked. The rationale for conducting this study was to determine levels of SARS-CoV-2 seropositivity in our study population. With that, this study was not designed to investigate mechanisms of LC and results surrounding the immune response to LC should be interpreted with caution. Furthermore, experiments conducted in this study, such as the N protein measurement, intergroup antibody comparisons, and RT-qPCR measurement were underpowered, and a larger sample size is required to definitively support these findings and reduce the effect of confounding variables in these conclusions. The LC biomarker results would also benefit from a remeasuring at later post infection timepoints as the majority of collected samples (90%) fall within a 10-month post infection window. This would strengthen the link between biomarker levels and LC immune status in younger individuals. Finally, during nasal buffer processing for RT-qPCR analysis, we did not validate the protein levels in buffer prior to RNA extraction, limiting the interpretability of these findings. It is also likely that host RNA was extracted during the isolation of viral RNA, thus potentially reducing the purity of input material for PCR amplification.

4.6 Future aims

Future aims for this project include exploring alternative mechanisms responsible for LC symptoms and adding to our current findings. Available LC literature posits that LC is driven by a myriad of mechanisms, including viral antigen persistence in sanctuary tissues, the reactivation of latent herpesvirus infections (such as Epstein-Barr Virus), and autoantibody production against host proteins(110). The first aim would be to re-enroll previous participants for a follow-up study visit and remeasure biomarker and viral antigen levels in blood (N protein and S

protein). These results would provide a better understanding of whether endothelial biomarkers remain elevated at post infection timepoints greater than 10 months post infection as well as the role of lingering spike protein in contributing to continued LC immune activation. Additionally, adding an older age cohort (65 years plus) would provide a comprehensive biomarker framework for understanding how the age spectrum (young, middle aged, and older participants) contributes to LC disease progression. A secondary aim would be to obtain tissue biopsies from ACE2 tropic tissues (gastrointestinal tissues, lung tissues, kidney tissues, etc.) in LC individuals and measure the levels of both viral antigens (N protein and S protein) for further explaining the role of viral antigen persistence in sanctuary tissue reservoirs during a prolonged LC immune activation. Finally, adding the measurement of tissue factor (an initiator of the extrinsic coagulation pathway) in blood samples using an ELISA assay would provide additional evidence towards endothelial involvement and how pathogenesis of hypercoagulability contributes to the endothelial response in LC.

4.7 Conclusion

Despite the stated limitations of this work, these results augment our understanding of the SARS-CoV-2 immune response in young individuals. These findings suggest that young individuals mount a robust humoral immune response to acute COVID-19 and that are also susceptible to LC, where endothelial involvement (activation, transformation, and damage) appears to be a significant driver of prolonged infection in this age cohort. Previously infected students had detectable lingering N protein in circulation as well as a robust anti-N IgG antibody response in 92% of participants. Interestingly, common predictors of disease outcome such as BMI, sex, vaccine makeup, and LC status did not appear to influence antigen or antibody levels,

while younger aged participants had higher IgG concentrations, and those on a plant-based diet had low antibody levels.

Inflammatory biomarkers linked to acute COVID-19 infection (such as IFN-γ, IL-6, CCL2, IL-15, and CXCL10) are negatively associated with time, aside from TNF-α, which follows a weakly positive correlation with time and significantly elevated levels in the older age comparison group. The endothelial adhesion markers ICAM-1 and VCAM-1 are significantly elevated in the younger aged cohort, suggesting their role in leukocyte attachment and possibly in the coagulation/clotting response associated with LC. The biomarkers E-selectin, ANG-2, and D-dimer, which are all associated with vascular permeability, vascular sprouting, and clotting are weakly, positively associated with time, indicating prolonged activation and dysregulation in the endothelium.

This study provides both a level of understanding regarding COVID-19 seroprevalence in a university setting and early evidence towards the mechanisms and biomarkers that contribute to LC in young individuals. These results may help contribute to the development of a standardized biomarker panel that is highly predictive of LC status, addressing an important gap in COVID-19 research.

REFERENCES

1. Artika IM, Wiyatno A, Ma'roef CN. Pathogenic viruses: Molecular detection and characterization. Infection, Genetics and Evolution. 2020 Jul 1;81:104215.

2. Sanjuán R, Domingo-Calap P. Mechanisms of viral mutation. Cell Mol Life Sci. 2016 Dec 1;73(23):4433–48.

3. Ma X, Lu J, Liu W. Knowledge of Emerging and Reemerging Infectious Diseases in the Public of Guangzhou, Southern China. Frontiers in Public Health [Internet]. 2022 [cited 2022 Apr 25];10. Available from: https://www.frontiersin.org/article/10.3389/fpubh.2022.718592

4. Ye ZW, Yuan S, Yuen KS, Fung SY, Chan CP, Jin DY. Zoonotic origins of human coronaviruses. Int J Biol Sci. 2020 Mar 15;16(10):1686–97.

5. Enjuanes L, Zuñiga S, Castaño-Rodriguez C, Gutierrez-Alvarez J, Canton J, Sola I. Chapter Eight - Molecular Basis of Coronavirus Virulence and Vaccine Development. In: Ziebuhr J, editor. Advances in Virus Research [Internet]. Academic Press; 2016 [cited 2022 Apr 25]. p. 245–86. (Coronaviruses; vol. 96). Available from: https://www.sciencedirect.com/science/article/pii/S0065352716300422

6. Kumar S, Nyodu R, Maurya VK, Saxena SK. Morphology, Genome Organization, Replication, and Pathogenesis of Severe Acute Respiratory Syndrome Coronavirus 2 (SARS-CoV-2). In: Saxena SK, editor. Coronavirus Disease 2019 (COVID-19): Epidemiology, Pathogenesis, Diagnosis, and Therapeutics [Internet]. Singapore: Springer; 2020 [cited 2022 Apr 26]. p. 23–31. (Medical Virology: From Pathogenesis to Disease Control). Available from: https://doi.org/10.1007/978-981-15-4814-7_3

7. Liu DX, Liang JQ, Fung TS. Human Coronavirus-229E, -OC43, -NL63, and -HKU1 (Coronaviridae). Encyclopedia of Virology. 2021;428–40.

8. V'kovski P, Kratzel A, Steiner S, Stalder H, Thiel V. Coronavirus biology and replication: implications for SARS-CoV-2. Nat Rev Microbiol. 2021 Mar;19(3):155–70.

9. Wacharapluesadee S, Tan CW, Maneeorn P, Duengkae P, Zhu F, Joyjinda Y, et al. Evidence for SARS-CoV-2 related coronaviruses circulating in bats and pangolins in Southeast Asia. Nat Commun. 2021 Feb 9;12(1):972.

10. Lewis D, Kozlov M, Lenharo M. COVID-origins data from Wuhan market published: what scientists think. Nature. 2023 Apr 5;616(7956):225–6.

11. Guruprasad L. Human coronavirus spike protein-host receptor recognition. Progress in Biophysics and Molecular Biology. 2021 May 1;161:39–53.

12. Cucinotta D, Vanelli M. WHO Declares COVID-19 a Pandemic. Acta Biomed. 2020 Mar 19;91(1):157–60.

13. Wood RM. Modelling the impact of COVID-19 on elective waiting times. Journal of Simulation. 2022 Jan 2;16(1):101–9.

14. Wood S. Daily Maverick. 2022 [cited 2022 May 4]. PANDEMIC TOLL ANALYSIS: Covid-19 has so far cost the world as much as $114-trillion — and counting. Available from: https://www.dailymaverick.co.za/article/2022-02-02-covid-19-has-so-far-cost-the-world-as-much-as-114-trillion-and-counting/

15. Rahimi A, Mirzazadeh A, Tavakolpour S. Genetics and genomics of SARS-CoV-2: A review of the literature with the special focus on genetic diversity and SARS-CoV-2 genome detection. Genomics. 2021 Jan 1;113(1, Part 2):1221–32.

16. Jackson CB, Farzan M, Chen B, Choe H. Mechanisms of SARS-CoV-2 entry into cells. Nat Rev Mol Cell Biol. 2022 Jan;23(1):3–20.

17. Murgolo N, Therien AG, Howell B, Klein D, Koeplinger K, Lieberman LA, et al. SARS-CoV-2 tropism, entry, replication, and propagation: Considerations for drug discovery and development. PLOS Pathogens. 2021 Feb 17;17(2):e1009225.

18. Duan L, Zheng Q, Zhang H, Niu Y, Lou Y, Wang H. The SARS-CoV-2 Spike Glycoprotein Biosynthesis, Structure, Function, and Antigenicity: Implications for the Design of Spike-Based Vaccine Immunogens. Frontiers in Immunology [Internet]. 2020 [cited 2022 May 4];11. Available from: https://www.frontiersin.org/article/10.3389/fimmu.2020.576622

19. Jaimes JA, Millet JK, Whittaker GR. Proteolytic cleavage of the SARS-CoV-2 spike protein and the role of the novel S1/S2 site. SSRN. 2020 May 5;3581359.

20. Essalmani R, Jain J, Susan-Resiga D, Andréo U, Evagelidis A, Derbali RM, et al. Distinctive Roles of Furin and TMPRSS2 in SARS-CoV-2 Infectivity. J Virol. 96(8):e00128-22.

21. Yuan M, Wu NC, Zhu X, Lee CCD, So RTY, Lv H, et al. A highly conserved cryptic epitope in the receptor binding domains of SARS-CoV-2 and SARS-CoV. Science. 2020 May 8;368(6491):630–3.

22. Wang Y, Chen XY, Yang L, Yao Q, Chen KP. Human SARS-CoV-2 has evolved to increase U content and reduce genome size. International Journal of Biological Macromolecules. 2022 Apr 15;204:356–63.

23. Fehr AR, Perlman S. Coronaviruses: an overview of their replication and pathogenesis. Methods Mol Biol. 2015;1282:1–23.

24. Romano M, Ruggiero A, Squeglia F, Maga G, Berisio R. A Structural View of SARS-CoV-2 RNA Replication Machinery: RNA Synthesis, Proofreading and Final Capping. Cells. 2020 May 20;9(5):1267.

25. Wu C rong, Yin W chao, Jiang Y, Xu HE. Structure genomics of SARS-CoV-2 and its Omicron variant: drug design templates for COVID-19. Acta Pharmacol Sin. 2022 Dec;43(12):3021–33.

26. Rastogi M, Pandey N, Shukla A, Singh SK. SARS coronavirus 2: from genome to infectome. Respiratory Research. 2020 Dec 1;21(1):318.

27. Zhang J, Xiao T, Cai Y, Chen B. Structure of SARS-CoV-2 spike protein. Current Opinion in Virology. 2021 Oct 1;50:173–82.

28. Chai J, Cai Y, Pang C, Wang L, McSweeney S, Shanklin J, et al. Structural basis for SARS-CoV-2 envelope protein recognition of human cell junction protein PALS1. Nat Commun. 2021 Jun 8;12(1):3433.

29. Thomas S. The Structure of the Membrane Protein of SARS-CoV-2 Resembles the Sugar Transporter SemiSWEET. Pathog Immun. 2020 Oct 19;5(1):342–63.

30. Cubuk J, Alston JJ, Incicco JJ, Singh S, Stuchell-Brereton MD, Ward MD, et al. The SARS-CoV-2 nucleocapsid protein is dynamic, disordered, and phase separates with RNA. Nat Commun. 2021 Mar 29;12(1):1936.

31. Ye Q, Lu S, Corbett KD. Structural Basis for SARS-CoV-2 Nucleocapsid Protein Recognition by Single-Domain Antibodies. Frontiers in Immunology [Internet]. 2021 [cited 2022 May 4];12. Available from: https://www.frontiersin.org/article/10.3389/fimmu.2021.719037

32. Marshall JS, Warrington R, Watson W, Kim HL. An introduction to immunology and immunopathology. Allergy, Asthma & Clinical Immunology. 2018 Sep 12;14(2):49.

33. Amarante-Mendes GP, Adjemian S, Branco LM, Zanetti LC, Weinlich R, Bortoluci KR. Pattern Recognition Receptors and the Host Cell Death Molecular Machinery. Frontiers in Immunology [Internet]. 2018 [cited 2022 May 25];9. Available from: https://www.frontiersin.org/article/10.3389/fimmu.2018.02379

34. Hato T, Dagher PC. How the Innate Immune System Senses Trouble and Causes Trouble. CJASN. 2015 Aug 7;10(8):1459–69.

35. Carty M, Guy C, Bowie AG. Detection of Viral Infections by Innate Immunity. Biochemical Pharmacology. 2021 Jan 1;183:114316.

36. Murira A, Lamarre A. Type-I Interferon Responses: From Friend to Foe in the Battle against Chronic Viral Infection. Frontiers in Immunology [Internet]. 2016 [cited 2022 May 30];7. Available from: https://www.frontiersin.org/article/10.3389/fimmu.2016.00609

37. Schoggins JW, Rice CM. Interferon-stimulated genes and their antiviral effector functions. Curr Opin Virol. 2011 Dec;1(6):519–25.

38. Lacy P, Stow JL. Cytokine release from innate immune cells: association with diverse membrane trafficking pathways. Blood. 2011 Jul 7;118(1):9–18.

39. Hughes CE, Nibbs RJB. A guide to chemokines and their receptors. FEBS J. 2018 Aug;285(16):2944–71.

40. Johansson C, Kirsebom FCM. Neutrophils in respiratory viral infections. Mucosal Immunol. 2021 Jul;14(4):815–27.

41. Portales-Cervantes L, Haidl ID, Lee PW, Marshall JS. Virus-Infected Human Mast Cells Enhance Natural Killer Cell Functions. JIN. 2017;9(1):94–108.

42. Knoll R, Schultze JL, Schulte-Schrepping J. Monocytes and Macrophages in COVID-19. Frontiers in Immunology [Internet]. 2021 [cited 2022 Jun 2];12. Available from: https://www.frontiersin.org/article/10.3389/fimmu.2021.720109

43. Gracia-Hernandez M, Sotomayor EM, Villagra A. Targeting Macrophages as a Therapeutic Option in Coronavirus Disease 2019. Frontiers in Pharmacology [Internet]. 2020 [cited 2022 Jun 2];11. Available from: https://www.frontiersin.org/article/10.3389/fphar.2020.577571

44. Chaplin DD. Overview of the Immune Response. J Allergy Clin Immunol. 2010 Feb;125(2 Suppl 2):S3-23.

45. Saylor K, Gillam F, Lohneis T, Zhang C. Designs of Antigen Structure and Composition for Improved Protein-Based Vaccine Efficacy. Frontiers in Immunology [Internet]. 2020 [cited 2022 Jun 2];11. Available from: https://www.frontiersin.org/article/10.3389/fimmu.2020.00283

46. Zhao F, Ma Q, Yue Q, Chen H. SARS-CoV-2 Infection and Lung Regeneration. Clinical Microbiology Reviews. 2022 Feb 2;35(2):e00188-21.

47. Bridges JP, Vladar EK, Huang H, Mason RJ. Respiratory epithelial cell responses to SARS-CoV-2 in COVID-19. Thorax. 2022 Feb 1;77(2):203–9.

48. Shivshankar P, Karmouty-Quintana H, Mills T, Doursout MF, Wang Y, Czopik AK, et al. SARS-CoV-2 Infection: Host Response, Immunity, and Therapeutic Targets. Inflammation. 2022;45(4):1430–49.

49. Voiriot G, Dorgham K, Bachelot G, Fajac A, Morand-Joubert L, Parizot C, et al. Identification of bronchoalveolar and blood immune-inflammatory biomarker signature associated with poor 28-day outcome in critically ill COVID-19 patients. Sci Rep. 2022 Jun 9;12(1):9502.

50. Brabander J de, Boers LS, Kullberg RFJ, Zhang S, Nossent EJ, Heunks LMA, et al. Persistent alveolar inflammatory response in critically ill patients with COVID-19 is associated with mortality. Thorax [Internet]. 2023 May 4 [cited 2023 May 24]; Available from: https://thorax.bmj.com/content/early/2023/05/04/thorax-2023-219989

51. Martinez G, Garduno A, Mahmud-Al-Rafat A, Ostadgavahi AT, Avery A, Silva S de A e, et al. An artificial neural network classification method employing longitudinally monitored immune biomarkers to predict the clinical outcome of critically ill COVID-19 patients. PeerJ. 2022 Dec 12;10:e14487.

52. Biering SB, Gomes de Sousa FT, Tjang LV, Pahmeier F, Zhu C, Ruan R, et al. SARS-CoV-2 Spike triggers barrier dysfunction and vascular leak via integrins and TGF-β signaling. Nat Commun. 2022 Dec 9;13(1):7630.

53. Bruni F, Charitos P, Lampart M, Moser S, Siegemund M, Bingisser R, et al. Complement and endothelial cell activation in COVID-19 patients compared to controls with suspected SARS-CoV-2 infection: A prospective cohort study. Frontiers in Immunology [Internet]. 2022 [cited 2023 May 26];13. Available from: https://www.frontiersin.org/articles/10.3389/fimmu.2022.941742

54. Birnhuber A, Fließer E, Gorkiewicz G, Zacharias M, Seeliger B, David S, et al. Between inflammation and thrombosis: endothelial cells in COVID-19. European Respiratory Journal [Internet]. 2021 Sep 1 [cited 2023 May 26];58(3). Available from: https://erj.ersjournals.com/content/58/3/2100377

55. Yu Y, Esposito D, Kang Z, Lu J, Remaley AT, De Giorgi V, et al. mRNA vaccine-induced antibodies more effective than natural immunity in neutralizing SARS-CoV-2 and its high affinity variants. Sci Rep. 2022 Feb 16;12(1):2628.

56. Moss P. The T cell immune response against SARS-CoV-2. Nat Immunol. 2022 Feb;23(2):186–93.

57. Rha MS, Shin EC. Activation or exhaustion of CD8+ T cells in patients with COVID-19. Cell Mol Immunol. 2021 Oct;18(10):2325–33.

58. Xiang Q, Feng Z, Diao B, Tu C, Qiao Q, Yang H, et al. SARS-CoV-2 Induces Lymphocytopenia by Promoting Inflammation and Decimates Secondary Lymphoid Organs. Frontiers in Immunology [Internet]. 2021 [cited 2023 Aug 18];12. Available from: https://www.frontiersin.org/articles/10.3389/fimmu.2021.661052

59. van der Ploeg K, Kirosingh AS, Mori DAM, Chakraborty S, Hu Z, Sievers BL, et al. TNF-α+ CD4+ T cells dominate the SARS-CoV-2 specific T cell response in COVID-19 outpatients and are associated with durable antibodies. Cell Reports Medicine. 2022 Jun 21;3(6):100640.

60. Pavan M, Bassani D, Sturlese M, Moro S. From the Wuhan-Hu-1 strain to the XD and XE variants: is targeting the SARS-CoV-2 spike protein still a pharmaceutically relevant option against COVID-19? J Enzyme Inhib Med Chem. 37(1):1704–14.

61. Canada PHA of. aem. 2020 [cited 2021 Dec 8]. COVID-19 daily epidemiology update. Available from: https://health-infobase.canada.ca/covid-19/epidemiological-summary-covid-19-cases.html?stat=num&measure=deaths&map=pt#a2

62. Campbell F, Archer B, Laurenson-Schafer H, Jinnai Y, Konings F, Batra N, et al. Increased transmissibility and global spread of SARS-CoV-2 variants of concern as at June 2021. Eurosurveillance. 2021 Jun 17;26(24):2100509.

63. Liu Y, Rocklöv J. The effective reproductive number of the Omicron variant of SARS-CoV-2 is several times relative to Delta. J Travel Med. 2022 Mar 9;29(3):taac037.

64. Harvey WT, Carabelli AM, Jackson B, Gupta RK, Thomson EC, Harrison EM, et al. SARS-CoV-2 variants, spike mutations and immune escape. Nat Rev Microbiol. 2021 Jul;19(7):409–24.

65. Hewins B, Richardson C, Rubino S, Kelvin A, Ostadgavahi AT, Kelvin DJ. Molecular mechanisms responsible for SARS-CoV-2 antibody waning and vaccine escape in Omicron sublineages BA.4 and BA.5. The Journal of Infection in Developing Countries. 2022 Jul 28;16(07):1122–5.

66. Alkhatib M, Salpini R, Carioti L, Ambrosio FA, D'Anna S, Duca L, et al. Update on SARS-CoV-2 Omicron Variant of Concern and Its Peculiar Mutational Profile. Microbiol Spectr. 10(2):e02732-21.

67. Montgomerie I, Bird TW, Palmer OR, Mason NC, Pankhurst TE, Lawley B, et al. Incorporation of SARS-CoV-2 spike NTD to RBD protein vaccine improves immunity against viral variants. iScience. 2023 Apr 21;26(4):106256.

68. Cosar B, Karagulleoglu ZY, Unal S, Ince AT, Uncuoglu DB, Tuncer G, et al. SARS-CoV-2 Mutations and their Viral Variants. Cytokine & Growth Factor Reviews. 2022 Feb 1;63:10–22.

69. SARS-CoV-2 variants of concern as of 24 August 2023 [Internet]. 2021 [cited 2023 Aug 29]. Available from: https://www.ecdc.europa.eu/en/covid-19/variants-concern

70. Mortazavi SA, Jooyan N, Baha'addini Baigy Zarandi BF, Jooyan N, Faraz M, Mortazavi SMJ. Coming Out of Nowhere: The Paradox of the Birth of Omicron. J Biomed Phys Eng. 2022 Aug 1;12(4):325–6.

71. Mallapaty S. Where did Omicron come from? Three key theories. Nature. 2022 Feb;602(7895):26–8.

72. Ball P. The lightning-fast quest for COVID vaccines — and what it means for other diseases. Nature. 2020 Dec 18;589(7840):16–8.

73. Kalinke U, Barouch DH, Rizzi R, Lagkadinou E, Türeci Ö, Pather S, et al. Clinical development and approval of COVID-19 vaccines. Expert Review of Vaccines. 2022 May 4;21(5):609–19.

74. WHO – COVID19 Vaccine Tracker [Internet]. [cited 2023 Aug 30]. Available from: https://covid19.trackvaccines.org/agency/who/

75. Fiolet T, Kherabi Y, MacDonald CJ, Ghosn J, Peiffer-Smadja N. Comparing COVID-19 vaccines for their characteristics, efficacy and effectiveness against SARS-CoV-2 and variants of concern: a narrative review. Clinical Microbiology and Infection. 2022 Feb 1;28(2):202–21.

76. Buschmann MD, Carrasco MJ, Alishetty S, Paige M, Alameh MG, Weissman D. Nanomaterial Delivery Systems for mRNA Vaccines. Vaccines. 2021 Jan;9(1):65.

77. Dolgin E. The tangled history of mRNA vaccines. Nature. 2021 Sep 14;597(7876):318–24.

78. Thomas SJ, Moreira ED, Kitchin N, Absalon J, Gurtman A, Lockhart S, et al. Safety and Efficacy of the BNT162b2 mRNA Covid-19 Vaccine through 6 Months. New England Journal of Medicine. 2021 Nov 4;385(19):1761–73.

79. Levin EG, Lustig Y, Cohen C, Fluss R, Indenbaum V, Amit S, et al. Waning Immune Humoral Response to BNT162b2 Covid-19 Vaccine over 6 Months. New England Journal of Medicine. 2021 Oct 6;0(0):null.

80. Hewins B, Rahman M, Bermejo-Martin JF, Kelvin AA, Richardson CD, Rubino S, et al. Alpha, Beta, Delta, Omicron, and SARS-CoV-2 Breakthrough Cases: Defining Immunological Mechanisms for Vaccine Waning and Vaccine-Variant Mismatch. Frontiers in Virology [Internet]. 2022 [cited 2022 Jun 12];2. Available from: https://www.frontiersin.org/article/10.3389/fviro.2022.849936

81. Willett BJ, Grove J, MacLean OA, Wilkie C, De Lorenzo G, Furnon W, et al. SARS-CoV-2 Omicron is an immune escape variant with an altered cell entry pathway. Nat Microbiol. 2022 Aug;7(8):1161–79.

82. Verywell Health [Internet]. [cited 2022 Feb 4]. Will the COVID-19 Vaccines Provide Sterilizing Immunity? Available from: https://www.verywellhealth.com/covid-19-vaccines-and-sterilizing-immunity-5092148

83. Singh C, Verma S, Reddy P, Diamond MS, Curiel DT, Patel C, et al. Phase III Pivotal comparative clinical trial of intranasal (iNCOVACC) and intramuscular COVID 19 vaccine (Covaxin®). npj Vaccines. 2023 Aug 18;8(1):1–9.

84. 2 NIAID Studies Highlight COVID-19 Nasal Vaccine Potential | NIH: National Institute of Allergy and Infectious Diseases [Internet]. 2022 [cited 2023 Aug 30]. Available from: https://www.niaid.nih.gov/news-events/covid-nasal-vaccines

85. Wang B, Andraweera P, Elliott S, Mohammed H, Lassi Z, Twigger A, et al. Asymptomatic SARS-CoV-2 Infection by Age: A Global Systematic Review and Meta-analysis. Pediatr Infect Dis J. 2023 Mar;42(3):232–9.

86. Cascella M, Rajnik M, Aleem A, Dulebohn SC, Di Napoli R. Features, Evaluation, and Treatment of Coronavirus (COVID-19). In: StatPearls [Internet]. Treasure Island (FL): StatPearls Publishing; 2023 [cited 2023 Aug 31]. Available from: http://www.ncbi.nlm.nih.gov/books/NBK554776/

87. CDC. Centers for Disease Control and Prevention. 2023 [cited 2023 Aug 31]. Post-COVID Conditions. Available from: https://www.cdc.gov/coronavirus/2019-ncov/long-term-effects/index.html

88. Auld SC, Caridi-Scheible M, Blum JM, Robichaux C, Kraft C, Jacob JT, et al. ICU and ventilator mortality among critically ill adults with COVID-19. medRxiv. 2020 Apr 26;2020.04.23.20076737.

89. Kenny G, Mallon PW. COVID19- clinical presentation and therapeutic considerations. Biochemical and Biophysical Research Communications. 2021 Jan 29;538:125–31.

90. Rovito R, Augello M, Ben-Haim A, Bono V, d'Arminio Monforte A, Marchetti G. Hallmarks of Severe COVID-19 Pathogenesis: A Pas de Deux Between Viral and Host Factors. Frontiers in Immunology [Internet]. 2022 [cited 2023 Aug 31];13. Available from: https://www.frontiersin.org/articles/10.3389/fimmu.2022.912336

91. de Morais Batista F, Puga MAM, da Silva PV, Oliveira R, dos Santos PCP, da Silva BO, et al. Serum biomarkers associated with SARS-CoV-2 severity. Sci Rep. 2022 Sep 26;12(1):15999.

92. Parotto M, Gyöngyösi M, Howe K, Myatra SN, Ranzani O, Shankar-Hari M, et al. Post-acute sequelae of COVID-19: understanding and addressing the burden of multisystem manifestations. The Lancet Respiratory Medicine. 2023 Aug 1;11(8):739–54.

93. Proal AD, VanElzakker MB. Long COVID or Post-acute Sequelae of COVID-19 (PASC): An Overview of Biological Factors That May Contribute to Persistent Symptoms. Frontiers in Microbiology [Internet]. 2021 [cited 2023 Aug 31];12. Available from: https://www.frontiersin.org/articles/10.3389/fmicb.2021.698169

94. Davis HE, McCorkell L, Vogel JM, Topol EJ. Long COVID: major findings, mechanisms and recommendations. Nat Rev Microbiol. 2023 Mar;21(3):133–46.

95. Swank Z, Senussi Y, Manickas-Hill Z, Yu XG, Li JZ, Alter G, et al. Persistent Circulating Severe Acute Respiratory Syndrome Coronavirus 2 Spike Is Associated With Post-acute Coronavirus Disease 2019 Sequelae. Clinical Infectious Diseases. 2023 Feb 1;76(3):e487–90.

96. Patel MA, Knauer MJ, Nicholson M, Daley M, Van Nynatten LR, Martin C, et al. Elevated vascular transformation blood biomarkers in Long-COVID indicate angiogenesis as a key pathophysiological mechanism. Molecular Medicine. 2022 Oct 10;28(1):122.

97. Zhou M, Yin Z, Xu J, Wang S, Liao T, Wang K, et al. Inflammatory Profiles and Clinical Features of Coronavirus 2019 Survivors 3 Months After Discharge in Wuhan, China. The Journal of Infectious Diseases. 2021 Nov 1;224(9):1473–88.

98. Chen B, Julg B, Mohandas S, Bradfute SB. Viral persistence, reactivation, and mechanisms of long COVID. eLife. 12:e86015.

99. Diseases TLI. Where are the long COVID trials? The Lancet Infectious Diseases. 2023 Aug 1;23(8):879.

100. Clarke KEN. Seroprevalence of Infection-Induced SARS-CoV-2 Antibodies — United States, September 2021–February 2022. MMWR Morb Mortal Wkly Rep [Internet]. 2022 [cited 2023 Sep 10];71. Available from: https://www.cdc.gov/mmwr/volumes/71/wr/mm7117e3.htm

101. Bajema KL, Wiegand RE, Cuffe K, Patel SV, Iachan R, Lim T, et al. Estimated SARS-CoV-2 Seroprevalence in the US as of September 2020. JAMA Internal Medicine. 2021 Apr 1;181(4):450–60.

102. Abhold J, Wozniak A, Mulcahy J, Walsh S, Zepeda E, Demmer R, et al. Demographic, social, and behavioral correlates of SARS-CoV-2 seropositivity in a representative, population-based study of Minnesota residents. PLoS One. 2023 Jun 15;18(6):e0279660.

103. Murphy TJ, Swail H, Jain J, Anderson M, Awadalla P, Behl L, et al. The evolution of SARS-CoV-2 seroprevalence in Canada: a time-series study, 2020–2023. CMAJ. 2023 Aug 14;195(31):E1030–7.

104. News · JW· C. CBC. 2022 [cited 2023 Sep 10]. Back to campus: Students face starkly different COVID-19 protocols at Canada's colleges, universities | CBC News. Available from: https://www.cbc.ca/news/canada/universities-colleges-campus-return-policies-1.6560643

105. Ioannidis JPA, Salholz-Hillel M, Boyack KW, Baas J. The rapid, massive growth of COVID-19 authors in the scientific literature. Royal Society Open Science. 2021 Sep 7;8(9):210389.

106. Patterson BK, Francisco EB, Yogendra R, Long E, Pise A, Rodrigues H, et al. Persistence of SARS CoV-2 S1 Protein in CD16+ Monocytes in Post-Acute Sequelae of COVID-19 (PASC) up to 15 Months Post-Infection. Front Immunol. 2022 Jan 10;12:746021.

107. Lee N, Jeong S, Lee SK, Cho EJ, Hyun J, Park MJ, et al. Quantitative Analysis of Anti-N and Anti-S Antibody Titers of SARS-CoV-2 Infection after the Third Dose of COVID-19 Vaccination. Vaccines (Basel). 2022 Jul 18;10(7):1143.

108. Maine GN, Krishnan SM, Walewski K, Trueman J, Sykes E, Sun Q. Clinical and analytical evaluation of the Abbott AdviseDx quantitative SARS-CoV-2 IgG assay and comparison with two other serological tests. J Immunol Methods. 2022 Apr;503:113243.

109. Azak E, Karadenizli A, Uzuner H, Karakaya N, Canturk NZ, Hulagu S. Comparison of an inactivated Covid19 vaccine-induced antibody response with concurrent natural Covid19 infection. Int J Infect Dis. 2021 Dec;113:58–64.

110. Peluso MJ, Deeks SG. Early clues regarding the pathogenesis of long-COVID. Trends Immunol. 2022 Apr;43(4):268–70.

111. Wang X, Tang G, Liu Y, Zhang L, Chen B, Han Y, et al. The role of IL-6 in coronavirus, especially in COVID-19. Frontiers in Pharmacology [Internet]. 2022 [cited 2023 Sep 23];13. Available from: https://www.frontiersin.org/articles/10.3389/fphar.2022.1033674

112. Schultheiß C, Willscher E, Paschold L, Gottschick C, Klee B, Henkes SS, et al. The IL-1β, IL-6, and TNF cytokine triad is associated with post-acute sequelae of COVID-19. Cell Rep Med. 2022 Jun 21;3(6):100663.

113. Queiroz MAF, Neves PFM das, Lima SS, Lopes J da C, Torres MK da S, Vallinoto IMVC, et al. Cytokine Profiles Associated With Acute COVID-19 and Long COVID-19 Syndrome. Frontiers in Cellular and Infection Microbiology [Internet]. 2022 [cited 2023 Sep 23];12. Available from: https://www.frontiersin.org/articles/10.3389/fcimb.2022.922422

114. Kalaivani MK, Dinakar S. Association between D-dimer levels and post-acute sequelae of SARS-CoV-2 in patients from a tertiary care center. Biomark Med. 2022 Aug;16(11):833–8.

115. Teo A, Chan LLY, Cheung C, Chia PY, Ong SWX, Fong SW, et al. Myeloperoxidase inhibition may protect against endothelial glycocalyx shedding induced by COVID-19 plasma. Commun Med (Lond). 2023 May 5;3:62.

116. Martinez GS, Ostadgavahi AT, Al-Rafat AM, Garduno A, Cusack R, Bermejo-Martin JF, et al. Model-interpreted outcomes of artificial neural networks classifying immune biomarkers associated with severe infections in ICU. Frontiers in Immunology [Internet]. 2023 [cited 2023 Sep 26];14. Available from: https://www.frontiersin.org/articles/10.3389/fimmu.2023.1137850

117. Yonker LM, Swank Z, Bartsch YC, Burns MD, Kane A, Boribong BP, et al. Circulating Spike Protein Detected in Post-COVID-19 mRNA Vaccine Myocarditis. Circulation. 2023 Mar 14;147(11):867–76.

118. Zhang Y, Ong CM, Yun C, Mo W, Whitman JD, Lynch KL, et al. Diagnostic Value of Nucleocapsid Protein in Blood for SARS-CoV-2 Infection. Clin Chem. 2021 Aug 6;hvab148.

119. Sganzerla Martinez G, Hewins B, LeBlanc JJ, Ndishimye P, Toloue Ostadgavahi A, Kelvin DJ. Evaluating the effectiveness of lockdowns and restrictions during SARS-CoV-2 variant waves in the Canadian province of Nova Scotia. Front Public Health. 2023;11:1142602.

120. Shang W, Kang L, Cao G, Wang Y, Gao P, Liu J, et al. Percentage of Asymptomatic Infections among SARS-CoV-2 Omicron Variant-Positive Individuals: A Systematic Review and Meta-Analysis. Vaccines (Basel). 2022 Jun 30;10(7):1049.

121. Wondeu ALD, Talom BM, Linardos G, Ngoumo BT, Bello A, Soufo AMN, et al. The COVID-19 wave was already here: High seroprevalence of SARS-CoV-2 antibodies among staff and students in a Cameroon University. Journal of Public Health in Africa [Internet]. 2023 Jan 27 [cited 2023 Oct 25]; Available from: https://www.publichealthinafrica.org/jphia/article/view/2242

122. Aydillo T, Gonzalez-Reiche AS, Aslam S, van de Guchte A, Khan Z, Obla A, et al. Shedding of Viable SARS-CoV-2 after Immunosuppressive Therapy for Cancer. N Engl J Med. 2020 Dec 24;383(26):2586–8.

123. Ciarambino T, Para O, Giordano M. Immune system and COVID-19 by sex differences and age. Womens Health (Lond). 2021 Jun 6;17:17455065211022262.

124. Huang B, Cai Y, Li N, Li K, Wang Z, Li L, et al. Sex-based clinical and immunological differences in COVID-19. BMC Infectious Diseases. 2021 Jul 5;21(1):647.

125. Mahamat-Saleh Y, Fiolet T, Rebeaud ME, Mulot M, Guihur A, El Fatouhi D, et al. Diabetes, hypertension, body mass index, smoking and COVID-19-related mortality: a systematic review and meta-analysis of observational studies. BMJ Open. 2021 Oct 25;11(10):e052777.

126. Neubauerova E, Tulinska J, Kuricova M, Liskova A, Volkovova K, Kudlackova M, et al. The Effect of Vegetarian Diet on Immune Response. Epidemiology. 2007 Sep;18(5):S196.

127. Bayart JL, Morimont L, Closset M, Wieërs G, Roy T, Gerin V, et al. Confounding Factors Influencing the Kinetics and Magnitude of Serological Response Following Administration of BNT162b2. Microorganisms. 2021 Jun 21;9(6):1340.

128. Yang HS, Costa V, Racine-Brzostek SE, Acker KP, Yee J, Chen Z, et al. Association of Age With SARS-CoV-2 Antibody Response. JAMA Network Open. 2021 Mar 22;4(3):e214302.

129. Zhai B, Clarke K, Bauer DL, Moehling Geffel KK, Kupul S, Schratz LJ, et al. SARS-CoV-2 Antibody Response is Associated with Age and Body Mass Index in Convalescent Outpatients. J Immunol. 2022 Apr 1;208(7):1711–8.

130. Nittas V, Gao M, West EA, Ballouz T, Menges D, Wulf Hanson S, et al. Long COVID Through a Public Health Lens: An Umbrella Review. Public Health Rev. 2022;43:1604501.

131. Holms RD. Long COVID (PASC) Is Maintained by a Self-Sustaining Pro-Inflammatory TLR4/RAGE-Loop of S100A8/A9 > TLR4/RAGE Signalling, Inducing Chronic Expression of IL-1b, IL-6 and TNFa: Anti-Inflammatory Ezrin Peptides as Potential Therapy. Immuno. 2022 Sep;2(3):512–33.

132. Talla A, Vasaikar SV, Szeto GL, Lemos MP, Czartoski JL, MacMillan H, et al. Persistent serum protein signatures define an inflammatory subcategory of long COVID. Nat Commun. 2023 Jun 9;14(1):3417.

133. Williams ES, Martins TB, Shah KS, Hill HR, Coiras M, Spivak AM, et al. Cytokine Deficiencies in Patients with Long-COVID. J Clin Cell Immunol. 2022;13(6):672.

134. Ranjbar M, Rahimi A, Baghernejadan Z, Ghorbani A, Khorramdelazad H. Role of CCL2/CCR2 axis in the pathogenesis of COVID-19 and possible Treatments: All options on the Table. Int Immunopharmacol. 2022 Dec;113:109325.

135. Teuwen LA, Geldhof V, Pasut A, Carmeliet P. COVID-19: the vasculature unleashed. Nat Rev Immunol. 2020;20(7):389–91.

136. Arnhold J. The Dual Role of Myeloperoxidase in Immune Response. Int J Mol Sci. 2020 Oct 29;21(21):8057.

137. Al-Hakeim HK, Al-Rubaye HT, Al-Hadrawi DS, Almulla AF, Maes M. Long-COVID post-viral chronic fatigue and affective symptoms are associated with oxidative damage, lowered antioxidant defenses and inflammation: a proof of concept and mechanism study. Mol Psychiatry. 2023 Feb;28(2):564–78.

138. Soni A, Herbert C, Filippaios A, Broach J, Colubri A, Fahey N, et al. Comparison of Rapid Antigen Tests' Performance Between Delta and Omicron Variants of SARS-CoV-2. Ann Intern Med. 2022 Oct 11;M22-0760.

139. Lau CS, Aw TC. SARS-CoV-2 Antigen Testing Intervals: Twice or Thrice a Week? Diagnostics [Internet]. 2022 May [cited 2023 Oct 30];12(5). Available from: https://www.ncbi.nlm.nih.gov/pmc/articles/PMC9139623/

140. Chu VT, Schwartz NG, Donnelly MAP, Chuey MR, Soto R, Yousaf AR, et al. Comparison of Home Antigen Testing With RT-PCR and Viral Culture During the Course of SARS-CoV-2 Infection. JAMA Internal Medicine. 2022 Jul 1;182(7):701–9.

141. Cedro VQM, de Lima Gomes S, Simões ACCD, Sverzut T do VL, Bertti KCX, Tristão MT, et al. Cost-effectiveness analysis of COVID-19 tests in the unified health system. Cost Eff Resour Alloc. 2023 Sep 13;21:64.

APPENDIX I

Table A.1 Student cohort demographics collected during enrolment.

Variable	*n*	(%)	±SD
Age			
18-20	10	13.0	0.52
21-25	29	37.7	1.52
26-30	23	29.9	1.41
31-35	15	19.5	1.30
Age (avg.)	26.7	-	4.4
Sex			
Male	22	28.6	0.00
Female	55	71.4	
Total	77	100.0	
BMI (kg/m^2)			
Male (avg.)	25.88	-	5.44
Female (avg.)	24.17	-	5.16
BMI (avg.)	25.03	-	-
Comorbidities			
No comorbidities	62	80.1	0.00
Autoimmune disorder	1	1.3	
Renal condition	1	1.3	
ADHD	3	3.9	
IBS	1	1.3	
Hypothyroidism	2	2.6	
Anxiety/mood disorder	3	3.9	
Migraine	2	2.6	
PCOS	1	1.3	
Beta thalassemia	1	1.3	

Table A.2 Lifestyle and social factors collected during enrolment for each study participant.

Variable	*n*	(%)
Smoking Status		
Non-smoker	74	96.1
Smoker	3	3.9
Cannabis Use		
Does not use	55	71.4
Smoker	15	19.5
Consumer	7	9.1
Cannabis Frequency (combined smoking and consuming)		
Less than monthly	8	38.1
Monthly	5	23.8
Weekly	5	23.8
Daily or almost daily	3	14.3
Alcohol Status		
Drinker	55	71.4
Non-drinker	22	28.6
Alcohol Frequency (more than five drinks/occasion)		
Less than monthly	28	50.0
Monthly	20	35.7
Weekly	8	14.3
Diet		
No preference	54	70.0
Vegetarian	14	18.2
Vegan	5	6.5
Pescatarian	4	5.2
Transportation		
Walk/bike/drive	52	67.5
Public transit (bus)	27	35.1
Taxi	2	2.3
Living Status		
With roommate	34	44.2
With partner or spouse	29	37.7
Alone	14	18.2
Housing		
Single occupancy	57	74.0
Shared room	20	26.0

Table A.3 COVID-19 infection and vaccination history of each study participant.

Variable	*n*	(%)
Infection History		
Previous infection	50	65.0
No infection	27	35.0
Vaccination History		
3 doses	63	82.0
2 doses	8	10.0
4 doses	6	8.0
Vaccine Brand- Dose 1		
Pfizer-BioNTech (BNT162b2)	61	79.0
Moderna (mRNA-1273)	9	12.0
AstraZeneca (ChAdOx1)	6	8.0
Sinopharm (BBIBP-CorV)	1	1.0
Vaccine Brand- Dose 2		
Pfizer-BioNTech (BNT162b2)	36	47.0
Moderna (mRNA-1273)	34	44.0
AstraZeneca (ChAdOx1)	6	8.0
Sinopharm (BBIBP-CorV)	1	1.0
Vaccine Brand- Dose 3		
Pfizer-BioNTech (BNT162b2)	48	71.0
Moderna (mRNA-1273)	18	26.0
AstraZeneca (ChAdOx1)	1	1.0
Sinovac (CoronaVac)	1	1.0
Vaccine Brand- Dose 4		
Pfizer-BioNTech (BNT162b2)	5	83.0
Moderna (mRNA Bivalent)	1	17.0
Breakthrough Infections		
Total	47	61.0
Total after 1 dose	2	4.3
Total after 2 doses	11	23.4
Total after 3 doses	32	68.0
Total after 4 doses	1	2.1

APPENDIX II

Table A.2.1 Primer/probe N gene sequences (5' → 3') used to amplify SARS-CoV-2 viral RNA in isolated throat/nasal samples. Sequences were provided by the Centers for Disease Control and Prevention (CDC) and synthesized by NEB (NEB #E3019S/L).

Primer/probe		Sequence
2019-nCoV_N1	Forward primer	5′ GAC CCC AAA ATC AGC GAA AT 3′
	Reverse primer	5′ TCT GGT TAC TGC CAG TTG AAT CTG 3′
	Probe	5′ HEX-ACC CCG CAT TAC GTT TGG TGG ACC-Q 3′
2019-nCoV_N2	Forward primer	5′ TTA CAA ACA TTG GCC GCA AA 3′
	Reverse primer	5′ GCG CGA CAT TCC GAA GAA 3′
	Probe	5′ 6-FAM-ACA ATT TGC CCC CAG CGC TTC AG-Q 3′
RNase P	Forward primer	5′ AGA TTT GGA CCT GCG AGC G 3′
	Reverse primer	5′ CAA CTG AAT AGC CAA GGT GAG C 3′
	Probe	5′ Cy5-TTC TGA CCT GAA GGC TCT GCG CG-Q 3′

Abbreviations: Q- quencher; FAM, HEX, Cy5- fluorophore assignments.

Table A.2.2 The type and documented role in infection of the serum biomarkers measured in this study.

Biomarker	Type	Role in Infection
Pro-inflammatory:		
CXCL10	Chemokine	Attracts macrophages/monocytes during infection (involved in cytokine storm). CXCL10 is released by monocytes, endothelial cells, and fibroblasts.
Granzyme B	Protease	Involved in extracellular matrix remodeling and promotes the activation of proinflammatory cytokines
GM-CSF	Cytokine	Promotes myeloid cell development and dendritic cell differentiation
IL-2	Cytokine	Promotes the development of T-regulatory cells
IL-4	Cytokine	Induces the differentiation of naïve helper T-cells to Th2 cells
IL-7	Cytokine	Regulates T-cell and B-cell development and homeostasis
IL-12	Cytokine	Activates T-cells and NK cells; increases IFN-γ production
IL-15	Cytokine	Progresses septic shock by maintaining natural killer cell populations
TNF-α	Cytokine	Inflammatory– contributes to the progression of acute respiratory distress syndrome
IFN-γ	Cytokine	Provides early defence against viral challenge
IL-6	Cytokine	Contributes to pulmonary inflammation
CCL2	Cytokine	Recruits immune cells and increases inflammation
Anti-inflammatory		
IL-10	Cytokine	Inhibits the release of pro-inflammatory cytokines during infection
IL-1ra	Cytokine	Controls systemic responses to inflammatory stimuli
Endothelial/vascular Repair and/or Transformation:		
ANG-2	Cytokine (proangiogenic factor)	Induces vascular sprouting, upregulated in inflammatory diseases
D-dimer	Fibrin degradation product	Elevated during COVID-19 in the lungs due to increased rate of thromboembolic complications
E-selectin	Adhesion molecule	Marker of endothelial activation

ICAM-1	Adhesion molecule	Regulates endothelial barrier function
VCAM-1	Adhesion molecule	Regulates inflammation associated with vascular adhesion
Ferritin	Iron storage protein	Plays a role in systemic and cellular iron homeostasis
SP-D	Surfactant protein	Surfactant protein that contributes to innate immunity in the lungs
Neutrophil Activity & Degranulation:		
Lipocalin 2/NGAL	Adipocytokine	Modulates oxidative stress and protects against bacterial infection
IL-17A	Cytokine	Induces proinflammatory cytokines and recruits neutrophils to the site of infection
MPO	Peroxidase enzyme	Released by stimulated neutrophils and can increase reactive oxygen species production during infection leading to oxidative stress